# The theory of two-electron atoms: between ground state and complete fragmentation

Gregor Tanner*

*Basic Research Institute in the Mathematical Sciences, Hewlett-Packard Laboratories Bristol, Filton Road, Stoke Gifford, Bristol BS12 6QZ, United Kingdom*

Klaus Richter and Jan-Michael Rost

*Max-Planck-Institut für Physik komplexer Systeme, Nöthnitzer Str. 38, D-01187 Dresden, Germany*

Since the first attempts to calculate the helium ground state in the early days of Bohr-Sommerfeld quantization, two-electron atoms have posed a series of unexpected challenges to theoretical physics. Despite the seemingly simple problem of three charged particles with known interactions, it took more than half a century after quantum mechanics was established to describe the spectra of two-electron atoms satisfactorily. The evolution of the understanding of *correlated* two-electron dynamics and its importance for doubly excited resonance states is presented here, with an emphasis on the concepts introduced. The authors begin by reviewing the historical development and summarizing the progress in measuring the spectra of two-electron atoms and in calculating them by solving the corresponding Schrödinger equation numerically. They devote the second part of the review to approximate quantum methods, in particular adiabatic and group-theoretical approaches. These methods explain and predict the striking regularities of two-electron resonance spectra, including propensity rules for decay and dipole transitions of resonant states. This progress was made possible through the identification of approximate dynamical symmetries leading to corresponding collective quantum numbers for correlated electron-pair dynamics. The quantum numbers are very different from the independent particle classification, suitable for low-lying states in atomic systems. The third section of the review describes modern semiclassical concepts and their application to two-electron atoms. Simple interpretations of the approximate quantum numbers and propensity rules can be given in terms of a few key periodic orbits of the classical three-body problem. This includes the puzzling existence of Rydberg series for electron-pair motion. Qualitative and quantitative semiclassical estimates for doubly excited states are obtained for both regular and chaotic classical two-electron dynamics using modern semiclassical techniques. These techniques set the stage for a theoretical investigation of the regime of extreme excitation towards the three-body breakup threshold. Together with periodic orbit spectroscopy, they supply new tools for the analysis of complex experimental spectra.

## CONTENTS



*Present address: School of Mathematical Sciences, Division of Theoretical Mechanics, University of Nottingham, University Park, Nottingham NG7 2RD, UK.

## I. INTRODUCTION

*Moon-earth-sun, the oldest, best known but least understood three-body problem*—this is how Martin Gutzwiller summarized research on the gravitational dynamics of three masses in a recent review (Gutzwiller, 1998; see also 1995). Probably a similar statement applies to the corresponding microscopic three-body system, the dynamics of three massive point charges, most abundantly exemplified in Nature by two-electron atoms. The reason in both cases is the nonseparability of the classical equations of motion and the existence of chaos in the classical dynamics of the three-body system.

Two-electron atoms have played an important role in the development of theoretical physics in this century: They were a catalyst for the quantum theory in the mid 1920s, since the old quantum mechanics of Niels Bohr and others could not cope with the seemingly simple problem of calculating the ground state of helium. The discovery of strong electron-electron correlation effects in doubly excited resonant states of helium in a seminal experiment by Madden and Codling in 1963 triggered the development of group-theoretical and adiabatic quantum approximations to understand these unexpected correlations. Almost 70 years after the failure of the Bohr-Sommerfeld quantization for helium, two-electron dynamics were again at the forefront of a revival of the old quantum theory. New semiclassical concepts were introduced by Gutzwiller and others in the early 1970s, for which Heller and Tomsovic (1993) coined the term *postmodern quantum mechanics*. In contrast to the old quantum theory, which was based on (mostly) *ad hoc* quantization rules for certain classical orbits, modern semiclassical theory exploits the full classical dynamics in a systematic way. Based on these ideas, the first successful semiclassical quantization of helium was performed by Ezra *et al.* in 1991.

*Bound-state* spectra of two-electron atoms could be calculated efficiently with the help of the Hartree-Fock self-consistent-field method shortly after the new quantum theory was established. They can be handled to such accuracy today that they are used for high-precision measurements and calculations to improve on the fundamental physical constants. *Doubly excited* resonant states could not, on the other hand, be tackled by an effective single-particle method, and over the last 35 years the struggle to understand doubly excited resonances has been the focus of theoretical research on two-electron atoms. The role of electron correlation has become more and more important with increasing double excitation, and the correlated three-body Coulomb dynamics have been found to cause an extremely rich and complicated resonance spectrum. Hence two-electron atoms represent a prototype of a (few-body) system strongly affected by electronic correlation.

From a general perspective the complexity of the atomic three-body problem can be related to the under-

lying chaotic classical dynamics, in particular if the system is highly excited in an energy regime where infinitely many resonances exist. In this respect, two-electron atoms are of basic interest not only in atomic physics but also for the development of concepts of quantum chaos (see Berry, 1983; Gutzwiller, 1990).

Hence two-electron dynamics remain an active field of research to the present day. The persistent interest in the two-electron atomic three-body system lies in the fact that it is indeed complex enough for rather involved theoretical concepts (which we shall review), yet it is simple enough to provide accurate numerical and experimental data to test the approximation schemes.

### A. Scope of this review and related work

After a historical overview we shall concentrate on the ideas on which our understanding of two-electron resonances is mainly based today. We distinguish here approximate quantum concepts such as adiabatic and group-theoretical methods on the one hand and semiclassical methods on the other. We shall use the unique opportunity provided by a review to compare these two groups of concepts and to work out their mutual relations. We are not, however, able to cover all aspects of two-electron systems. We take responsibility for our selection, which is and must be subjective. The selection has been guided by our aim of summarizing the most relevant historical developments and providing a perspective for future research directions. Therefore we emphasize qualitative issues and only briefly summarize the progress in experimental and numerical techniques (which undoubtedly made possible the present status of our understanding) in the first part of the review.

A second general restriction refers to the regime of energy: We shall review only the quasidiscrete spectrum, i.e., true bound states and resonances. Processes at energies above the three-particle breakup threshold will not be discussed. For accounts of this energy regime we refer the reader to the work of Rau (1984), Fano and Rau (1986), Byron and Joachain (1989), and Rost (1998).

On a more technical level, we restrict ourselves to the nonrelativistic problem of an infinitely heavy nucleus and two electrons. All three particles are assumed to be pointlike. This constitutes a well-defined and widely accepted framework for studying two-electron dynamics and allows us to compare different theoretical approaches. Only for deeply bound states and large nuclear charges do these restrictions lead to inaccurate approximations. In such cases relativistic and QED effects as well as the mass polarization terms accounting for the finite mass of the nucleus must be included in the theoretical treatment for a direct comparison with high-precision experimental results. Such calculations have been carried out by Drake and co-workers (Drake, 1988; Drake *et al.*, 1993). Although we shall mostly refer to a nucleus with variable charge $Z$ and two electrons, we shall almost exclusively discuss helium $(Z=2)$ and $H^-$ $(Z=1)$. Work on atoms with two active electrons and a structured core has been recently reviewed by Aymar *et al.* (1996). A detailed account of atomic negative-ion resonances has been given by Buckman and Clark (1994). Atomic and other Coulombic three-body systems have been reviewed by Lin (1995) within the framework of the hyperspherical approach.

Only within the restrictions stated is it possible to achieve a reasonable, coherent presentation of the overwhelming number of articles in this field and of the remarkable progress made understanding two-electron atoms.

We note that, more recently, the correlation problem of few bound electrons has also become important in the context of so-called ''artificial atoms.'' Heitmann and Kotthaus (1993) provide an overview of such systems in which the electrons are confined by an electrostatic potential in semiconductor heterostructures to form ''quantum dot helium.''

### B. Content of the review

The review is structured as follows: In a first, mostly historical, part we cover early attempts to quantize helium (starting from classical mechanics) by Bohr and the leading physicists who were his contemporaries. Those attempts were ended by the early quantum-mechanical proof that helium has a stable ground state. Here, the first refined semiclassical approaches for highly excited ''planetary atoms'' will be discussed. We briefly review the progress in complementary, quantum-variational methods for the computation of two-electron states including resonances. After summarizing the numerical methods most often used today, we introduce the complex rotation method, which is one of the most powerful contemporary techniques used to compute resonances. Simultaneously we describe the state of the art concerning relevant experiments.

In the second part we focus on theoretical concepts introduced in an effort to understand the regularity in the resonance spectrum of helium: With group-theoretical methods it has been possible to identify and predict multiplets of resonances that share common properties. Here resonances play a role similar to that of particles in group-theoretical approaches in elementary-particle physics. A second successful concept is based on the introduction of adiabatic variables. In the so-called ''molecular approximation'' the interelectronic distance is treated as an adiabatic variable. This approach is very similar to the Born-Oppenheimer approximation for molecules. In a second adiabatic approach, the ''hyperspherical approximation,'' the average volume of the atom characterized by the hyperspherical radius $\mathcal{R}=\sqrt{r_1^2+r_2^2}$ is the adiabatic variable. Here the $r_i$ are the electron-nucleus vectors. Both adiabatic approximations reveal similar key features of the two-electron system that have not been recognized in other theories. Most notably the surprising regularity in the decay pattern of two-electron resonances, the so-called propensity rules, becomes transparent in the adiabatic approximation. Finally, some interesting nonmainstream concepts are dis-

cussed, in particular, the extension of the two-electron problem from three to arbitrary spatial dimensions.

In the third part of the review we discuss the renaissance of semiclassical methods. They offer a viewpoint of two-electron dynamics complementary to those discussed in the previous two parts. The broad interest in understanding the influence of classical chaos on quantum systems has led to a variety of new semiclassical techniques that are also applicable to nonintegrable dynamics, which will be reviewed here briefly.

The semiclassical methods allow for a completely new approach to two-electron atoms. Instead of trying to solve the Schrödinger equation explicitly, the focus lies now on the study of the classical three-body Coulomb problem and its influence on spectral features of the corresponding quantum system. The classical dynamics differ quite considerably in different phase-space regions and range from nearly integrable behavior to complete chaos. In particular, the collinear subspaces (in which all particles move along the same line) turn out to be of great importance for the quantum spectrum, which can be justified on semiclassical grounds.

The systematics of Rydberg resonance series can be described qualitatively by a small number of characteristic short periodic orbits in the classical three-body system. On a more sophisticated level, periodic orbit theory provides a new way to analyze the spectral density of (resonant) states by Fourier transformation. By exploiting the classical information in detail, periodic orbit trace formulas are able to resolve quantitatively individual resonances and bound states from the ground state across the various two-body fragmentation thresholds. Rydberg series converging to these thresholds can be obtained from a semiclassical quantum defect theory with purely classical coupling parameters.

The review ends with a summary and a brief look at some open questions. These mostly concern the behavior of two-electron resonances with increasing energy in the nearly unexplored energy regime close to the complete fragmentation threshold, where all three particles can be free.

## II. HELIUMLIKE SYSTEMS: FROM OLD TO MODERN QUANTUM THEORY

Two-electron atoms share the intriguing property that, despite the seemingly simple form of the underlying Hamiltonian, their spectral features get exceedingly complicated with increasing (double) excitation. For a nucleus with charge $Z$ and infinite mass, the nonrelativistic Hamiltonian reads in atomic units (a.u.) ($e=m_e=1$)

$$H=\frac{\mathbf{p}_1^2+\mathbf{p}_2^2}{2}-\frac{Z}{r_1}-\frac{Z}{r_2}+\frac{1}{r_{12}}. \tag{1}$$

Here $r_k$ ($k=1,2$) denote the electron-nucleus distances, and the distance between the electrons is $r_{12}$ (see Fig. 1). The nonintegrability of this three-body Coulomb problem gives rise to a remarkably rich behavior with respect both to its quantum features and to its classical dynamics.

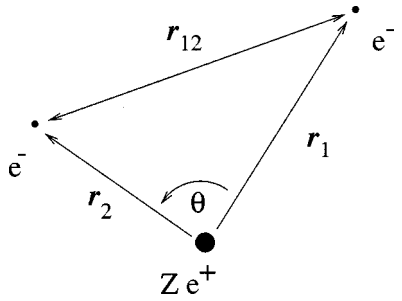


FIG. 1. The two-electron atom and its basic coordinates.

The helium atom not only represents a prototype of an atom with complex spectral structure, but also played a key role in the development of quantum mechanics until the end of the 1920s. At that time, the observation that atomic spectra display discrete levels called for a completely new type of theory—a quantum theory. The first theoretical approaches based on Bohr's quantum postulates, which were so successful in reproducing the hydrogen spectrum, failed, however, when applied to two-electron atoms; a satisfying calculation of the ground-state energy as well as of excited states of helium turned out to pose unsolvable problems to a Bohr-Sommerfeld-like quantization. This method is usually nowadays referred to as the ''old quantum theory.'' Its failure for helium led to a serious crisis of this original quantum approach to atoms, which was finally superseded by the ''new quantum theory'' formulated by Schrödinger (1926) and Heisenberg (1925). The latter formalism was first applied to the helium atom by Heisenberg (1926), taking into account wave mechanics, the electron spin, and the Pauli principle.

The two complementary pictures—the (semi)classical approach to the helium spectrum on the one hand and the wave-mechanical framework on the other hand—will guide us throughout this review, and both (after significant refinement) complement one another in the present understanding of three-body Coulomb systems. We therefore describe in the following section in some detail the early semiclassical and quantum approaches to the helium atom, mainly referring to its ground state. In Sec. II.B we then turn to doubly excited states. We summarize their basic properties and review advanced quantum-mechanical methods used today to take into account electron correlation effects. A corresponding novel approach in the spirit of the old quantum theory, a ''new old quantum theory,'' i.e., a modern semiclassical theory, which adequately describes highly (doubly) excited two-electron atoms, is presented in Sec. IV.

### A. Early calculations of two-electron ground states

#### 1. The failure of the ''old quantum theory''

It is instructive, not only from a historical point of view, to reconsider the reasons for the failure of the old

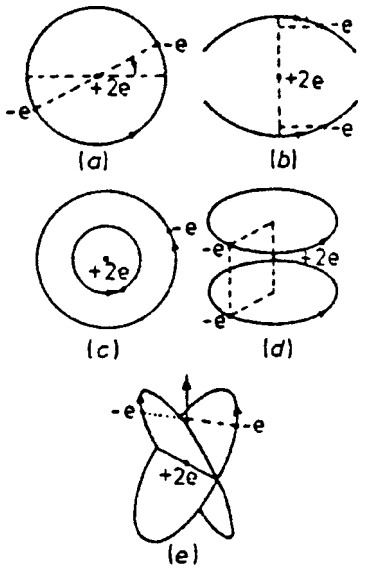


FIG. 2. Examples of periodic configurations of the electron pair in helium that served as classical models for the ground state: (a) Bohr, 1913; (b) and (d) Langmuir, 1921; (c) Landé, 1919; (e) Kemble, 1921 and Kramers, 1923 (from Leopold and Percival, 1980; see also Van Vleck, 1922).

quantum theory when applied to helium. This approach, which is more a collection of heuristic rules than a real theory, dates back to the early work on hydrogen by Bohr. Starting from his postulates on the quantization of the periodic Kepler motion, he presented a formula for the energy levels of hydrogen that showed remarkable agreement with measurements of that time. Hence it was natural to apply the same approach to helium, the simplest atom with more than one electron. In Bohr's first model of helium (Bohr, 1913) the two electrons revolve, opposite each other, on the same orbit about the nucleus as shown in Fig. 2(a). To obtain quantized energies he applied the condition

$$\oint p\, \mathrm{d}q = nh, \tag{2}$$

where $(p,q)$ are generalized coordinates and momenta of the electron pair, $h$ is Planck's constant, and $n$ is an integer. The result was discouraging: the ionization energy of the ground state was about 4 eV too high, compared with the then-experimental value of 24.5 eV.

The following ten years were characterized by a long sequence of attempts to find an appropriate classical periodic configuration for the electron-pair motion in helium and to apply quantization conditions of the type of Eq. (2). A proper computation of the helium ground-state energy became a challenge for leading theoretical physicists of that time, including Bohr, Born, Heisenberg, Kramers, Landé, Sommerfeld, and Van Vleck, to name a few.

Some of the proposed periodic orbits of paired-electron dynamics are depicted in Fig. 2. The corresponding ground-state energies obtained are summarized in Table I. (For a thorough historical account of this long and tortuous chain of work see, for example, Mehra and Rechenberg, 1982.) All models considered gave rather unsatisfactory results for the ground state of helium. For instance, in Langmuir's double-circle model, Fig. 2(d), the ionization energy came out negative, i.e.,

TABLE I. Ground-state energies (in a.u.) of the helium atom: left, semiclassical; right, quantum-mechanical and experimental. The good agreement of the energy obtained from the Heisenberg-Sommerfeld model (see Fig. 3) must be considered as accidental (see text). The given result from Solov'ev's approach was extracted from Fig. 4 of Solov'ev (1985). The asymmetric stretch orbit (Ezra *et al.*, 1991) is shown in Fig. 13(b), Sec. IV.B. The semiclassical cycle expansion is described in Sec. IV. The theoretical data do not include finite-mass, relativistic, or QED corrections, except for the result by Drake (1993), which contains relativistic effects. The difference between the latter result and the latest experimental figures (Bergeson *et al.*, 1998) reflects QED effects. Some of the data are from Leopold and Percival, 1980, Table I.

| Semiclassical | | | Quantal/Experimental | | |
|---|---|---|---|---|---|
| Year | Method | $-E$ | Year | Method | $-E$ |
| 1913 | orbit Fig. 2(a), Bohr (1913) | 3.06 | 1927 | first order pert. Unsöld (1927) | 2.75 |
| 1919 | orbit Fig. 2(c), Landé (1919) | | 1927 | molecularlike, Slater (1927) | 2.895 |
| 1921 | orbit Fig. 2(b), Langmuir (1921) | 2.17 | 1927 | variational, Kellner (1927) | 2.873 |
| 1921 | orbit Fig. 2(d), Langmuir (1921) | 2.31 | 1928 | variational, Hylleraas (1928) | 2.895 |
| 1922 | "hybrid orbit," Van Vleck (1922) | 2.765 | 1929 | var., 38 param., Hylleraas (1929) | 2.9037 |
| 1922 | orbit Fig. 3, Heisenberg (1922) | 2.904 | 1959 | var., 38 param., Kinoshita (1959) | 2.903 722 |
| 1923 | orbit Fig. 2(e), Kramers (1923) | 2.762 | 1959 | perimetric coord., Pekeris (1959) | 2.903 724 376 |
| 1980 | 1. order pert., Leopold *et al.* (1980) | 2.7410 | 1988 | Hylleraas type basis, | 2.903 724 377 |
| 1980 | variational, Leopold *et al.* (1980) | 2.8407 | | Drake (1988) | 03415 |
| 1985 | perturb. theory, Solov'ev (1985) | 3.05 | 1995 | perimetric coordinates, | 2.903 724 377 |
| 1991 | as. stretch orbit, Ezra *et al.* (1991) | 3.097 | | Bürgers *et al.* (1995) | 034 119 589 |
| 1991 | cycle expansion, Ezra *et al.* (1991) | 2.932 | 1993 | relativ. Drake (1993) | 2.903 700 023 |
| | | | 1924 | experimental, Lyman (1924) | 2.9035 |
| | | | 1998 | exp., Bergeson *et al.* (1998) | 2.903 693 775 |

the configuration was unstable. The approaches based on models (a)–(d) in Fig. 2 were critically summarized by Van Vleck (1922), who added another, no more successful, three-dimensional model (not shown) that can be viewed as a hybrid of configurations (b) and (d).

The failure of these early quantum approaches for helium was accompanied by a very unsatisfactory result obtained by Pauli (1922) in his Ph.D. thesis on another three-body Coulomb system, namely, the hydrogen molecule ion $H_2^+$: within the Born-Oppenheimer approximation, this system is reduced to the (separable) problem of an electron moving in the field of two fixed Coulomb centers. By using a Bohr-Sommerfeld quantization condition he calculated the equilibrium internuclear distance to be nearly three times as large as the correct one ($\sim$2 a.u.). Moreover, he found the system to be metastable instead of being bound.

The approaches to a description of the helium atom as presented above included all the principal problems of the old quantum theory: the calculations were based only on a number of *ad hoc* rules and postulates that were open for speculation. A rigorous theoretical framework, which could have been used as a guideline, was missing. Before presenting the principal shortcomings of this theory, it is worth mentioning some of the common beliefs at that time. They led to the models for periodic electron-pair motion shown in Fig. 2 and hindered a more rapid understanding of the helium problem. It was generally assumed that

(i) the ground state of helium was related to a single periodic orbit of the electron pair;

(ii) the electrons were supposed to move on symmetric orbits in which their distance to the nucleus was equal at each instant;

(iii) orbits in which the electrons hit the nucleus (''Pendelbahnen,'' Born, 1925) were excluded;

(iv) the quantum numbers in quantization conditions like Eq. (2) were supposed to be integers.

Two who did not take these assumptions for granted were Sommerfeld and his student Heisenberg. Although he was mainly involved in problems of turbulence at that time, Heisenberg's interest in the helium problem was stimulated by Bohr in 1922. Sommerfeld and Heisenberg devised as a possible classical ground-state configuration a model in which the electrons move on two different Kepler ellipses of the same shape but oriented in opposite directions: one electron passes through the perihelion while the second is at its aphelion. Figure 3 shows this configuration sketched by Heisenberg in a letter to Sommerfeld on October 1922 (Heisenberg, 1922; the role of Heisenberg at this stage of the ''old quantum theory'' is also described by Cassidy, 1995). In his letter, Heisenberg outlined a calculation of the ground-state energy on the basis of this electron-pair motion. As an important achievement from today's point of view, he introduced, in addition to the quantization of the radial motion, a second quantization condition (Heisenberg, 1922),

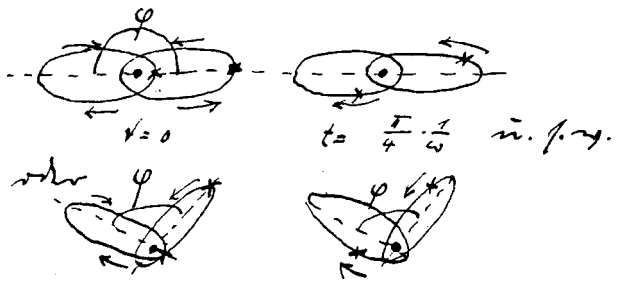


FIG. 3. Sketch of the periodic electron-pair motion proposed by Heisenberg and Sommerfeld as a candidate for a classical ground-state configuration of helium. The figure is copied from a letter of Heisenberg to Sommerfeld (Heisenberg, 1922). It was never published by Heisenberg.

$$\oint p_\varphi \mathrm{d}\varphi = n_\varphi h, \tag{3}$$

for the motion of the angle $\varphi$ between the major axes of the two orbits under the influence of the mutual electron interaction (see Fig. 3). Moreover, he introduced *half integer* quantum numbers, e.g., $n_\varphi = 1/2$ for the ground state. Including the interaction in a perturbative manner, Heisenberg arrived at an ionization potential of 24.6 V, compared to the best experimental value of 24.5 V at that time. However, this approach was strongly criticized by Pauli and Bohr. They did not accept the concept of noninteger quantum numbers, but thought at that time that the classical laws of motion had to be modified in order to achieve agreement with experiment. Heisenberg, discouraged by Bohr, never published his calculations, which may explain why the Heisenberg-Sommerfeld model, to the best of our knowledge, has never been mentioned in the atomic physics literature. Contrary to Bohr, Sommerfeld, encouraged by the results obtained by Heisenberg, wrote a paper (Sommerfeld, 1923), referring to Heisenberg's perturbative results, in which he suggested the underlying model of opposite electrons and half-integer quantum numbers as a possible classical ground-state configuration.

Heisenberg, together with Born, went ahead and started to attack the more ambitious problem of excited states in helium. They considered different types of asymmetric electron configurations and developed an effective Hamiltonian based on a multipole expansion scheme for the potential of the outer electron in the combined field of the nucleus and the inner electron. By that means they derived a Rydberg formula,

$$H = \frac{(Z-1)^2}{(n+\delta)^2}, \tag{4}$$

where $n$ is the principal quantum number of the outer electron. The quantum defect $\delta$ reflects non-Coulombic, short-ranged parts of the central potential and depends on the remaining quantum numbers and the configuration considered (Born and Heisenberg, 1923). However, the obtained energies of the excited states were unsatisfying and led Heisenberg and Born to the conclusion that ''the result of our investigation is completely nega-

tive'' (Born and Heisenberg, 1923).[1] For that reason Heisenberg also lost all confidence in his original ground-state calculations. From then on he no longer followed the ideas of the old quantum mechanics but started to devise his ''new'' quantum theory based on conceptually new postulates.

The good agreement between the result of Heisenberg's first perturbative calculations of the helium ground-state energy (see Table I) mentioned above and the experimental values must be considered as accidental: Heisenberg's perturbative scheme was not appropriate for the case of degenerate classical motion of two electrons[2] and he did not know the role of Maslov indices (see Sec. IV.A) in quantization conditions. However, from today's point of view, the great virtue of the Heisenberg-Sommerfeld model for the helium ground state lies in two facts:

(i) The electrons move out of phase on perturbed Kepler ellipses opposite each other. This type of classical motion comes rather close to the asymmetric stretch periodic orbit, a collinear out-of-phase motion of the electrons on opposite sides of the nucleus discussed in Sec. IV.B.2. This kind of electron-pair motion turned out to be crucial for the structure of ground and symmetrically excited states (Ezra *et al.*, 1991; Wintgen *et al.*, 1992), as described in detail in Secs. IV.C and IV.D.[3]

(ii) Heisenberg introduced *ad hoc* half integer quantum numbers, which simulate the effect of Maslov indices.

Due to these two facts the Heisenberg-Sommerfeld model and the related quantization condition (3) can be regarded as coming closest to a correct semiclassical description of the helium ground state compared to all other models employed in the old quantum theory. We note, however, that in a rigorous semiclassical treatment the ground state is more precisely represented by a whole number of periodic orbits, as will be discussed in Secs. IV.A and IV.D.2.

The pessimistic mood in the early 1920s concerning a semiclassical treatment of two-electron atoms becomes apparent in a conclusion given by Van Vleck (1922):

> The conventional quantum theory of atomic structure does not appear to be able to account for the properties of even such a simple element as helium, and to escape from this dilemma some radical modification in the ordinary conceptions of the quantum theory or of the electron may be necessary. [p. 842]

The same negative point of view is expressed in the *Vorlesungen über Atommechanik* (*Lectures on the Mechanics of the Atom*) by Born (1925). These conclusions, which mark the end of the old quantum theory, address the need for a completely different approach, namely quantum wave mechanics. The essential shortcomings of the old quantum theory can be summarized as follows:

(i) The role of conjugate points along classical trajectories and their importance in a semiclassical approach to quantum states (via Maslov indices) were not properly accounted for.

(ii) The precise role of periodic orbits and their stability for systems with nonintegrable or even chaotic classical dynamics was unknown.

The failure of the old methods on the one hand and the success of the new quantum theory on the other hand influenced subsequent research for several decades. Still, in 1941, the helium problem was considered as ''raising unsolvable problems'' (Bachelard, 1941). We are not aware of any serious and successful attempts to attack the problem using a semiclassical framework until the 1980s.

For the separable $H_2^+$ problem only item (i) had to be accounted for. Strand and Reinhardt (1979) employed an Einstein-Brillouin-Keller quantization procedure for $H_2^+$ (see Keller, 1958; Gutzwiller, 1990), combined with a uniform treatment at potential barrier maxima. They obtained agreement with quantum results to within a fraction of a percent. As already pointed out by Einstein (1917), such a quantization scheme, based on the existence of invariant tori, cannot be applied to nonintegrable systems. It is therefore not an appropriate framework for the description of the helium atom.

Leopold and Percival (1980) and Solov'ev (1985) attacked the helium problem using improved variational and perturbative semiclassical methods, respectively. Although these approaches ignore item (ii) they represent important steps towards a rigorous semiclassical treatment of two-electron atoms. Thus they will be briefly reviewed in the following subsection before we turn to quantum approaches for two-electron atoms.

### 2. Semiclassical perturbative and variational approaches

#### *a. Planetary atoms*

More than 50 years after the first attempts to treat helium, Percival and co-workers were the first to reconsider the helium problem from the point of view of the old quantum theory (Leopold *et al.*, 1980; Leopold and Percival, 1980). Percival had pointed out that in highly (doubly) excited atoms the electrons should carry features of classically moving particles. He thus coined the term *planetary atoms* for these systems (Percival, 1977) due to their similarity to the gravitational three-body problem.[4] This picture is physically appealing, although one should keep in mind that a direct transfer of results

[1] Heisenberg's and Born's calculations of asymmetrically excited states are based on schemes that were later reconsidered by different authors (e.g., Nikitin and Ostrovskii, 1982; Belov and Khveshchenko, 1985).

[2] An appropriate semiclassical perturbative treatment was later performed by Solov'ev (1985), which will be briefly discussed in Sec. II.A.2.

[3] A periodic orbit of the Heisenberg-Sommerfeld type (Fig. 3) does not really exist as a solution of the classical Hamilton function, but only as a quasiperiodic motion of that type, shown in Fig. 4.

[4] For a recent review of a celestial three-body problem, see Gutzwiller (1998) on the three-body system moon-earth-sun.

from the celestial to the atomic three-body problem is generally not possible for two reasons: First, in gravitational three-body systems, the masses of the three bodies involved usually differ by orders of magnitude. This often allows for a perturbative treatment since the gravitational interaction depends on the masses (Arnold, 1991). The mutual Coulomb interactions in two-electron atoms are, on the other hand, of the same magnitude, and perturbation theory is therefore not *a priori* applicable. Second, gravitational forces are always attractive, while the repulsive Coulomb interaction between electrons usually leads to a destabilization of the two-electron atom. Depending on the initial conditions, the *classical* two-electron atom generally autoionizes after a few revolutions of the electrons around the nucleus. For a typical example of such a classical autoionizing configuration of equally excited electrons see Fig. 4. The classical two-electron atom is thus an unbound system at all energies. Quantum mechanically, the electrons cannot exchange an arbitrary amount of energy since the (remaining) $He^+$ ion has a minimum ground-state energy. This allows for the existence of quantum bound states.


FIG. 4. Typical classical out-of-phase motion of the electron pair in helium obtained from a numerical integration of the full Hamilton equations of motion. The electrons evolve on perturbed Kepler ellipses around the nucleus until they autoionize after a few revolutions (from Richter, 1991).

#### *b. Percival's and Solov'ev's treatments*

Leopold and Percival (1980) could improve upon the results of the old quantum theory by introducing a variational semiclassical approach and, in particular, by pointing out the relevance of a correct inclusion of Maslov indices, which lead to noninteger quantum numbers. They showed that the ideas of the old quantum theory were not intrinsically wrong. Moreover, they argued that semiclassical techniques should be powerful in dealing with highly doubly excited states in which quantum approaches become increasingly involved. Their work thus redirected attention to semiclassical approaches for two-electron systems.

In a first paper, Leopold *et al.* (1980) used a first-order perturbative semiclassical scheme. In zero order, electron-electron interaction is neglected and the dynamics are integrable. The electrons evolve on tori and their motion can be described in terms of the respective action variables $\mathbf{I}=(I_r,I_\theta,I_\phi)$ where $(r,\theta,\phi)$ represent the usual spherical coordinates. According to the Einstein-Brillouin-Keller quantization, the quantal states of the two unperturbed electrons ($k=1,2$) in helium correspond to those tori whose actions fulfill

$$I_{n_k}=n_k\hbar; \quad I_{l_k}=\left(l_k+\frac{1}{2}\right)\hbar; \quad I_{m_k}=m_k\hbar, \tag{5}$$

with the corresponding quantum numbers $n_k,l_k,m_k$ and actions $I_n=I_r+I_\theta+I_\phi$; $I_l = I_\theta + I_\phi$ and $I_m=I_\phi$ (Goldstein, 1980).

First-order perturbative corrections to the independent electron energies were computed by taking the average $\langle 1/r_{12}\rangle$ over the six angle variables corresponding to the actions $I_{n_k},I_{l_k},I_{m_k}$. The resulting electron model obtained by Leopold *et al.* (1980) for the ground state is close to configuration (e) in Fig. 2. The ionization potential is still about 4 eV lower than the experimental value (see Table I).

In a second paper, Leopold and Percival (1980) introduced a semiclassical variational treatment of the ground state and excited states of helium, which turns out to be superior to perturbative methods. They found for the ground-state energy $E=-2.8407$ a.u., compared to the exact energy $E=-2.9037$ a.u. (see Table I).

In this context, a related semiclassical approach by Solov'ev (1985) should be mentioned, which, in our opinion, has not received the attention it deserves. Solov'ev argued that the unperturbed angular momentum eigenstates (or corresponding tori) used in the approach of Leopold *et al.* (1980) are inadequate as zero-order reference states in a first-order perturbative treatment of the helium ground state and of symmetrically excited states. The degeneracy in energy of these states, classically related to the commensurate periods of the motion along Kepler trajectories, has to be accounted for in an appropriate perturbation theory.

Solov'ev starts from a configuration of two equivalent electrons moving out of phase on Kepler-like orbits similar to those shown in Fig. 4. As suitable coordinates he introduces, besides the single-electron Kepler motion, the angle between the major axes of the two Kepler ellipses and the time difference between the passage of the first and second electron through the perihelion. Solov'ev achieves an adiabatic separation of the corresponding frequency scales and thereby a decomposition of the full problem into oscillatory motions in one-dimensional effective potentials which can be semiclassically quantized. This method, which is particularly well suited to a description of highly symmetrically excited states, also gives a reasonable estimate, $E\approx -3.05$ a.u., for the helium ground state.

#### *c. Discussion and summary of further approaches*

It is by now well known (Richter and Wintgen, 1990a; Ezra *et al.*, 1991; Wintgen *et al.*, 1992) that a considerable part of helium phase space is classically chaotic. Hence an Einstein-Brillouin-Keller approximation based on classical tori, as performed by Leopold *et al.* (1980), is in principle not adequate for a description of the full problem. The same is true of Solov'ev's treatment applied to helium, since it assumes an effective decoupling of the different degrees of freedom.

We close this section by noting that the collinear configuration of two electrons on opposite sides of the

nucleus but moving symmetrically in phase ($r_1=r_2$), known as the Wannier orbit, has frequently been proposed in the literature as relevant for symmetrically doubly excited states (Miller, 1972; Fano, 1983; Harris *et al.*, 1990a; 1990b; Sadeghpour, 1991). This type of motion and its importance for doubly excited states is critically reviewed in Sec. IV.

The periodic orbit originally proposed by Langmuir for the helium ground state [orbit (b) in Fig. 2] was reexamined by Dimitrijević and Grujić (1984) and Wesenberg *et al.* (1985). However, the latter authors overlooked the fact that the Langmuir orbit is indeed stable (Richter and Wintgen, 1990a), a fact that was not accounted for in their Einstein-Brillouin-Keller-type quantization. Finally, Klar (1986) reconsidered the Langmuir double-circle model [Fig. 2(d)] and showed that it is classically stable.

We end the historical review of semiclassical approaches to two-electron atoms here in the mid 1980s. We shall return to semiclassical concepts in Sec. IV. There we review more recent advances in modern semiclassical theory and apply it to two-electron atoms, taking into account that the corresponding classical system is chaotic. In particular, a generalized Einstein-Brillouin-Keller scheme for excited states will be derived that leads in a natural way to the structure of perturbed Rydberg series and quantum defects. In the following, we shall summarize related pure quantum-mechanical techniques to solve the Schrödinger equation directly.

#### 3. Wave-mechanical perturbative and variational results

It is helpful to contrast the semiclassical perturbative and variational techniques with the corresponding early quantum-mechanical methods. After Heisenberg's first application of the new quantum theory to the helium problem (Heisenberg, 1926), the quantum-mechanically calculated ground-state energy of helium was rapidly improved in a number of publications in the late twenties. The ground-state energies obtained are summarized in Table I. Unsöld (1927), using first-order quantum perturbation theory, obtained an energy with still a rather large error. Slater (1927) treated helium by reducing it to the "molecular" problem of one electron in the presence of two fixed Coulomb centers of charge $-e$ and $Ze$, representing the nucleus and the second electron. (Similar molecular models were later employed to describe doubly excited states of two-electron atoms; see Secs. III.B.1 and III.B.4.)

Quantum-variational methods have proven most suitable for obtaining precise results for the ground state or low-lying states of two-electron atoms and are superior to perturbative methods. As a very simple trial wave function for a variational calculation of the ground state one may use $\psi(r_1,r_2,r_{12})=\exp[-(Z-\sigma)(r_1+r_2)]$, where $\sigma$ represents screening in a rather approximate way. Minimizing the energy functional gives $E=-(Z-5/16)^2$, i.e., $E=-2.85$ a.u. for the helium ground state (Bethe and Salpeter, 1977). However, for the case of $H^-$ this ansatz does not lead to a bounded ground state.

Kellner (1927) was the first to use the Ritz variational principle and obtained a rather precise ground-state energy, $E=-2.895$ a.u.

His results were improved upon by the variational calculations of Hylleraas (1928, 1929), who finally obtained $E=-2.9037$ a.u. using a trial wave function with 38 variational parameters. This method was again taken up using large-scale variational calculations by Kinoshita (1959); see Table I.

First-order perturbation theory is also significantly improved upon by Hartree's method (see Bethe and Salpeter, 1977). It turns out that Hartree-type wave functions are convenient and sufficient approximations to the ground state for many applications in which electron correlation effects need not be considered.

For a comprehensive and more detailed discussion of the different methods used to obtain low-lying states of two-electron atoms see, for example, Bethe and Salpeter (1977). A recent overview of ground-state energies in general Coulombic three-body systems, including exotic two-electron atoms, is given by Lin (1995). Most accurate ground-state energies are nowadays achieved by diagonalization of the two-electron Hamiltonian matrix, Eq. (1), using large basis sets (see Table I for the case of He). These methods, which were introduced by Pekeris (1958, 1959) in his pioneering calculation of the helium ground state (see Table I), will be presented in Sec. II.C.2.

### B. Doubly excited states: Basic spectral structure and experimental developments

Since the famous experiment of Madden and Codling (1963) showed that doubly excited states of two-electron atoms represent the paradigm for electron correlations in atomic systems, these states have attracted the continuous interest of both theoreticians and experimentalists. We shall approach these correlation effects stepwise: in this section we give a preliminary overview of excited states of helium and $H^-$. Starting from singly excited states, we introduce doubly excited resonances on the traditional level of single-particle quantum numbers. We then review in Secs. II.B.2–II.B.4 progress in the understanding of doubly excited states from the experimental side by pointing out some of the key experiments, which represent the variety of techniques used and the advances in spectroscopic precision. Experimental results such as those of Madden and Codling were incompatible with classification schemes based on the picture of two independent electrons and have prompted much theoretical work. In Secs. II.C.1 and II.C.2, we summarize related computational advances and outline numerical techniques used at present for accurate quantum-mechanical calculations of highly doubly excited states. Both the numerical and the experimental facts provided here will act as starting and reference points for the physical pictures, classification schemes, and approximate methods that represent our

understanding of correlation effects in doubly excited atoms up to the present day. They will be developed in detail in Secs. III and IV.

### 1. Basic spectral properties

The last section dealt exclusively with the computations of two-electron ground states, the main issue of early quantum theory. The question naturally arises of how to characterize and calculate singly and doubly excited states. Certain exact symmetries of the three-body Coulomb problem allow, at least partly, for a classification of these quantum states. The overall rotational symmetry, related to conservation of the total angular momentum $\mathbf{L}$ and its projection, give rise to $L$ and $M$ as good quantum numbers. The quantum numbers of the total spin $S$ and its $z$ component are linked to electron exchange $\mathbf{r}_1 \leftrightarrow \mathbf{r}_2$ through the antisymmetry of the total wave function. This leads to the distinction between singlet ($S=0$) and triplet ($S=1$) states. Furthermore, reflection symmetry infers that the wave functions of the electron pair are eigenfunctions of the parity operator $P$: $\mathbf{r}_1, \mathbf{r}_2 \rightarrow -\mathbf{r}_1, -\mathbf{r}_2$ with eigenvalue $\pi$ describing even and odd states. These properties lead to the usual spectroscopic notation ${}^{2S+1}L^{\pi}$ (assuming $LS$ coupling).

It may appear appealing to treat two-electron atoms analogously to many-electron systems, in a mean-field approach, possibly in a self-consistent way. As a result, the two electrons both evolve in an effective central potential that suggests their classification in terms of the usual hydrogenic principal quantum numbers $N,n$ and angular momentum quantum numbers $l_1, l_2$. In such a conventional description, (excited) states, e.g., in helium, are organized in Rydberg series $(N, l_1; n \rightarrow \infty, l_2)$, which converge to one-particle fragmentation thresholds, $I_N$, of the remaining $He^+(N)$ ion. Here $N$ stands for the principal quantum number of the inner electron. This model, being based on the individual quantum numbers, neglects electronic correlations completely but accounts at least qualitatively for certain general features of two-electron states.

In the following, we shall mainly use helium to illustrate the general spectral characteristics emerging from the above model as well as its considerable deficiencies. Figure 5 shows the ${}^1S^e$-level diagram of helium as an example of a spectrum of doubly excited resonant states. The resonance energies shown were numerically computed by complex rotation (see Sec. II.C.2). Roughly, the helium spectrum can be divided into three distinct parts: (i) the ground and singly excited bound states, (ii) doubly excited resonant states, and (iii) the continuum above the three-particle breakup threshold, 79 eV (or 2.9037 a.u.) above the ground-state energy.

(i) For the discrete singly excited states ($N=1; n=1,\ldots,\infty$), singlet $({}^1S, {}^1P, {}^1D, \ldots)$ and triplet $({}^3S, {}^3P, {}^3D, \ldots)$ configurations are usually distinguished. States of the two subsystems with the same principal quantum numbers differ significantly in their quantum defects. Triplet levels lie noticeably higher in energy. This, and the fact that singlet and triplet states do not combine optically with each other, led early investigators to think of two different kinds of helium, parahelium ($S=0$) and orthohelium ($S=1$) (Bethe and Salpeter, 1977). Singly excited states converge to the first ionization threshold $I_1$, which lies at $-Z^2/2$ a.u. This corresponds to an ionization energy of ~24.58 eV for helium.

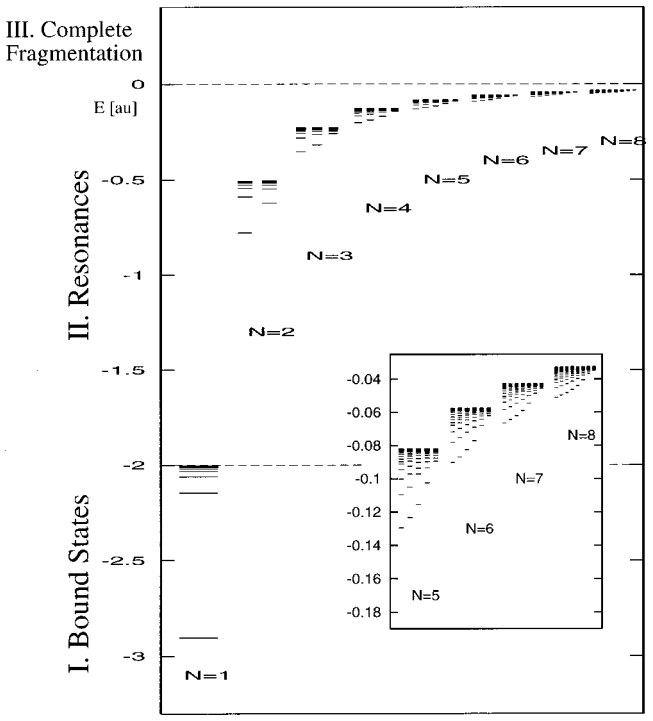


FIG. 5. Level diagram of the ${}^1S^e$ states of helium from the ground state to the $N=8$ resonance series close to the three-particle breakup threshold. There are $N$ Rydberg series converging to each ionization threshold $I_N$. The inset shows the $N=5-8$ levels on an enlarged scale.

(ii) Helium doubly excited states form a doubly infinite (in $N$ and $n$) sequence of levels lying above the first ionization threshold. Their (perturbed) Rydberg series converge to ionization thresholds $I_N$ at energies $-Z^2/(2N^2)$ (in a.u.), which are characterized by the excited state $N$ of the remaining inner electron. For example, for ${}^1S^e$ states (Fig. 5) there are $N$ different Rydberg series converging to each $I_N$.

Doubly excited states are embedded in the continua above the fragmentation thresholds of energetically lower Rydberg series. Hence they form resonances that can decay by autoionization, due to the electron-electron interaction, via coupling to the continua. This distinguishes them qualitatively from the stable singly excited states in which the inner electron, in its ground state, cannot further transfer energy to ionize the outer one. This picture of singly and doubly excited states and their difference is purely quantum mechanical and does not exist for classical two-electron atoms (see Sec. IV.B.)

(iii) The three-body dynamics in the energy regime above the three-particle breakup threshold $E=0$ have been probed by photo double ionization and collision

experiments. Theoretical descriptions of electron-impact ionization, often called $(e,2e)$ reactions, are reviewed by, for example, Byron and Joachim (1989). In particular, the region close to the threshold has been studied extensively. In this region the energy dependence of the total cross section for three-particle breakup is strongly influenced by electron-electron correlation leading to the famous Wannier threshold law (Wannier, 1953). The physics in this energy region is beyond the scope of this review; see Rau (1984) and Rost (1998) for extensive discussions.

The experiment of Madden and Codling (1963) revealed that the simple model of independent-particle angular momentum quantum numbers $l_1,l_2$ mentioned above proves inappropriate to characterize a series of doubly excited states if the electrons can occupy a number of quasidegenerate (individual electron) configurations. Depending on the degree of excitation, these configurations can be strongly mixed through the electron-electron interaction, so that there remains no dominant independent-particle configuration $(l_1,l_2)$ that could be assigned to a given resonance. In helium or $H^-$ this mixing of independent-particle states is particularly pronounced since, due to the absence of a core, each electron-nucleus subsystem possesses the high hydrogenic degeneracy of the energy levels (Eichmann *et al.*, 1990). Hence, in such doubly excited atoms, independent-particle states are fragile and correlation effects should be strongest. Instead of using $(l_1,l_2)$, it is more appropriate to label the different Rydberg series converging to the same ionization threshold $I_N$ by a Stark-type quantum number $K$, which for $^1S$ states runs from $K=-N+1,-N+3$, to, $N-3,N-1$ (see Sec. III).

Approximate quantum numbers can be uniquely assigned for energies in which Rydberg series, converging to different ionization thresholds, do not overlap. Figure 5 shows that Rydberg series converging to different $I_N$ start to overlap for $N\geq 4$. The mutual interaction of the Rydberg series in the energy regime shown in Fig. 5 can still be treated within quantum defect theory (Seaton, 1983); see, for example, Domke *et al.* (1991, 1995). This is only possible for moderate $N$, where individual perturbers can still be identified. However, the assignment of quantum numbers becomes increasingly difficult when more than two series of different $N$ overlap (Bürgers *et al.*, 1995). The number of resonance series that interact simultaneously increases further with $N$, which renders the conventional description schemes almost impossible. This regime close to $E=0$, which is characterized by a large number of strongly overlapping resonances, is far from being understood and is becoming a focus of current research activities.

Before we enter into the theory for correlated doubly excited states we review the related experimental observations.

### 2. Early experimental observation of electronic correlations

After the ground state and singly excited states of two- and more-electron atoms were fairly well understood, theoretical surprises from doubly excited states were not expected. Apart from the regime close to the double ionization threshold, where an increasing number of Rydberg series starts to overlap and to interact, the spectral structure in the energy regime of isolated, nonoverlapping Rydberg series in Fig. 5 may suggest that the related doubly excited states behave similar to singly excited states. Hence an improvement of the simple independent particle model introduced above along the lines of a Hartree-Fock description, which had proven very successful for multielectron atoms, was appealing. Such an approach implies that two-electron states are more or less products of single-particle configurations. Given the helium ground state as a dominant $1s^2$ configuration, the lowest doubly excited states were therefore expected to be roughly $2s^2,2s2p,2snp$ states and so on.

Although the existence of doubly excited resonant states has been known for about 60 years, the primary role of correlations in forming collective states of the electron pair became suddenly evident with the key experiment of Madden and Codling in 1963. This revealed dramatic deviations from the expectations of Hartree-Fock-like models. Using synchrotron radiation and recording the absorption spectrum of helium, they could observe a series of $^1P^o$ states converging to the $N=2$ ionization threshold. $^1P^o$ states are strongly favored due to dipole selection rules when probing the helium ground state $^1S^e$ by photo excitation. Within the independent-particle picture three series were expected: $2snp$, $2pns$, and $2pnd$. Instead, Madden and Codling observed one dominant, intense series. A second very faint series could only be guessed and the third series was not detected. The difference in the intensities was a clear indication that the electron-electron interaction leads to so far unknown selection or propensity rules for radiative excitation. Moreover, the position of the resonances in the strong and weak series did not match any of the expected combinations $2s2p,2p2s$.

In an early theoretical interpretation of the experimental findings, Cooper *et al.* (1963) proposed as explanation a strong configuration mixing of the $^1P^o(2l_12l_2)$ states due to their perfect degeneracy in the limit of vanishing electron interaction. For reasons of exchange symmetry, they suggested using combinations of the sum $(+)$ and the difference $(-)$ of the atomic product wave functions of the $2snp$ and $2pns$ states as an appropriate basis. Corresponding calculations showed that these linear combinations indeed shifted the resonance positions towards the experimentally observed ones. This led to the original classification of these doubly excited states as $+$ and $-$ series. The $+$ labels were assigned to states of the intense series. The observed linewidths, a measure of the autoionization rates, were reflected in the photoionization yield: intense lines exhibit large widths.

It took more than 20 years of research before the early description of doubly excited atomic states could be backed by a systematic treatment and consistent un-

derstanding of the astonishing symmetries of two-electron atoms. The corresponding approaches will be discussed in Sec. III.

### 3. Overview of modern spectroscopic techniques

Until about ten years ago, the existing spectroscopic data for doubly excited two-electron atoms lagged considerably behind theoretical results. This was mainly due to the fact that appropriate monochromatic light sources, suitable for high-resolution spectroscopy, were missing. Such sources could bridge the rather large energy gap between the ground state and doubly excited states: in the case of helium, the doubly excited $^1P^o$ resonances lie approximately between 60 and 79 eV above the ground state. This problem was tackled experimentally along two main routes, either by direct double excitation using synchrotron radiation (see Sec. II.B.3.a) or by studying doubly excited alkaline-earth atoms with conventional dye lasers operating in the optical regime (see Sec. II.B.3.b). Further experimental efforts, partly based on nonphotonic double excitation, will be summarized in Sec. II.B.4.

#### *a. Double excitation of helium using synchrotron radiation*

Until 1990, reliable measurements of resonant states in helium were limited to the $N=2$ Rydberg series (Madden and Codling, 1963; Morgan and Ederer, 1984; Kossmann *et al.*, 1988) and to the lowest states of higher Rydberg series (Woodruff and Samson, 1982; Kossmann *et al.*, 1988; Zubek *et al.*, 1989). More recently, the development of high-resolution monochromators for synchrotron radiation has led to a striking improvement in the precision of photo cross sections, which will be discussed below. Complementary experiments based on emission spectroscopy even achieved the observation of *partial* decay widths. Due to the dipole selection rule for the single-photon process from the $^1S^e$ ground state, only final doubly excited states of $^1P^o$ symmetry can be detected with this technique. This restriction, however, facilitates identification of the resonances.

Single-photon double excitation with synchrotron radiation, combined with high-resolution monochromators such as those at BESSY, Berlin (Domke *et al.*, 1991, 1992, 1995, 1996), and even further improved monochromators at the Advanced Light Source in Berkeley (Schulz *et al.*, 1996) made it possible to reveal for the first time several additional Rydberg series. Moreover, each Rydberg series could be followed up to higher excited states of the outer electron. In an experimental breakthrough, Domke *et al.* (1992) resolved for the first time the third Rydberg series, $2pnd$, below the $N=2$ ionization threshold. This series had been "missing" since the observation of the famous principal $(sp,2n+)$ and secondary $(sp,2n-)$ resonances by Madden and Codling (1963).

The latest experiments on doubly excited helium using synchrotron radiation at the Advanced Light Source with further increased photon flux and a resolution of 1 meV (Schulz *et al.*, 1996) were able to measure all three series converging to the $N=2$ threshold with improved precision. The spectra of the three series of autoionizing states are shown in Fig. 6, which illustrates the experimental progress since the early measurements of Madden and Codling. The most intense (principal, or $+$) series appears in panel (a) as a pure sequence of pronounced Beutler-Fano profiles (Fano, 1961). It is resolved up to $n=26$. The first secondary $(-)$ series in Fig. 6(b), which is visible in panel (a) as a sequence of tiny peaks, is roughly 100 times less intense than the $+$ series. It is convenient to label the different series converging to the same threshold by the (Stark-type) quantum numbers $K$. This assignment, which is due to Herrick (1983), will not be justifed at this stage. (See Sec. III.C for details, including the introduction of a further quantum number, $T$.) The differences in the observed intensities will be explained in Sec. III.B.3.a; see also Fig. 10 below. The three observed series in Figs. 6(a)–(c) can then be classified according to $(N,K)_n$ with $K=0$, 1, and $-1$, respectively.

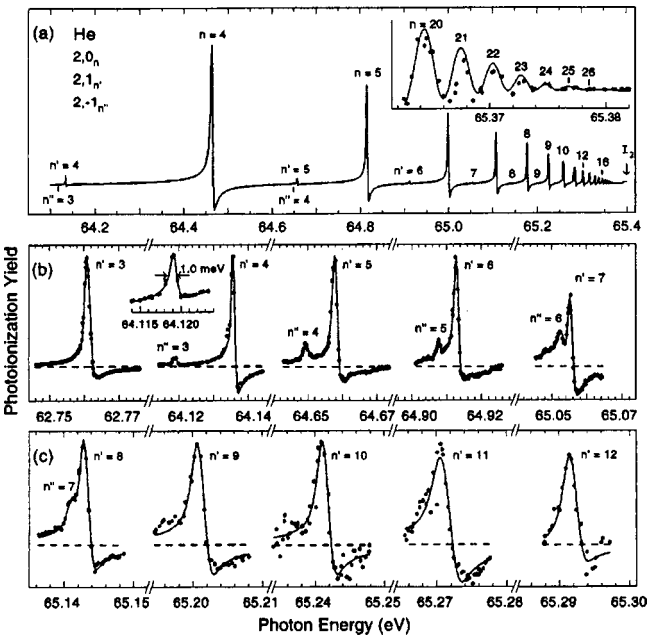


FIG. 6. Observed spectra of autoionizing resonances in helium after double excitation through synchrotron radiation. Panel (a) shows an overview spectrum of all three $^1P^o$ resonance series below the $N=2$ ionization threshold $I_2$, with the dominant, classic Beutler-Fano profiles of the intense principal series discovered by Madden and Codling (1963). Panels (b) and (c) depict the secondary series $(N,K)_n=(2,1)_{n'}$ and $(2,-1)_{n''}$; see Sec. III.C for the notation (from Schulz *et al.*, 1996).

Besides being able to investigate in detail doubly excited states below the $I_2$ threshold, Domke *et al.* (1996) were able to observe members of all the strongest (principal) Rydberg series up to the $N=9$ ionization threshold as well as further secondary series with relatively weak intensities. The interesting regime of strongly overlapping and interacting Rydberg series is thus accessible today.

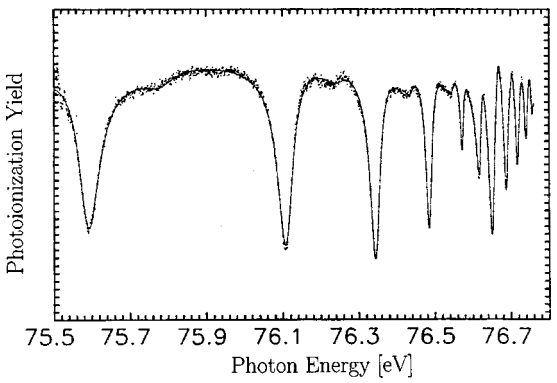


FIG. 7. Double excitation resonances $^1P^o$ of He in an energy regime below the $N=5$ threshold. The dots denote experimental photoabsorption cross sections from the helium ground state using synchrotron radiation (Domke *et al.*, 1996). The solid line shows the theoretical prediction based on complex rotation (see Sec. II.C.2) by Wintgen (1994). The strong dips represent the principal Rydberg series with approximate quantum numbers $n=5,\ldots,14$ of the outer electron. The irregular structure at $\sim 76.7$ eV is due to interference of the $N=5$ series with the lowest state in the $N=6$ series.

Figure 7 shows as an example highly doubly excited resonances of helium in an energy region below the $N=5$ threshold, in order to illustrate the recent experimental achievements and to compare them with theoretical results. The dots mark measured cross sections (Domke *et al.*, 1995). The solid line is *not* a fit but the numerical result from a complex rotation calculation (see Sec. II.C.2) by Wintgen (1994). The pronounced resonances are related to the principal ($K=3$ in Herrick's classification) Rydberg series with ($N=5$, $n=5,\ldots,14$). The tiny dips visible in between the pronounced states $n=5,\ldots,9$ reflect the lowest states of a secondary Rydberg series $(N,K)_n=(5,1)_n$. Similar agreement between theory and experiment has been obtained by hyperspherical close-coupling calculations (Tang and Shimamura, 1994; see Sec. II.C.1).

The high-resolution experiments of Schulz *et al.* (1996) allowed for the first time observation of the secondary series $(N,K)_n=(3,2)_n$ and $(3,0)_n$. Recent comprehensive accounts of these fascinating experimental developments can be found in Domke *et al.* (1996) and Rost *et al.* (1997). They also include detailed comparisons between experiment and theory with respect to quantum defects, resonance widths, oscillator strengths, and shape parameters.

The photoabsorption experiments described above have been recently complemented by electron emission measurements of partial photoionization cross sections and photoelectron angular distributions of helium in the energy region up to the $I_5$ threshold (Menzel *et al.*, 1995, 1996). These experiments also use the Advanced Light Source to study the resonant photoionization process $\mathrm{He}(1s^2)+h\nu\rightarrow\mathrm{He}^*(N,K_n)\rightarrow\mathrm{He}^+(j)+e^-$. The photoelectron is detected, which makes possible the determination of the corresponding photoelectron angular distribution parameters $\beta_j$ (Menzel *et al.*, 1995). The energy dependence of the related partial cross section $\sigma_j$ is obtained by scanning simultaneously the incident photon energy and the pass energy of the analyzers of the emitted electron. A thorough investigation of partial cross sections and angular distributions is given by Menzel *et al.* (1996) for a large variety of Rydberg series up to the $I_5$ threshold, including for instance, the weak-intensity series $(N,K)_n=(N,N-4)_n$. The measured spectra for $\sigma_j$ and $\beta_j$ are in substantial agreement with the numerical results of Tang and Shimamura (1994). Recently Sokell *et al.* (1996) detected long-lived neutral particles that were generated through the decay of doubly excited states. In their setup, the observed strengths of different series of doubly excited states are very different from the conventional findings by detecting charged fragments.

### *b. Laser double excitation of alkaline-earth atoms*

Compared to helium, alkaline-earth atoms have the experimental advantage of a total two-electron excitation energy of about 15 eV, which can be reached by resonant multiphoton laser excitation.[5] Rydberg states in alkaline-earth atoms are also thoroughly discussed in the book by Gallagher (1994). Compared to direct double excitation from the ground state by synchrotron excitation, the use of several lasers has the advantage of making accessible not only $^1P^o$ states but a variety of doubly excited states with different total angular momenta in a controlled way. While these facts render them favorites for experimental investigations, alkaline-earth atoms differ from the pure three-body problem that is preferentially considered in theory. The difference arises from the spatial extension of the core, which adds a non-Coulombic potential term and removes the $l$ degeneracy of valence electron states that penetrate the core. The corresponding nondegenerate single-electron configurations are therefore much less affected by electron-electron interaction, which renders the observation of related electron correlation effects rather difficult. Hence elaborate multistep laser excitation techniques have been developed (Camus *et al.*, 1989; Eichmann *et al.*, 1990; Jones and Gallagher, 1990) involving up to six lasers, which allow for the controlled excitation of the two valence electrons into states with nonzero angular momenta and reduced overlap with the inner core. In particular, excited states with angular momenta $l>3$ do not penetrate the core and should behave similarly to those in helium. If the electrons are in addition asymmetrically excited, $\langle r_1\rangle<\langle r_2\rangle$, they are supposed to move in different regions of space, and these systems can be considered as experimental realizations of *planetary atoms* (Roussel *et al.*, 1990; Eichmann *et al.*, 1992; Seng *et al.*, 1995).

[5]See Morita and Suzuki (1988) for calcium, Bloomfield *et al.* (1984), Camus *et al.* (1989), Eichmann *et al.* (1989, 1990) Jones and Gallagher (1990), and Roussel *et al.* (1990) for barium, and Eichmann *et al.* (1992), Hogervorst (1993), and Seng *et al.* (1995) in the case of strontium.

In two impressive experiments by the groups of Camus (Camus *et al.*, 1989) and Sandner (Eichmann *et al.*, 1990), the polarization of the inner electronic wave function by the outer electron could be observed. This can be interpreted as a correlation effect. Sandner and coworkers, for instance, used six lasers to bring the first valence electron to a highly excited $nd$ state ($60 \leqslant n \leqslant 100$) and then excited the second valence electron to $l=4$ states with $N=6$ using isolated core excitation. The nonpenetrating inner wave function is hydrogenlike and can therefore be polarized by the outer electron. This experiment, like the experiment of Camus *et al.* (1989), showed a Stark-like energy splitting of the inner electronic states due to the electric field of the slow outer electron, which can be assumed to be "frozen." As will be discussed in Secs. III.B.4, IV.C.2.a, and IV.D.1, similar highly correlated states have been predicted theoretically for helium by Richter and Wintgen (1990b, 1991). However, in those "frozen planet" states the outer electron is truly (dynamically) localized in space.

#### 4. Further methods for double excitation

We briefly review further important experimental approaches here. They probably cannot compete in precision with high-resolution measurements using synchrotron radiation; however, they represent smart and ingenious alternative techniques to observe doubly excited states and are in particular suitable for two-electron systems other than helium.

##### *a. Laser excitation of $H^-$*

In a seminal experiment, Bryant and co-workers were able to reveal several series of doubly excited resonant states in a relativistic $H^-$ beam (Harris *et al.*, 1990a, 1990b). The spectrum of the negative hydrogen ion $H^-$ exhibits a similar overall structure to that of helium. However, the border between discrete and continuum levels, known as the detachment threshold in the case of $H^-$, is very low and lies at 0.75 eV. Only the $H^-$ ground state is bound. Furthermore, the series in $H^-$ have dipole character at the ionization thresholds stemming from the long-range potential formed by the polarized inner $H$ subsystem. This is in contrast to the typical Rydberg series found for all other two-electron atoms. In the experiments of Harris *et al.*, $H^-$ atoms, provided by a linear accelerator and moving with relativistic velocities, intercept a laser beam of laboratory photon energy $E_0$ at a variable angle $\alpha$. The experiments made use of the relativistic Doppler shift leading to an angle-dependent barycentric photon energy $E=E_0(1+\beta\cos\alpha)/(1-\beta^2)^{1/2}$ with $\beta=v/c$. This powerful tool allowed for a tuning of $E$ over a large range, from approximately 0.03 eV up to 21 eV, covering the whole interesting regime of resonances in $H^-$, in particular high-lying states at energies of 10–14 eV. The work by Harris *et al.* (1990a, 1990b) contains a comprehensive account of measured resonance series converging to threshold from $N=4$ up to $N=8$ and compares these with numerical results.[6] For a review with emphasis on atomic negative-ion resonances, we refer the reader to the work of Buckman and Clark (1994).

##### *b. Dielectronic recombination*

Kilgus *et al.* (1990) made use of the time-reversed autoionization process (followed by the emission of a photon), namely, *dielectronic recombination* of a positive ion and a free electron, for the formation of doubly excited states. These experiments were performed in a heavy-ion storage ring generating stored and cooled $O^{7+}$ ions and an intense electron beam provided by an electron cooling device. The experiment allowed the observation of low-lying doubly excited resonant states of the fairly exotic two-electron system $(O^{6+})^{**}$.

##### *c. Electron- and ion-impact experiments*

In contrast to the rapid advances in photoexcitation spectroscopy for highly excited states, electron-impact measurements reveal mainly doubly excited resonances below the $N=2$ ionization limit in helium (Hicks and Comer, 1975; van den Brink *et al.*, 1989) and, more recently, below the $N=3$ threshold (Brotton *et al.*, 1997; Montesquieu *et al.*, 1988). Experiments by Buckmann *et al.* (1983) and Buckmann and Newman (1987) have reached doubly excited states up to $N=9$, but with very limited energy resolution. However, the advantage of electron-impact spectroscopy lies in the fact that it allows for the observation of both optically allowed *and* forbidden transitions. Hence this method makes it possible to unveil the full spectral richness. For instance, in the experiment by Brotton *et al.* (1997), eleven states that are optically inaccessible have been observed and relative cross sections measured.

A more recent alternative technique for double excitation was presented by Moretto-Capelle *et al.* (1997), who measured double excitation cross sections of low-lying states in helium produced in collisions with 100 keV protons. The experimental information was extracted from electron emission spectra. In related experiments, double excitation was achieved earlier by double electron capture processes in slow collisions of highly charged ions with atoms; see, for example, Stolterfoht *et al.* (1986), Mack *et al.* (1989), and Sakaue *et al.* (1990).

In conclusion, there exist today a variety of ingenious experimental techniques for studying the properties of two-electron atoms. At present, spectra using synchrotron radiation exhibit the highest resolution, reaching the accuracy of state-of-the-art numerical calculations reviewed in the following section.

---

[6]The assignment by Harris *et al.* (1990a, 1990b) for the so-called + and − intrashell Feshbach resonances with symmetric and asymmetric stretch motion is incompatible with the present understanding of these resonances; see Sec. IV.C.

### C. Doubly excited states: numerical approaches

#### 1. Brief review of modern numerical methods

A huge number of numerical investigations have improved our understanding of electron-electron correlations in two-electron atoms. In recent years it has become possible to calculate cross sections of two-electron processes with a number of different numerical methods. Here we can only briefly mention a few of them that may be considered as examples of the techniques currently in use. For further accounts on computational techniques we refer the reader to previous reviews on related topics, for instance, those by Fano (1983), Fano and Rau (1986), Lin (1986, 1995), Buckman and Clark (1994), and Aymar *et al.* (1996).

##### *a. Feshbach projection formalism*

Among earlier methods that were applied to obtain the resonance parameters (energies or widths) numerically, we mention those of Bhatia and Temkin (1975, 1984) based on a *Feshbach projection formalism*. More recently, Martin and co-workers proposed an $\mathcal{L}^2$ method combined with the Feshbach formalism that takes into account interchannel coupling in an algebraic way [see Cortés and Martin (1993) for $H^-$, Sánchez and Martin (1993) for He].

##### *b. Hyperspherical approaches*

One of the most widely used theoretical approaches during the last three decades employs *hyperspherical coordinates* for the solution of the three-particle Schrödinger equation (for reviews see Fano, 1983; Starace, 1988, 1993; Lin, 1995). The application of the adiabatic hyperspherical approach is twofold:

Starting with the work of Macek (1968), hyperspherical coordinates have built the framework for the (qualitative) understanding and classification (Lin, 1984, 1986) of resonant states, as will be reviewed in Sec. III.D.

Second, the hyperspherical treatment has been used for numerical computations of adiabatic energy curves, wave functions, and transition amplitudes of doubly excited resonances (see, for example, Sadeghpour and Greene, 1990; Liu *et al.*, 1991; Park *et al.*, 1991; Sadeghpour, 1991). More recently, accurate numerical algorithms based on hyperspherical coordinates have been developed. The *hyperspherical close-coupling method* has become one of the most powerful techniques for obtaining *ab initio* results (Tang *et al.*, 1992a, 1992b; Tang and Shimamura, 1994; for a detailed account see the review of Lin, 1995). It allows one to compute partial cross sections with high precision (about 1%) and has recently been extended to provide angular distribution parameters and differential cross sections as well (Menzel *et al.*, 1995, 1996), as they are obtained in the electron emission experiments described in Sec. II.B.3.a. We note that, in addition to the hyperspherical close-coupling technique, conventional close-coupling methods have also been employed (Oza, 1986) to compute cross sections for two-electron phenomena.

##### *c. R-matrix method*

A further important method, which is among the most widely used numerical techniques for atomic resonances and collision processes, is the *R-matrix method*. We forego a more detailed account of this method in view of the recent review by Aymar *et al.* (1996), which includes a thorough description of the eigenchannel $R$-matrix method. The $R$-matrix approach has been applied to doubly excited resonances by Hayes and Scott (1988), Hamacher and Hinze (1989), Sadeghpour *et al.* (1992), and Cheng Pan *et al.* (1994), to name only a few.

##### *d. Multiconfigurational Hartree-Fock method*

The *multiconfigurational Hartree-Fock method* was extended to autoionizing states by Froese-Fischer and Indrees (1990). Nicolaides and co-workers proposed a related method that they called ''state-specific solution of the complex-eigenvalue Schrödinger equation.'' They developed this approach to study resonant states of negative ions like $H^-$ (Chrysos *et al.*, 1990) and $He^-$ (Chrysos *et al.*, 1992). This method allows for a calculation of partial decay widths, in contrast to the complex rotation method, which is an efficient means to compute resonance positions and widths and will be presented next.

#### 2. Complex rotation method

Different methods exist for computing resonance energies directly by diagonalizing the two-electron Hamiltonian using large $\mathcal{L}^2$ basis sets. Besides the *stabilization method* (Mandelshtam *et al.*, 1993; Müller *et al.*, 1994), the *complex rotation method* (Balslev and Combes, 1971; Junker, 1982; Reinhardt, 1982; Ho, 1983) has become a standard approach to various atomic systems with states coupled to a continuum. This technique allows one to use bound-state methods to calculate resonant energies, widths, cross sections, and wave functions of autoionizing states.

Complex rotation is achieved by complex scaling of the radial coordinates and momenta according to $r \rightarrow r\exp(i\theta)$; $p \rightarrow p\exp(-i\theta)$ (Ho, 1983). Resonance positions and widths are obtained from the complex eigenvalues, $E_n - i\Gamma_n/2$, of the corresponding rotated Hamiltonian $H(\theta)$, after diagonalizing $H(\theta)$ in a basis set of real square integrable wave functions. This means that continuum properties are represented by a discrete basis set.

This method was introduced by Doolen *et al.* (1974) for doubly excited two-electron atoms and was then extensively employed by Ho and co-workers.[7] While Ho has used a Hylleraas-type basis set, Wintgen and coworkers applied the complex rotation method within a Sturmian basis set using perimetric coordinates (James and Coolidge, 1937; Pekeris, 1958); for details see Rich-

[7]See, for example, Ho and Callaway (1985), Ho (1986), and Ho (1989) for helium, Ho (1990, 1992) for $H^-$, and Ho and Bhatia (1992) for $^3P^e$ states in $Ps^-$.

ter and Wintgen (1991), Richter *et al.* (1992), and Bürgers *et al.* (1995). Perimetric coordinates, together with the Sturmian-type basis set, have the great advantage that they lead to a sparse and banded matrix representation of the Hamiltonian in algebraic form. The accuracy of this method, is such that the nonrelativistic helium ground state, for instance, has been computed with a precision of up to 18 significant digits (see Table I).[8]

An extensive list of energies and widths of $^1S$ and $^3S$ states of helium has been presented by Bürgers *et al.* (1995), and for asymmetrically excited electrons (frozen planet states; see Secs. IV.C.2.a and IV.D.1) by Richter *et al.* (1992). A listing of $^1P^o$ He resonances converging to the $N=2-7$ thresholds is given by Rost *et al.* (1997). Results from the complex rotation method will also be used as a check of the semiclassical calculations in Sec. IV.

Experimentally, resonant energies are usually not directly observed but indirectly deduced by excitation through electron impact or photoabsorption. As reviewed in Sec. II.B.3.a, high-precision photoabsorption spectra have been obtained in state-of-the-art experiments that challenge theory to calculate cross sections for comparison. This is again possible by using complex rotation in terms of complex (dipole) matrix elements (Wintgen and Delande, 1993; Domke *et al.*, 1995; Rost *et al.*, 1997). An example of such a numerical calculation of the photoabsorption cross section in helium is given in Fig. 7. The excellent agreement between the numerical and the measured curves shows the high precision of the current state-of-the-art theoretical and experimental techniques. The most recent complex-scaling photoabsorption calculations for helium by Grémaud and Delande (1997) cover the energy regime up to the $N=9$ threshold, where various resonances strongly overlap.

In the next section, we present a thorough classification and interpretation of the resonances, given so far only numerically, in terms of approximate quantum numbers which account for the collective dynamics of the electron pair (Herrick, 1983; Lin, 1984; Feagin and Briggs, 1986).

## III. APPROXIMATE QUANTUM-MECHANICAL CONCEPTS FOR TWO-ELECTRON DYNAMICS

Following the discovery of the effects of correlated electron motion by Madden and Codling (1963), surprisingly different, powerful, and intellectually involved theoretical concepts such as adiabatic approximations, group-theoretical methods, and advanced semiclassical techniques have been necessary to obtain the level of understanding of two-electron resonances we have achieved today. With this understanding we can answer the following crucial questions raised by the experimental and full numerical data, as summarized in Figs. 5 and 6.

(1) The single-particle picture is not applicable for two-electron atoms (see Sec. II). Why are two-electron resonances nevertheless organized in regular (Rydberg) series? What distinguishes different Rydberg series quantitatively, i.e., can one calculate quantum defects of the form introduced in Eq. (4)?

(2) What is the common structure of the wave functions from states belonging to the same Rydberg series?

(3) How can we understand the extreme selectivity in the photoabsorption cross section for different Rydberg series, as can be seen, for example, in Fig. 6? What is the origin of the characteristic autoionization behavior that leads to differences in the resonance widths of orders of magnitude for states belonging to different Rydberg series, as in Fig. 6?

The last question addresses the possible existence of selection rules, or at least propensity rules, for transitions between two-electron states, in analogy to the well-known angular momentum selection rules for dipole matrix elements between single-electron states.

### A. Overview

Among the many contributions towards answering the questions raised above, three major theoretical concepts can be identified: the hyperspherical approach, the algebraic approach, and the molecular approximation. These three qualitative and semiquantitative descriptions could not have been developed without a continuously increasing set of two-electron resonance data, mostly from numerical, converged calculations.

*The adiabatic hyperspherical approximation* was introduced to the problem of two electrons by Macek (1968) and was later mainly pursued by Fano and co-workers (for reviews see Fano, 1983; Fano and Rau, 1986; Lin, 1986, 1995). However, it was also followed by collaborations around Matzsusawa and Watanabe in Japan (e.g., Atsumi *et al.*, 1990; Tang *et al.*, 1992a; Tolstikhin *et al.*, 1995) and Klar in Europe (Klar and Klar, 1980; Pelikan and Klar, 1983). The separation of one variable, the hyperradius, leads to a set of adiabatic potential curves converging to each $He^+(N)$ threshold, similar to the Born-Oppenheimer approximation in molecules. Each of these potential curves carries an entire Rydberg series. The non-Coulombic short-range form of the potential curves accounts naturally for a quantum defect that is different for each Rydberg series. Hence, by construction, the hyperspherical adiabatic approximation provides a partial answer to question (1). Moreover, in days when computers were not as powerful as today, the hyperspherical approach was a convenient way to lower the computational effort, since the calculation of adiabatic potential curves, still a substantial numerical task (see Sec. III.D), is not as involved as the numerical solution of the full problem. However, the structure un-

[8]One should, however, keep in mind that relativistic and finite-mass corrections, which are not included in these calculations, become relevant at such a level of precision. Results including these effects were obtained by Drake (1993; see Table I). They differ from the recent experimental results of Eikema *et al.* (1996) and Bergeson *et al.* (1998; see Table I) due to the Lamb shift of the helium ground state.

derlying each potential curve, i.e., question (2) and therefore also (3), could not be determined. This goal was pursued by the algebraic approach.

*The algebraic approximation* was initiated by Wulfman (1968), who tried to use the well-known dynamical $SO(4)$ symmetry of hydrogen to understand the structure of two electrons from a coupled representation $SO(4)\times SO(4)$. The idea led Herrick and co-workers to an enlightening description of two-electron resonances that yielded for the first time an approximate but complete set of collective quantum numbers (for a review see Herrick, 1983). Various *ad hoc* coupling schemes of $SO(4)$ led to the discovery of an astonishing degree of order in the two-electron resonance spectrum. In a series of papers, Lin (1983a) succeeded in attaching approximate quantum numbers from the algebraic approach uniquely to hyperspherical potential curves. This was a great step forward and answered, in addition to question (1), question (2) to a large extent: The existence of approximate quantum numbers *per se* revealed a common structure for each Rydberg series, and Lin assigned the quantum numbers by following morphological similarities in the wave functions for the hyperspherical potential curves. Still, it was not known if the approximate quantum numbers corresponded to quasiseparability of the problem in a suitable coordinate system. Such a coordinate system would automatically lead to an answer for the still open question (3). Could one find a quasiseparable approximation for two-electron states that would explain possible selection rules? It was the third major concept of two-electron states that provided this separation.

*The adiabatic molecular separation* was introduced by Feagin and Briggs (1986); for a review see Rost and Briggs (1991). This approximation treats the two-electron atom literally as a molecule, assigning the role of the adiabatic internuclear axis to the interelectronic axis. The structure of the adiabatic potential curves is rather similar to the hyperspherical approach, with one important difference: the Hamiltonian for fixed interelectronic vector $\mathbf{r}_{12}$ is separable in elliptical coordinates, thereby providing a full set of quantum numbers (which are in one-to-one correspondence to those derived by Herrick within the algebraic approach). In addition, separability implies a coordinate system in which the wave function for the two electrons can be written approximately as a product of functions with a well-defined number of nodes along each coordinate corresponding to the quantum numbers. Hence the achievements of the hyperspherical and algebraic approaches could be combined in the molecular approximation, with the additional benefit of a set of coordinates in which the two-electron resonant wave functions are approximately separable. The separability permits the identification and formulation of propensity rules, and therefore, finally, in addition to answering questions (1) and (2), also answers question (3).

The molecular description provides the most detailed information about two-electron resonances since it takes into account the rather special feature of the singular Coulomb potentials. Hence it is probably difficult to transfer this approach to other (non-Coulombic) few-body systems.

The algebraic approach also makes heavy use of the $SO(4)$ structure of the Coulomb problem. Nevertheless, constructing level multiplets from group-theoretical considerations is a common technique in few-body dynamics and is probably best known from the theory of quarks (Halzen and Martin, 1984). The algebraic approach is much more ''transferable'' between different few-body problems. In fact, it is the preferred theoretical concept if the interparticle forces are not known in detail.

The most general few-body concept is the adiabatic hyperspherical approximation, especially if the potentials are known. It produces in most cases good quantitative estimates for the energy levels and it has been used in nuclear physics as well as for the nuclear (non-Coulombic) motion in molecules containing a small number of atoms (see, e.g., Hernandez and Clary, 1996).

We shall discuss all three concepts in this section, as well as a selection of interesting alternative approaches. For the sake of a pedagogical presentation we present the molecular approximation first because it appears to provide the most complete qualitative description of doubly excited states within a single concept. In particular, the two limiting collinear cases with $\Theta\approx 180^\circ$ (electrons on opposite sides of the nucleus) and with $\Theta\approx 0$ (electrons on the same side of the nucleus) will become clear: in the first case the interelectronic axis $r_{12}$ is taken as the adiabatic variable $R$; in the second case the distance $r_>$ from the nucleus to the outer electron is defined as the adiabatic $R$. The two collinear configurations persist as structural elements of doubly excited states even for very high excitation of both electrons, where the approximate quantum numbers (to be derived in the present section) lose their meaning. This fact is based on classical and semiclassical considerations, which will be presented in Sec. IV.

### B. The molecular adiabatic approximation

#### 1. Symmetries and wave functions

Feagin and Briggs (1986, 1988) introduced and formulated the idea of viewing doubly excited atomic states in terms of molecular potential curves known from $H_2^+$. This idea has the appealing consequence that each potential curve comes from a separable adiabatic two-center Coulomb Hamiltonian (Slater, 1977) with well-defined quantum numbers and carrying naturally a (Rydberg) series of two-electron resonances.

In molecular Jacobi coordinates, with $\mathbf{R}=\mathbf{r}_{12}$ connecting the two electrons and $\mathbf{r}=(\rho,z,\phi)$ pointing from the middle of the two electrons to the nucleus, the two-electron Hamiltonian reads

$$H=-\nabla_R^2-\frac{1}{4}\nabla_r^2-\frac{Z}{|\mathbf{R}/2-\mathbf{r}|}-\frac{Z}{|\mathbf{R}/2+\mathbf{r}|}+\frac{1}{R}. \tag{6}$$

Treating the interelectronic axis **R** as a slow variable in analogy to the internuclear axis for $H_2^+$ does not seem to make sense on first glance, since the light electrons are expected to move *fast* compared to the heavy nucleus. However, first, the mass argument must refer to the reduced masses involved, which are of comparable magnitude for the two electrons and the center of mass of the nucleus with respect to the electrons, as can be seen from Eq. (6). Second, the success of adiabatic separations is not necessarily linked to slow and fast variables but can also originate in quasiseparability of the system in the respective variables. Finally, an intuitive argument can be given in support of the interelectronic axis as an adiabatic variable for highly excited two-electron resonances, more specifically, if $N/Z \gg 1$. In this case, the effect of the attraction between an electron and the nucleus is much weaker than that of the repulsion between the electrons, which is expected to dominate the structure of the resonant states. This is not the case for the ground state, in which $N/Z \leqslant 1$, and it is not too surprising that a molecular adiabatic separation leads to a binding energy for helium that is 20% too small (Hunter and Pritchard, 1967a, 1967b; Hunter *et al.*, 1968).

In a molecular expansion the spatial wave function is represented as a sum over products of rotational, $\mathcal{D}^{L,S,t}_{Mm}(\Psi,\vartheta,\phi)$, vibrational, $f^L_{im}(R)$, and molecular-orbital, $\psi^t_{im}(\rho,z;R)$, wave functions:

$$\Psi^{S,t}_{LM}(\mathbf{r},\mathbf{R}) = \sum_{im} \mathcal{D}^{L,S,t}_{Mm}(\Psi,\vartheta,\phi)\frac{f^L_{im}(R)}{R}\psi^t_{im}(\rho,z;R). \quad (7)$$

In a body-fixed frame, connected to the lab-fixed frame by the Euler angles $\Psi,\vartheta,\phi$, the interelectronic vector **R** is parallel to the $z$ axis. As in Rost *et al.* (1997), the azimuthal angular dependence on $\phi$ is described by the rotational wave function $\mathcal{D}^{L,S,t}_{Mm}(\Psi,\vartheta,\phi)$, and the molecular orbital (MO) $\psi^t_{im}(\rho,z;R)$ is a wave function for the center-of-mass motion of the nucleus in the coordinates $\rho$, $z$ at fixed internuclear distance $R$ and for a given quantized azimuthal motion $m$. The index $i$ counts the quantized states in $(\rho,z)$.

The wave function in Eq. (7) has been constructed to respect all exact two-electron symmetries; see also Sec. II.B.1. In particular, the rotational parts consist of a symmetry-adapted linear combination of Wigner functions $D^L_{Mm}(\Psi,\vartheta,\phi)$ for the Euler angles (Feagin and Briggs, 1988),

$$\mathcal{D}^{L,S,t}_{Mm} = D^L_{Mm} + (-1)^{S+t+L+m} D^L_{M-m}. \quad (8)$$

Hence the wave function in Eq. (7) is an eigenfunction of the permutation operator $P_{12}$ for the (identical) electrons $P_{12}$: $\mathbf{R}\to-\mathbf{R}, \mathbf{r}\to\mathbf{r}$ with eigenvalue $(-1)^S$ where $S$ is the spin of the electron pair, either singlet $(S=0)$ or triplet $(S=1)$. Furthermore, it is an eigenfunction of the parity operator $P$: $\mathbf{R}\to-\mathbf{R}, \mathbf{r}\to-\mathbf{r}$ with eigenvalues $p=\pm1$. The product operator $PP_{12}$ thus has eigenvalues $(-1)^S p = (-1)^t$, which defines the quantum number $t$ in Eq. (7). The quantum number $m$ is the eigenvalue of the projection operator $l_z$ where $\mathbf{l} = -i\mathbf{r}\wedge\nabla_r$ and also of the body-fixed component $L_z$ of the total angular momentum **L**.

The solution of the eigenvalue equation $(H-E)\Psi^{S,t}_{LM}=0$ reduces, after integration over **r** and the Euler angles, to the following set of coupled equations for the vibrational amplitudes:

$$-\{\partial^2/\partial R^2 - 2[U^L_{im}(R)-E]\}f^L_{im}(R) = \sum_{j\neq i} A^0_{ij}(R)f^L_{jm}(R) + A^+_{ij}(R)f^L_{jm+1}(R) + A^-_{ij}(R)f^L_{jm-1}(R), \quad (9)$$

where we omitted the dependence on $M$, $S$, and $t$ to simplify the notation. The rotational coupling terms

$$A^{\pm}_{ij}(R) = [(L\mp m)(L\pm m+1)]^{1/2}\langle\psi_{im}|l_\pm/R^2|\psi_{jm\pm1}\rangle \quad (10)$$

change the angular momentum quantum number $m$, while the radial coupling term

$$A^0_{ij}(R) = \langle\psi_{im}|2\partial/\partial R|\psi_{jm}\rangle\partial/\partial R \quad (11)$$

leaves $m$ unchanged.

In the adiabatic approximation the sum in Eq. (7) is collapsed to one term $im$ with the consequence that the right-hand side of Eq. (9) is zero, i.e., all couplings to channels $jm'\neq im$ are ignored, and Eq. (9) reduces to a conventional eigenvalue equation for $f^L_{im}(R)$. For fixed $R$ the adiabatic molecular wave function $\psi^t_{im}(\rho,z;R)$ approximately diagonalizes the two-electron Hamiltonian if it is an eigenfunction of the two-center Hamiltonian ($Z=2$ for helium)

$$h_m(R) = -\frac{1}{2}\frac{\partial^2}{\partial z^2} - \frac{1}{2\sqrt{\rho}}\frac{\partial^2}{\partial\rho^2}\sqrt{\rho} - \frac{Z}{r_1} - \frac{Z}{r_2} + \frac{m^2}{2r^2}, \quad (12)$$

which depends parametrically via $r_1$ and $r_2$ on the interelectronic distance $R$. In the adiabatic approximation the vibrational wave function $f^L_{im}(R)$ is an eigenstate of the adiabatic potential

$$U^L_{im}(R) = \mathcal{E}_{im}(R) + C^L_{im}(R) + 1/R, \quad (13)$$

where $\mathcal{E}_{im}(R)$ is an eigenvalue of $h_m(R)$ and $C^L_{im}(R) = \langle\psi_{im}|H-h_m|\psi_{im}\rangle$ is the expectation value of the part of the Hamiltonian that is not diagonalized by $\psi_{im}$.

Note that this is *not* the standard Born-Oppenheimer approach, since we have left out parts of the kinetic energy in $r$ to define the two-center Hamiltonian in Eq. (12). Therefore the residual kinetic energy $\frac{1}{4}\nabla_r^2$ [see Eq. (6)], not diagonalized in Eq. (12), is part of $C^L_{im}(R)$. This modified Born-Oppenheimer treatment acknowledges the fact that the reduced masses along both Jacobi coordinates to be separated adiabatically are of the same order of magnitude (Rost and Briggs, 1991). Using the kinetic energy as in Eq. (12) ensures by construction that the adiabatic correction term $C^L_{im}(R)$ is zero in the large-$R$ limit.

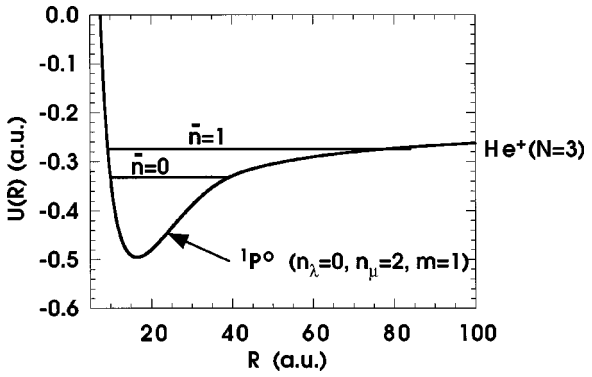


FIG. 8. Schematic representation of doubly excited states in helium in an adiabatic approximation. The resonances appear as vibrational eigenstates (the first two are shown) in a potential curve that is constructed from an eigenfunction of all exact symmetries $^{2S+1}L^{\pi}$ and of the two-center Coulomb problem with the respective quantum numbers $n_\lambda, n_\mu, m$; see text. The states $\bar{n}$ form a Rydberg series with the limiting energy of the excited $He^+(N)$ ion for $\bar{n}\to\infty$ (from Rost *et al.*, 1997).

### 2. Quasiseparability and quantum numbers

The most important feature of the molecular approximation is the fact that the two-center Hamiltonian in Eq. (12) is separable in prolate spheroidal coordinates (Slater, 1977),

$$\lambda=\frac{r_1+r_2}{R},\quad \mu=\frac{r_1-r_2}{R}, \tag{14}$$

with

$$r_{1,2}=\sqrt{\rho^2+(z\pm R/2)^2}. \tag{15}$$

The separability implies a product form for the molecular orbital

$$\psi_{im}=\Lambda^m_{n_\lambda}(\lambda)M^m_{n_\mu}(\mu), \tag{16}$$

with quantum numbers $n_\lambda, n_\mu$ that count the nodes along the respective coordinates.

To summarize, in the molecular approximation individual resonances are obtained by computing vibrational eigenstates according to the Schrödinger equation,

$$\left(-\frac{\partial^2}{\partial R^2}+U^L_{n_\lambda,n_\mu,m}(R)-E_{\bar{n}}\right)f_{\bar{n}}(R)=0. \tag{17}$$

The vibrational quantum number $\bar{n}$ specifies the excitation of one electron along a Rydberg series. Physically, $\bar{n}$ counts the same states as $n$ in Sec. II.B.1, and the relation between both quantum numbers is $\bar{n}=n-N$, where $N$ is the principal quantum number of the $He^+(N)$ hydrogenic level for $\bar{n}\to\infty$. The exact quantum numbers $L,M,S,M_S,\pi$ and the approximate quantum numbers $\bar{n},n_\lambda,n_\mu,m$ constitute a complete classification of doubly excited states. Moreover, they imply an approximate nodal structure of the wave functions, which in turn leads to propensity rules for radiative transitions involving doubly excited states as well as autoionization. Figure 8 illustrates schematically the calculation of a doubly excited two-electron state with all its quantum numbers in the molecular approximation.

As for other separable problems, the quantum numbers do not have to represent the actual number of nodes along some coordinates. Hydrogen itself is the best example, in which only the azimuthal quantum number $m=n_\phi$ specifies directly the number of nodes of the wave function in the coordinate $\phi$. The number of nodes in $\theta$ are given by $n_\theta=l-m$, and the radial nodes are counted by $n_r=N-l-1$; see also Eq. (5). Moreover, the hydrogen problem separates into many other coordinates besides spherical coordinates (due to its high degree of degeneracy). Relevant for the two-electron problem is the separation of hydrogen into parabolic coordinates, where again two sets of quantum numbers are used, the nodal quantum numbers $[N_1,N_2,m]$ with $N=N_1+N_2+m+1$ and the "Stark" quantum numbers $(N,K,T)$ with $K=N_1-N_2$ and $T=m$ (see Bethe and Salpeter, 1977). While the nodal quantum numbers count the nodes of the wave function along the parabolic coordinates, the Stark quantum numbers directly describe the energy eigenvalues in the presence of a static electric field (the Stark effect).

To characterize the two-electron potential curves $U(R)$ from Eq. (13) one can also use parabolic quantum numbers that classify each $U(R)$ uniquely in the "separated-atom" limit $R\to\infty$, when the outer electron has been removed to infinity and merely represents a static electric field for the inner one. Along an adiabatic molecular-orbital curve the nodes of the wave functions do not change. Hence numbers are in one-to-one correspondence:

| parabolic | molecular | Herrick/Stark | |
|---|---|---|---|
| $N_1$ | $=n_\lambda=$ | $\frac{1}{2}(N-K-1-T)$, | (18a) |
| $N_2$ | $=[n_\mu/2]=$ | $\frac{1}{2}(N+K-1-T)$, | (18b) |
| $\lvert m\rvert$ | $=m=$ | $T$, | (18c) |
| $A=(-1)^{n_\mu}(=)A.$ | | | (18d) |

The notation $[x]$ stands for the closest integer lower than $x$. Herrick was the first to introduce the set of Stark quantum numbers $N,K,T$ for two-electron states. They emerged from his algebraic approach (Herrick, 1983), to be discussed in Sec. III.C. Since the information of even and odd nodes $n_\mu$ is lost in the parabolic/Stark classification, an additional quantum number must be introduced, which has been done by Herrick and Sinanoglu (1975); see Sec. III.C.1. Today this quantum number is commonly denoted by $A$, as coined by Lin (1983a). He used $A$ as a label to characterize hyperspherical potential curves for two-electron atoms with the values $A=\pm 1$ for an antinodal $(+)$ or nodal $(-)$ line of the corresponding adiabatic wave functions at $r_1=r_2$. Moreover, Lin (1983a) introduced the label $A=0$ for no apparent symmetry with respect to the line $r_1=r_2$; see Sec. III.D. In the two-center adiabatic approach, $A$ is the

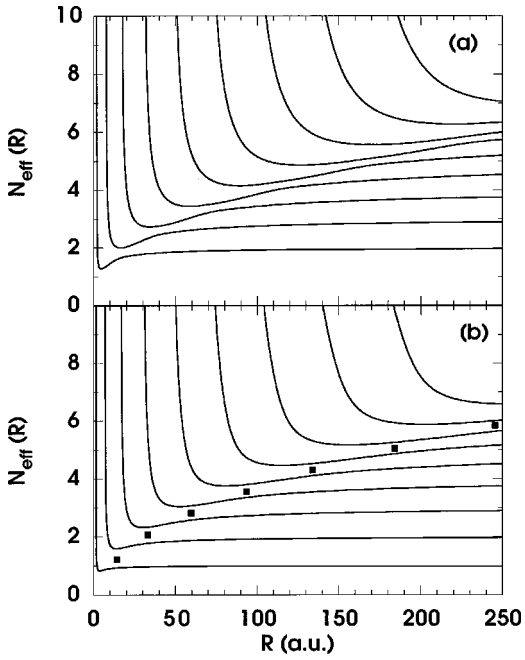


FIG. 9. Adiabatic molecular potential curves for two-electron doubly excited states as a function of the interelectronic distance $R$. The resonances appear as vibrational eigenstates in the potential curves. The energy is plotted as effective quantum number $N_{\rm eff}(R)=[-2/U(R)]^{1/2}$ with $N_{\rm eff}(R\to\infty)=2,3,4,\ldots$ indicating directly the $He^+(N)$ ionization thresholds. Part (a) shows potential curves that carry the resonances of the principal series with quantum numbers $[N_1,N_2,m]^A=[0,N-1,1]^+$, $N=2,\ldots,10$ from below. Part (b) shows resonances of $A=-1$ symmetry for $N=1,\ldots,9$ corresponding to the quantum numbers $[0,N-1,0]^-$ from below. To guide the eye the black squares indicate the locus of the avoided crossing; see text (from Rost *et al.*, 1997).

eigenvalue of the *body-fixed* electron exchange operator with values $A=\pm 1$ from $A=(-1)^{n_\mu}$. $A=0$ does not occur in this description. This is the reason why we put the last equality of Eq. (18d) in parentheses. The correspondence to a hyperspherical potential curve with the empirical label $A=0$ would be a linear combination of several molecular potential curves of different symmetry $A$.

### 3. Propensity rules for radiative and nonradiative transitions

#### *a. Autoionization*

The approximate constants of motion of Eq. (18) for correlated two-electron dynamics imply a nodal structure for the respective resonant states (Rost, Gersbacher, *et al.*, 1991). In turn this nodal structure leads to preferences for autoionization (Rost and Briggs, 1990) and dipole transitions (Vollweiter *et al.*, 1991), which may be easily understood in the molecular language of adiabatic potential curves identified by a set $[N_1N_2m]^A$ of quantum numbers. A small subset of such potential curves as a function of the adiabatic interelectronic distance $R$ is shown in Fig. 9. The most obvious features in Fig. 9 are avoided crossings between two potential curves. Their locus as a function of $R$, indicated by black squares in Fig. 9(b), follows closely the saddle point of the two-center Coulomb potential that plays a crucial role for the three-body Coulomb problem. The saddle point for fixed $R$ is defined by $\mathbf{r}_1+\mathbf{r}_2=0$, where the $\mathbf{r}_i$ are the two electron-nucleus vectors. Moreover, this is exactly the definition of configuration space occupied by the classical Wannier orbit, which plays a prominent role in the classical understanding of two-electron dynamics; see Sec. IV.B.2.b.

The avoided crossings may be interpreted in the following way: To the right of such a crossing, the adiabatic two-electron wave function $\psi^m_{n_\lambda n_\mu}(R)$ has its main contribution in the Coulombic wells, and the contributions in each well are separated from each other by a classically forbidden region with a probability density that is small at the saddle point. To the left of the avoided crossing, the wave function has its main contribution at the saddle point. Hence the avoided crossings separate two regions in $R$ in which the wave function has a different character. As can be seen in Fig. 9, potential curves whose quantum numbers differ by $\Delta N_2=1$ (i.e., $\Delta n_\mu=2$) display avoided crossings, which are narrower for $A=+1$ states [whose wave functions have an antinode on the saddle, Fig. 9(a)] than for $A=-1$ states [with a node on the saddle, Fig. 9 (b)]. In the latter case the change in character of the wave function as a function of $R$ passing an avoided crossing is not so dramatic, since for reasons of symmetry the wave function is zero exactly at the saddle point for all $R$.

The mechanism of autoionization relies on nonadiabatic transitions in this description, in full analogy to electronic transitions in molecules. *Radial* transitions via Eq. (11) are sensitive to the change of the wave function as a function of $R$. Hence they occur preferentially through an avoided crossing of two potential curves. The second kind of nonadiabatic transition is due to rotational coupling $\Delta m=1$ between potential curves according to Eq. (10). Finally, there is no explicit mechanism to change $N_1$ $(n_\lambda)$. Hence transitions with $\Delta N_1\neq 0$ are strongly suppressed. From these observations one can extract three propensity rules for autoionization, which are labeled according to the relative efficiency of the underlying decay mechanism:

$$\text{(A)}\ \Delta N_2=-1 \quad \text{or} \quad \Delta N=-1,\ \Delta K=-1, \tag{19a}$$

$$\text{(B)}\ \Delta m=-1 \quad \text{or} \quad \Delta T=-1, \tag{19b}$$

$$\text{(C)}\ \Delta N_1=-1 \quad \text{or} \quad \Delta N=-1,\ \Delta K=+1. \tag{19c}$$

In general, states with $A=+1$ have larger widths than those with $A=-1$. This can be expected following the discussion of Fig. 9 and it can be directly seen from the experiments, e.g., from Fig. 6. As an example we show in Fig. 10 the decay systematics for the lowest resonance $n=N$ of $^1P^o$ symmetry in a series $[N_1N_2,m]_n$. Each box contains the width of the lowest resonance of the respective series with quantum numbers $[N_1N_2m]$. Simultaneously, the box represents the continuum $[N_1N_2m]$ into which a higher-lying resonance may de-

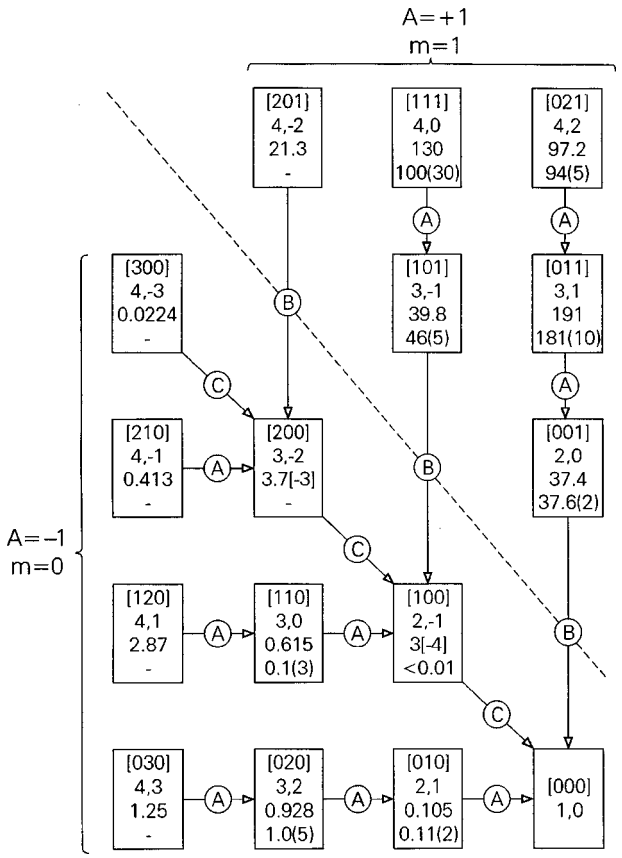


FIG. 10. Decay modes indicated by arrows with the respective rule from Eq. (19) for the lowest $^1P^o$ resonances in the manifolds $N=2-4$. Each box stands for a continuum channel and the lowest resonance in this channel. The quantum numbers $[N_1N_2m]$ and $N,K$ are given together with the theoretical and experimental width in meV from Rost *et al.* (1997; uncertainty in parentheses). The dashed diagonal separates $A=+1$ and $A=-1$ states.

cay, as indicated by the arrows and the respective mechanism (A), (B), or (C).

The states with $A=+1$ are located in the upper right triangle. Those that can decay according to rule (A) have the largest widths (of the order of $10^2$ meV). The arrows point to quantum numbers of the continuum into which these states decay according to rule (A). Close to the (dashed) diagonal separating $A=+1$ and $A=-1$ states we see those resonances that cannot decay by (A). Instead they decay according to (B) by changing their rotational quantum number. Since this change also implies a change of the quantum number $A$, the decay arrow has to cross the diagonal and points to a continuum state with $A=-1$. The rotational decay of these $A=+1$ states is only slightly less effective (by about a factor of 5) than the decay of the $A=+1$ states according to (A). Hence we combine all $A=+1$ states located in the upper triangle into class-I states with the relatively largest widths.

The $A=-1$ states below the diagonal that can decay according to (A) define the class-II states. Their widths (of the order of $10^0$ meV) are one to two orders of magnitude smaller than the widths of the class-I states. Among the $A=-1$ states are also class-III states located directly below the diagonal. They can only decay according to (C) along the diagonal, and their widths ($10^{-4}-10^{-2}$ meV) are more than two orders of magnitude smaller than those of class-II resonances; for more details, see Rost *et al.* (1997) and Rost and Briggs (1990).

To summarize, the three propensity rules (A), (B), and (C) group resonant two-electron states into three classes I–III. For helium, widths between members of two classes differ typically by at least two orders of magnitude, $\Gamma_I:\Gamma_{II}:\Gamma_{III}\approx 10^4:10^2:1$. For a semiclassical interpretation of the propensity rules discussed above see Sec. IV.C.

### b. Dipole transitions

Propensity rules for radiative transitions can be derived by analyzing the dipole matrix elements according to the nodal structure of the resonant wave functions, which is a simple analytical task on the potential saddle at $2\mathbf{r}\equiv\mathbf{r}_1+\mathbf{r}_2=0$. This region in configuration space is most relevant for symmetrically excited electrons with $N\approx n$. It corresponds to the equilibrium geometry of a linear $ABA$ molecule (Hunter and Berry, 1987). Not surprisingly, the relevant quantum number,

$$v_2=2N_1+m, \tag{20}$$

for radiative propensities quantizes the twofold-degenerate bending motion of triatomic molecules and can be derived by normal-mode analysis about the saddle point. Dipole matrix elements within the saddle approximation follow the selection rule (Vollweiter *et al.*, 1991)

$$\text{(D)}\ \ \Delta v_2=0,\pm 1, \tag{21}$$

which survives for the entire dynamics as a propensity rule. Rule (D) has been derived from properties of the doubly excited state involved in the dipole transition. A preference among the possible transitions according to (D) can be induced by the second state of the dipole matrix element (Rost *et al.*, 1997). Such a preference has also been worked out by Gerasimovich *et al.* (1996); see Sec. III.E.3. The propensity rules are also confirmed by the latest measurements of partial ionization cross sections (Menzel *et al.*, 1995, 1996).

## 4. The molecular description of planetary states

For a long time the symmetrically excited states with $N\approx n$ were the center of research activities. After 1990 the development of sophisticated laser excitation schemes of alkaline-earth atoms permitted the preparation of non-core-penetrating doubly excited states and the examination of heliumlike three-body systems with high-resolution laser spectroscopy (Eichmann *et al.*, 1992). Many features of the experimental spectra for very asymmetrically doubly excited states (e.g., $N=6,n>25$) could be understood in the "frozen planet approximation" (Eichmann *et al.*, 1990) in which the outer,

very slow electron represents a static electric field for the inner electron; see also Sec. II.B.3.b.

#### a. Characteristics of planetary states

In 1990, Richter and Wintgen discovered a new class of strongly correlated but asymmetrically excited states. They have remarkable properties, discussed in detail by Richter *et al.* (1992), namely, distinct angular *and* radial correlations, extremely small decay widths, and respective wave functions that are quasiseparable into collective semiclassical and molecular coordinates. The strong radial and angular correlations of the electrons lead to the mixing of all single-particle angular momenta $l_i$ resulting in the formation of a molecular- (or Stark-) type inner electronic wave function and a vibrational, highly nonhydrogenic wave function for the outer electron. As will be discussed in Sec. IV.B.2.a, the resonances are associated with a classical phase-space region, where the three-body Coulomb system becomes nearly integrable.

The resonances exist for arbitrary *finite* nuclear charges $Z>1$. Their existence is inherently tied to the repulsive electron-electron interaction. In particular, they do not possess a limiting independent-particle motion. Hence standard perturbation theory in $1/Z$ starting from the independent-particle limit fails in describing these states. However, they can be described within an adiabatic approximation.

#### b. Structure of planetary states from the adiabatic approximation

The suitable adiabatic variable **R** for planetary states is the coordinate $\mathbf{r}_>$ of the slow outer electron. If the origin of the internal coordinate **r** describing the fast electron is taken as the geometrical midpoint of **R**, i.e., $\mathbf{r}=\mathbf{r}_>-\mathbf{R}/2$ the Hamiltonian for fixed **R** is that of a two-center Coulomb problem in which one center, the nucleus, is attractive while the other center, the slow electron, is repulsive. The adiabatic wave function for fixed $R$ is again separable into prolate spheroidal coordinates $\bar{\lambda},\bar{\mu}$; however, they obviously have a different meaning from that of Eq. (14), namely,

$$\bar{\lambda}=\frac{r_>+r_{12}}{R},\quad \bar{\mu}=\frac{r_>-r_{12}}{R}. \tag{22}$$

The adiabatic potential curves (Fig. 11) also look very different from Fig. 8. For each manifold $N$ the uppermost curve, in which the fast inner electron is highly polarized towards the outer electron, develops a secondary potential well around $R\sim 100$ a.u. These curves have $n_{\bar{\lambda}}=0$ and the maximum number of nodes in $\bar{\mu}$, $n_{\bar{\mu}}=N-1$. In helium, the minimum is for $N\geqslant 6$ deep enough for vibrational bound states with oscillatorlike eigenfunctions for the outer electron.

The occurrence of minima in the Born-Oppenheimer potentials is not restricted to MO states with $n_{\bar{\lambda}}=0$. If $N$ is large enough (i.e., $N\geqslant 16$ in the case of helium), the polarization of an inner-electron state with one off-radial node ($n_{\bar{\lambda}}=1$) is strong enough to produce a potential well in the adiabatic potential. The adiabatic picture not only describes the number of nodes in the wave functions correctly, but also predicts the shape of the nodal surfaces: In $\bar{\lambda}$ and $\bar{\mu}$ they appear as nearly straight lines (Richter *et al.*, 1992), which proves the approximate separability of the *ab initio* quantum wave functions in these coordinates (Richter and Wintgen, 1992).

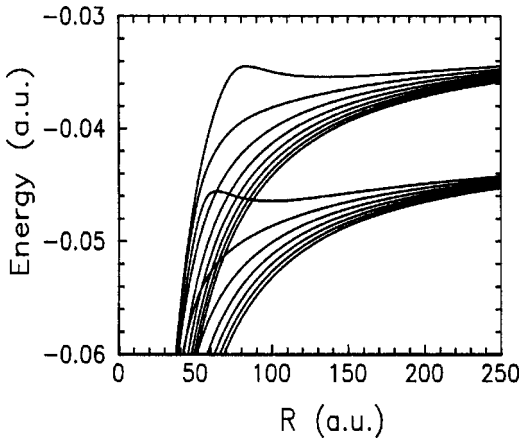


FIG. 11. Born-Oppenheimer potential curves for molecular-orbital-states belonging to the manifolds $N=6$ and $N=7$ of helium (from Richter *et al.*, 1992).

Although the planetary atom resonances are adiabatically separable into prolate spheroidal coordinates as the intrashell resonances are, one has to keep in mind the different meaning of the coordinates and the radically different character of these two sets of states, which becomes obvious in their decay characteristics.

#### c. Decay widths

While the adiabatic potential curves representing intrashell resonances show pronounced avoided crossings responsible for an efficient and characteristic decay mechanism (see Sec. III.B.3.a), such avoided crossings do not occur for potential curves representing the planetary states (see Fig. 11). Indeed, these states are oscillatorlike and they are so different from the hydrogenic states into which they must decay that they have a remarkably long lifetime. Moreover, the lifetime increases exponentially with $N$ such that for states starting from $N\approx 20$ radiative decay is more probable than autoionization (Richter and Wintgen, 1991; Richter *et al.*, 1991). Their asymptotic stability for $N\to\infty$ is connected with the fact that the classical periodic orbit that supports these states is stable. This again is in sharp contrast to the intrashell states in which the collinear subspace with electrons on different sides of the nucleus contains only unstable periodic orbits, reflecting the larger instability of intrashell states; see Sec. IV.B.2.a for a discussion of the classical collinear dynamics.

### 5. Conclusions from the adiabatic molecular treatment

The insight into the structure of two-electron resonances gained from the adiabatic molecular treatment

leads to the conclusion that there are two important limiting cases of collinear arrangement of the three particles:

(i) In an $H_2^+$-like symmetric molecular approximation with the two electrons forming the adiabatic axis, a collinear configuration emerges for increasing $N$, keeping the wave function nodeless in the $\lambda$ coordinate of Eq. (14). Pronounced avoided crossings between the corresponding potential curves belonging to different $N$ indicate the relative instability, i.e., large decay widths, of these states.

(ii) In a molecular adiabatic approximation, treating the vector of the outer electron as the slow variable, states without nodes along the $\overline{\mu}$ coordinate form for increasing $N$ a collinear arrangement with both electrons on the same side of the nucleus ($\Theta \approx 0°$).

These so-called planetary states have very small decay widths. In Sec. IV.B.2.a, we shall see that these two collinear configurations emerge very naturally from a classical analysis. The difference in the decay properties of these two groups of resonances reflects the difference in the classical stability of representative periodic orbits belonging to the respective classical collinear configurations.

A comparison of the two adiabatic molecular descriptions reveals that the long-lived planetary states correspond in the symmetric $H_2^+$-like description to states with the maximum bending excitation for a given $N$, $n_\lambda = N-1$. The propensity rules in Eq. (19), especially the forbidden transition (19c), also reflect the stability of planetary states. This shows that the adiabatic molecular approximation with the interelectronic axis $\mathbf{r}_{12}$ as the adiabatic variable provides a good overall picture of the resonance properties. The quantitative representation for the states with maximal $n_\lambda$ is, however, rather poor. The character of adiabatic wave functions changes quite drastically in this limit, and the frozen planet states are quantitatively much better represented in the corresponding adiabatic molecular treatment with $\mathbf{R} = \mathbf{r}_>$ as the adiabatic variable.

### C. The algebraic approach

The idea of understanding the structure of the levels of doubly excited states in terms of group symmetries dates back to the work by Wulfman (1968). The real breakthrough of the algebraic approach, which is mainly based on properties of the $SO(4)$ group, came with later work initiated by Wulfman (1973) and Sinanoglu and Herrick (1975) and completed by Herrick and coworkers in a series of papers (Herrick and Sinanoglu, 1975; Herrick, 1975a, 1975b; Herrick and Kellman, 1980; Herrick *et al.*, 1980). A good overview is given by Herrick (1983).

#### 1. Dynamical *SO*(4) representations for one- and two-electron atoms

For the dynamics of the hydrogen atom there is a second constant of motion, apart from the angular momentum $\mathbf{l}$, the Runge-Lenz vector (Schiff, 1968),

$$\mathbf{A} = \tfrac{1}{2}(\mathbf{l}\times\mathbf{p} - \mathbf{p}\times\mathbf{l}) + \hat{\mathbf{r}}. \tag{23}$$

For bound states $\mathbf{l}$ and $\mathbf{b} = (-2H)^{-1/2}\mathbf{A}$ satisfy commutation relations that correspond to an $SO(4) = SU(2) \times SU(2)$ generating coupling scheme of angular momenta. Each irreducible representation of the dynamical $SO(4)$ group can be labeled by two indices $[p,q]$ (Herrick, 1983).

For two electrons indicated by indices $i = 1,2$ Wulfman (1968) used initially coupled angular momenta $\mathbf{L} = \mathbf{l}_1 + \mathbf{l}_2$ and $\mathbf{B}' = \mathbf{b}_1 + \mathbf{b}_2$ to generate an $SO(4)$ algebra. However, as he himself (Wulfman, 1973) and Sinanoglu and Herrick (1975) showed later, one should use $\mathbf{B} = \mathbf{b}_1 - \mathbf{b}_2$ instead of $\mathbf{B}'$ to describe doubly excited states. States within irreducible representations generated by $\mathbf{L}$ and $\mathbf{B}$ are labeled by $|PQLM\rangle$, where $L,M$ are the total angular momentum and its projection onto a space-fixed axis, while $P,Q$ are two new collective quantum numbers (Herrick, 1983). Linear combinations of $\pm|Q|$ states can be constructed to be eigenfunctions of the parity operator. For convenience Herrick and Sinanoglu (1975) defined $T = |Q|$ and $K = P - n - 1$ where $n$ is the principal quantum number of the outer electron, i.e., $n \geqslant N$. From configuration-interaction (CI) calculations in the basis $|PQLM\rangle$ Herrick and Sinanoglu found that the Hamilton matrix for intrashell states with $N = n$ is approximately block diagonal according to $\Delta|Q| = 0$, $\Delta K = 0$, which means that $K$ and $Q$ are approximate quantum numbers for doubly excited states. This empirically found dynamical symmetry was a real surprise, in particular for the strongly coupled intrashell electrons with $n = N$. The existence of the approximate collective quantum numbers was rationalized as a consequence of angular correlation by looking at the operator $\cos\Theta$, where $\Theta$ is the interelectronic angle (see Fig. 1). The evaluation of $\langle\cos\Theta\rangle$ is simplified in the absence of exchange of the electrons by the operator replacement $\cos\Theta \to \mathbf{b}_1\mathbf{b}_2/Nn$. In the $SO(4)$ basis $|PQLM\rangle$ this replacement leads to

$$\cos\Theta \to -\frac{K}{N} + \frac{N^2 - 1 + K^2 - T^2 + 2\mathbf{l}_1\mathbf{l}_2}{2Nn}. \tag{24}$$

The pictorial interpretation of Eq. (24) in the two limits $\cos\Theta \approx \pm 1$ is easily given in terms of two Kepler ellipses for the two electrons, oriented according to their Runge-Lenz vectors $\mathbf{b}_i$. If the two ellipses point in the same direction we have $\cos\Theta \approx 1$. The opposite case leads to $\cos\Theta \approx -1$. Note that, for $\cos\Theta \approx 1$, complete degeneracy of the two single-electron ellipses describing intrashell electrons will not be possible for finite nuclear charges $Z$ because the electron-electron interaction would lead to infinite energy at the point where the two electrons meet each other. The observation suggests a nontrivial change in this type of configuration if the electron-electron repulsion is successively increased from the independent-electron limit. The existence of so-called planetary states is an interesting consequence; see Secs. III.B.4, IV.C.2.a, and IV.D.1.

For $n \gg N$, i.e., very asymmetrically excited states, Eq. (24) gives directly $\cos\Theta \approx -K/N$, while the operators $\mathbf{l}_i$ in

the second part lead for smaller $n$ to an admixture of other $SO(4)$ channels. Hence the explanation in terms of $\cos\Theta$ is not complete, at least for intrashell states $N=n$, where the assignment in terms of $K,T$ quantum numbers works very well. We have already seen that the separability of the two-center Coulomb problem supplies the missing link to understanding why the algebraic scheme of the coupled $SO(4)$ representation works so well for intrashell states. In fact the derived quantum numbers are in one-to-one correspondence, as can be seen from Eq. (18). We have so far not mentioned the molecular quantum number $A$, which can be interpreted as the body-fixed electron exchange operator. The algebraic approach has with $T=m$ basically the same projection onto a (body-fixed) quantization axis as the molecular approximation with the interelectronic axis $\mathbf{R}$, here defined by $\mathbf{B}\propto\mathbf{R}$. Herrick and Sinanoglu (1975) noticed the existence of $A$, which they called $\nu$ (see also Herrick, 1983). The difference between the two groups of states distinguished by the two possibilities for $A$ are most evident for states with total angular momentum $L=0$. Then $N=n$, i.e., intrashell states, are forbidden by the Pauli principle for $A=-1$. Basically, $A=\pm1$ is a generalization of the original classification $(2s,np)\pm(2p,ns)$ by Fano and Cooper (1965).

#### 2. Multiplets and supermultiplets for intrashell doubly-excited-state energies

If the $K,T$ quantum numbers mainly determine the correlation energy of the doubly excited states, energy levels ordered according to $K,T$ should show a characteristic pattern. Noting that $L=T$ defines the lowest possible total angular momentum for a given $T$, one can plot within a manifold for fixed $N$ and $A$ the lowest resonance energies as a function of $T$. As a result a typical "diamond" pattern is obtained in which the energy axis can be identified with the scale for the quantum number $K$ to a remarkable degree of accuracy (Herrick, 1983). Apparently, different angular momenta and discrete symmetries (spin, parity) have only a minor influence on the spectral ordering.

The $SU(2)\times SU(2)$ decomposition with its characteristic diamond pattern for the energy levels is the basic multiplet for two-electron resonant states. Herrick and co-workers investigated other coupling schemes and additional quantum labels leading to "supermultiplets" that reveal even more similarities between certain groups of resonances (Herrick and Kellman, 1980; Herrick *et al.*, 1980).

One supermultiplet structure emerges when the two-electron $SO(4)$ group is decomposed into a series of $SO(3)$ representations. In fact we deal with $[SO(4)]_1\times[SO(4)]_2=SU(2)\times SU(2)\times SU(2)\times SU(2)$. The $SO(3)$ representations of this product group are irreducible under the operator $\mathbf{d}_>^2$, where $\mathbf{d}_>$ is the angular momentum with the larger eigenvalue $d=\max(C,D)$ of $\frac{1}{2}(\mathbf{L}^2+\mathbf{B}^2)=D(D+1)$ and $\frac{1}{2}(\mathbf{L}^2-\mathbf{B}^2)=C(C+1)$. In terms of the coupled basis $|PQLM\rangle$ the quantum number for $\mathbf{d}_>$ is

$$d=\frac{P+Q}{2}=\frac{1}{2}(N-1+K+T), \tag{25}$$

where the last identity follows from the definition of $K$ and $T$ for intrashell states $N=n$. The quantum number $d$ cannot be related to the dynamics of a physical coordinate directly within the group-theoretical approach. However, a comparison with the molecular approximation [Eq. (18)] reveals that $d$ is nothing else but the number of nodes along the elliptical coordinate $\lambda$.

In this context we also note that Kellman and Herrick (1980) as well as Yuh *et al.* (1981) have formulated a model for doubly excited states as normal-mode vibrations about the equilibrium position of a linear triatomic molecule $X$-$Y$-$X$. Clearly, the molecular approximation directly justifies this model and the interpretation of certain features in the two-electron resonances as a rovibrational structure. Recent developments in the algebraic approach can be found in Kellman (1994).

### D. The hyperspherical adiabatic approximation

In 1968 Macek proposed an adiabatic separation of the "slow" radial variable $\mathcal{R}=\sqrt{r_1^2+r_2^2}$ to describe doubly excited states. A full set of hyperspherical coordinates for two electrons includes the hyperradius $\mathcal{R}$, the hyperangle $\alpha$ defined by $\tan\alpha=r_2/r_1$, and a set of four geometrical angles $\omega=(\theta_1,\phi_1,\theta_2,\phi_2)$ as usual to describe the positions of the vectors $\mathbf{r}_i$ in the physical space. Hyperspherical coordinates had previously been used in nuclear physics; a general theoretical description of hyperspherical coordinates is given, for example, by Fano and Rau (1986). The two-electron Hamiltonian reads in these coordinates

$$H=-\mathcal{R}^{-5/2}\frac{\partial^2}{\partial\mathcal{R}^2}\mathcal{R}^{5/2}+H_{\mathcal{R}} \tag{26}$$

with

$$H_{\mathcal{R}}=\frac{\mathbf{\Lambda}^2+15/4}{\mathcal{R}^2}+\frac{C(\alpha,\Theta)}{\mathcal{R}}, \tag{27}$$

where $\mathbf{\Lambda}$ is the grand angular momentum operator in six dimensions (see Fano and Rau, 1986). The three-body Coulomb potential in Eq. (27) may be interpreted as having an angular-dependent charge $C(\alpha,\Theta)$ where $\Theta$ is the angle between the two electron-nucleus vectors $\mathbf{r}_1$ and $\mathbf{r}_2$ (see Fig. 1). The "grand angular momentum" operator can be expressed in terms of the two individual angular momentum operators $\mathbf{l}_i$ and the hyperangle $\alpha$ (see Fano and Rau, 1986).

#### 1. Potential curves and channel functions

The hyperspherical two-electron wave function is constructed to be an eigenfunction of the same exact symmetries as Eq. (7) with quantum numbers $L,M,\pi,S$ and reads

$$\Psi^{S,t}_{L,M}(\mathcal{R},\omega)=\sum_{\mu}\mathcal{R}^{-5/2}F_{\mu}(\mathcal{R})\Phi_{\mu}(\omega;\mathcal{R}), \tag{28}$$

where the adiabatic channel function $\Phi_{\mu}(\omega;\mathcal{R})$ is an eigenfunction of $H_{\mathcal{R}}$ from Eq. (27) with eigenvalues $\mathcal{E}(\mathcal{R})$. The expansion equation (27) leads to a similar set of coupled differential equations for the $F_{\mu}(\mathcal{R})$ as in the molecular case for the $f_i(R)$ in Eq. (9). The adiabatic approximation is invoked by truncating the expansion in $\mu$ to a single term, which leads to the vibrational eigenvalue equation

$$\left(-\frac{\partial^2}{\partial\mathcal{R}^2}-\langle\Phi_{\mu}|\frac{\partial^2}{\partial\mathcal{R}^2}|\Phi_{\mu}\rangle+\mathcal{E}(\mathcal{R})-E\right)F_{\mu}(\mathcal{R})=0. \tag{29}$$

The adiabatic hyperspherical representation and the molecular representation of Eq. (7) have many aspects in common; a comparison can be found in Abramov *et al.* (1997). The differences are twofold. First, in the molecular approximation the interelectronic *vector* **R** is separated, leaving for fixed **R** the solution of a three-dimensional problem, the so-called two-center Coulomb problem. This separation includes the definition of a body-fixed frame (along the vector **R**), which has turned out to be an important structural property of doubly excited states. [The approximate quantum number $m$ as well as the body-fixed exchange quantum number $A$ result from this property, which is built into the algebraic approach by taking $\mathbf{B}=\mathbf{b}_1-\mathbf{b}_2\propto\mathbf{R}$ as an $SO(4)$ generator; see Sec. III.C.1.] The hyperspherical approach separates only the scalar hyperradius $\mathcal{R}$, leaving for fixed $\mathcal{R}$ a five-dimensional problem to be solved numerically. Clearly this requires much more numerical effort, and different methods have been developed to solve this problem (see Sec. II.C.1). The effort is rewarded by the better quantitative prediction of doubly excited resonance energies compared to the molecular approximation (Koyama *et al.*, 1986, 1989; Fukuda *et al.*, 1987). However, a qualitative interpretation is difficult. The numerically solved five-dimensional Hamiltonian is not separable. Hence the approximate separability of the body-fixed dynamics, built into the molecular approximation and in the algebraic approach from the beginning, must be reconstructed from the adiabatic potential curves. There it can be recognized in extremely narrow avoided crossings. A diabatic passage corresponds to a conservation of the quantum number $m$. Without knowing this molecular symmetry, Lin worked out in a series of papers how the algebraic quantum numbers $K,T,A$ could be uniquely assigned to hyperspherical potential curves (Lin, 1982a, 1982b, 1983b; Lin and Macek, 1984). He gave rules to identify which curves had to be diabatically connected by comparing patterns of adiabatic hyperspherical wave functions. A new feature emerged through the introduction of the value $A=0$ for potential curves that did not have the exchange symmetry $A=\mp 1$ in their eigenfunctions. Such potential curves have been interpreted as having a dominant "single-particle" character. However, as has been discussed in Sec. III.B.4, there exist highly correlated planetary states with another adiabatic axis $\mathbf{R}=\mathbf{r}_{>}$. The connection between Lin's $A=0$ states and the planetary states has never been worked out. Nevertheless, it is clear that the planetary states can be considered as those with maximum $\lambda$ excitation, $n_{\lambda}=N-1$, and therefore they can be regarded at least as a subset of Lin's $A=0$ states. For reviews of the hyperspherical work up to the mid eighties see Fano (1983) and Lin (1986).

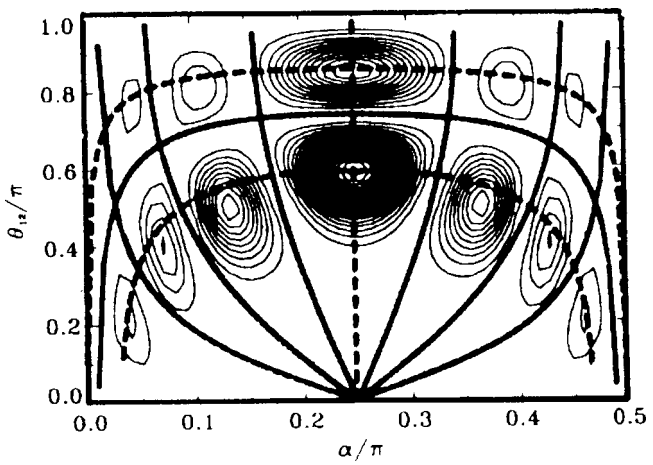


FIG. 12. Two-electron density for the $n_1=1,n_2=3,m=1$ state of $^1P^o$ symmetry of $H^-$ from an adiabatic hyperspherical calculation (Sadeghpour and Greene, 1990). Overlaid are the spheroidal nodal lines according to Eq. (14) from Rost *et al.* (1991).

In 1986 Watanabe and Lin reanalyzed the hyperspherical potential curves under the assumption that either $T$ or $m$ was the quantized projection of the total angular momentum onto a body-fixed axis; a more detailed investigation followed (Chen *et al.*, 1992). Around the same time Feagin and Briggs (1986) published the adiabatic molecular formulation and the close relation between both concepts became clear (Feagin and Briggs, 1988).

### 2. Nodal pattern of wave functions and propensity rules

A second major difference between the hyperspherical and the molecular adiabatic separation lies in the fact that the three-dimensional two-center Coulomb problem is separable, providing naturally a full set of quantum numbers to classify the potential curves (see Sec. III.B.1). If this quasiseparability is true, it must also show up in adiabatic hyperspherical wave functions. Based on their beautifully regular nodal pattern Sadeghpour and Greene (1990) recognized the importance of the quantum number $v_2$ of Eq. (20) and deduced the propensity rule $\Delta v_2=0$ for photoabsorption in $H^-$. This propensity rule was also verified for other two-electron systems (Atsumi *et al.*, 1990; Gou *et al.*, 1991; Sadeghpour, 1991). It is a special case of the general propensity rule Eq. (21). Moreover, the nodal pattern of the hyperspherical wave functions in Fig. 12 indeed follows the

spheroidal coordinates $\lambda,\mu$ [Eq. (14)] as predicted by the molecular approximation and pointed out by Rost, Briggs, and Feagin (1991).

To summarize our comparison of the molecular and hyperspherical adiabatic treatments, the hyperspherical approach provides a better quantitative picture, while the molecular approximation provides a better qualitative representation of two-electron resonances. With today's computing power it is possible to determine two-electron resonances fully numerically, making adiabatic approximations for quantitative predictions unnecessary. One of the fully numerical concepts, the hyperspherical coupled-channel method (Tang *et al.*, 1992a, 1992b; Abrashkevich *et al.*, 1995; see Sec. II.C.1), has evolved from the adiabatic hyperspherical approximation and has been very successful in predicting two-electron resonance phenomena, in particular photoabsorption spectra that are in impressive agreement with experiment (see Sec. II.B.3.a).

Recently, a hybrid formulation was proposed that combines the advantages of the hyperspherical and the molecular descriptions (Tolstikhin *et al.*, 1995).

### E. Other quantum-mechanical concepts for two-electron resonances

#### 1. Dimensional scaling

One of the intellectually most intriguing concepts concerning the hidden symmetries of doubly excited states is the idea of considering the two-electron Hamiltonian as a function of the dimension $D$, with $D=3$ representing reality. Early work dates back to Herrick (1975b) and Herrick and Stillinger (1975). More recently, Herschbach and co-workers have worked intensively on $D$-dimensional scaling in the context of atomic and molecular problems; for overviews see Witten (1980), Herschbach *et al.* (1993), and Herschbach (1993).

We sketch only briefly the idea of dimensional scaling using the simple one-electron case. General results for two-electron atoms are presented without going into detail but emphasizing the insight that this concept has added to our understanding of doubly excited states.

The one-electron problem is separable in $D$ dimensions into an angular part (depending on $D-1$ angles) and a radial part, for which the Schrödinger equation reads

$$\left(-\frac{1}{2}\frac{\partial^2}{\partial R^2}+\frac{L(D)[L(D)+1]}{2R^2}-\frac{Z}{R}-E\right)\Phi(R)=0. \quad (30)$$

Here $L(D)=L_3+\frac{1}{2}(D-3)$ is the angular momentum eigenvalue in $D$ dimensions with $L_3$ being the orbital angular momentum in $D=3$ (Herschbach, 1986). The function $L(D)$ constitutes the so-called "dimensional link," i.e.,

$$(D,L)\leftrightarrow(D-2i,L+i), \quad i=0,1,2,\ldots, \quad (31)$$

which means, for example, that the radial wave function for a spherically symmetric system of $L=2$ in $D=3$ is the same as the one for $L=0$ in $D=7$. The two-electron Hamiltonian does not have spherical symmetry. However, in the molecular adiabatic approximation it turns out that the body-fixed adiabatic wave function $\psi$ from Eq. (16) remains the same in different dimensions $D$ if its azimuthal quantum number $m(D)=m_3+\frac{1}{2}(D-3)$ is kept the same, where $m_3$ is the azimuthal quantum number for $D=3$. This demonstrates once again the strong influence of the spheroidal nodal structure of the wave function on two-electron states. This structure is preserved, even in arbitrary dimension $D$. The adiabatic vibrational motion for a $D$-dimensional two-electron state is determined by the potential

$$V(R)=V_{im}(R)+\frac{L(D)[L(D)+1]-m(D)^2}{R^2}+\frac{(D-3)(D-5)}{4R^2}, \quad (32)$$

where the first two terms are the adiabatic potential $U^L_{im}(R)$ in $D=3$ from Eq. (13) and $V_{im}$ does not depend on $L(D)$. The form of Eq. (32) confirms certain exact interdimensional degeneracies as already found by Herrick and Stillinger (1975) between ($D=3$, $L=1$) and ($D=5$, $L=0$), where the additional centrifugal barrier, the last term in Eq. (32), vanishes.

For higher angular momenta $L$, the interdimensional degeneracies according to the dimensional link, Eq. (31), for $L(D)$ and $m(D)$ are only approximate. Nevertheless, the similarity between certain sets of adiabatic hyperspherical potential curves of different symmetries, noticed earlier by Lin (1984), can easily be explained with the dimensional link Eq. (32). Moreover, one can define so-called generator states that are ground states of $^1S^e$ symmetry in some dimension $D>3$ and generate by virtue of the dimensional link states of different symmetry in $D=3$ (Rost *et al.*, 1992).

In a more general context, perturbation theory about the infinite-dimensional limit $1/D=0$ (which provides a simple but nonseparable approximation) has been used to determine zeroth-order normal modes for correlated dynamics (Herschbach, 1986). This approach also provides hints for the existence of approximate quantum numbers if the evolution of the normal modes is followed from $1/D=0$ to the physical case of $D=3$.

#### 2. The grandparent model and the double Rydberg formula

In analogy to the Rydberg formula for singly excited states (Friedrich, 1998), it seems tempting to look for a similar concept for doubly excited states. Indeed, as argued semiempirically and subsequently confirmed by numerical and experimental evidence,[9] the energies of

[9]See, for example, Read, 1977, 1982; Buckmann *et al.*, 1983; Wang, 1986; Buckmann and Newman, 1987; Lin and Watanabe, 1987; Lin, 1989; Molina, 1989; Read, 1990.

the lowest intrashell resonances $n=N$ in each manifold $N$ can be very well described by a ''double Rydberg'' formula,

$$E_{N,N}=-\frac{(Z-\sigma)^2}{(N-\mu)^2}, \tag{33}$$

where $Z-\sigma$ is the screened charge of the core and $\mu$ is a two-electron quantum defect.

Rau (1983) was the first to motivate the existence of Eq. (33) theoretically with a concept that treats the highly correlated electron pair as a single particle with internal degrees of freedom (see also Rau, 1984). Over the years it has turned out that this point of view leads to a kind of diabatic zeroth-order approximation (Rost and Briggs, 1988, 1989; Heim *et al.*, 1997). However, a diabatic approximation is, in contrast to an adiabatic one, not uniquely defined. This may be one reason why the concept of electron pairs, as appealing as it is, never really succeeded, despite the fact that the double Rydberg formula itself has been refined continuously to describe asymmetrically excited resonances as well (Sadeghpour and Greene, 1990; Burgdörfer *et al.*, 1995).

The most natural explanation for Eq. (33) and for double Rydberg formulas in general [see Eqs. (56) and (58)] is provided by a semiclassical treatment (see Sec. IV.C). A nice quantum-mechanical motivation including a generalization of Eq. (33) has emerged from analytical work in the high-$Z$ limit, which will be discussed briefly in the next section.

#### 3. Work in the limit of large nuclear charge $Z$

Apart from the well-known algebraic approach discussed in Sec. III.C a substantial number of papers have approached doubly excited states from the independent-electron limit $Z\to\infty$. Numerical results have been reported, for example, by Bachau (1984, 1988), Macias and Riera (1986a, 1986b), and Martin *et al.* (1988). An analytical method was developed by Dmitrieva and Plindov (1988a, 1988b, 1989, 1990, 1991) to determine from a perturbative quantum treatment for high $Z$ the behavior of symmetrically excited two-electron states at what they call the ''lower edge'' and the ''upper edge'' of each manifold $N$. These are exactly the two collinear symmetries with $\Theta\approx 180°$ and $\Theta\approx 0°$. In accordance with the existence of the double Rydberg formula, they find for the lower edge an analytical screening constant $\sigma=N^2\langle 1/r_{12}\rangle/2$ with the constant value $\sigma=1-2/\pi$, and for the upper edge a screening that increases logarithmically with $N$, $\sigma\propto\ln N$ (Dmitrieva and Plindov, 1988a). The results are only weakly dependent on the total angular momentum $L$ of the two electrons (Dmitrieva and Plindov, 1990), an observation that is again consistent with the classical considerations to be discussed below. More recently, the same group generalized their work to calculate propensity rules in the high-$Z$ limit that compare favorably with the rules stated in Eq. (21) (Gerasimovich *et al.*, 1996).

## IV. SEMICLASSICAL THEORY FOR TWO-ELECTRON ATOMS

The various methods developed so far to understand the structure of two-electron spectra and to describe decay widths and propensity rules for transitions between different Rydberg series are heavily based on quantum arguments. The various adiabatic approximations rely on the quasiseparability of the three-body Coulomb Schrödinger equation into suitable coordinate systems and the underlying group-theoretical structure of the problem.

In this section we shall analyze the complex structure of quantum spectra of two-electron atoms in terms of the dynamics of the classical problem, i.e., two electrons moving in the Coulomb potential of a positively charged nucleus. Modern developments in semiclassical theory provide a variety of techniques with which to study the connections between the structure of quantum spectra and the dynamics of the corresponding classical system. Quantum spectra for classically integrable problems tend to be ordered, and a set of quantum numbers can be assigned to each level. Wave functions are localized on classical tori, and there is no interaction between levels corresponding to series with different good quantum numbers. Quite the opposite is true for classically chaotic systems. The quantum spectra have no obvious structure, and wave functions are extended over the whole phase space. Energy-level statistics for quantum spectra are again very different for systems with an integrable or a chaotic classical counterpart (see, for example, Bohigas, 1991; Guhr *et al.*, 1998).

The classical two-electron atom is neither integrable nor fully chaotic. The apparently regular structure in the spectrum as well as the breakdown of approximate quantum numbers for highly doubly excited states and the enormous variation in the decay widths for resonances can be understood by studying the classical dynamics in detail. Qualitative results can be obtained by exploiting semiclassical periodic orbit theory.

A brief overview of modern semiclassical techniques is presented in Sec. IV.A. An analysis of the classical phase-space structure for two-electron atoms will be presented in Sec. IV.B. A qualitative description of the quantum spectrum in terms of only a few fundamental classical periodic orbits will emerge, as discussed in Sec. IV.C. A more refined picture allows one to calculate resonances belonging to various Rydberg series quantitatively from the ground state to the single-ionization thresholds, as discussed in Sec. IV.D.

### A. Introduction to modern semiclassical theory

In this section, we shall briefly review semiclassical concepts that have been developed over the past 20 years in order to understand the influence of classical order or chaos on quantum mechanics. The techniques have been especially useful in broadening our understanding of two-electron atoms.

### 1. Trace formulas and semiclassical zeta functions

We shall focus in the following mainly on the bound-state and resonance spectra of quantum systems. The information about the spectrum $\{E_n\}$ (with $E_n$ being complex in the case of resonances) is contained in the trace of the Green's function $G=(\hat{H}-E)^{-1}$, i.e.,[10]

$$g(E)=\mathrm{Tr}\,G(E)=\int \mathrm{d}^f q\; G(\mathbf{q},\mathbf{q};E)=\sum_n \frac{1}{E-E_n}, \tag{34}$$

where $G(\mathbf{q},\mathbf{q}';E)$ represents the energy-dependent Green's function in coordinate representation and $f$ denotes the dimension of the coordinate space.

Various other spectral functions of interest such as the density of states $d(E)=\Sigma_n \delta(E-\hat{H})$ or the spectral determinant $D(E)=\det(E-\hat{H})$ are connected to the trace (34) via the relations

$$d(E)=-\frac{1}{\pi}\mathrm{Im}\,g(E)=\sum_n \delta(E-E_n); \tag{35}$$

$$D(E)=\exp\left[\int \mathrm{d}E'\, g(E')\right]=\prod_n (E-E_n). \tag{36}$$

Closed semiclassical formulas for the trace of the Green's function were first given by Gutzwiller (1971, 1990), Balian and Bloch (1972, 1974), and Berry and Tabor (1976, 1977). The original derivation by Gutzwiller starts by writing the time-dependent Green's function as a Feynman path integral (Feynman and Hibbs, 1965) and by recovering the semiclassical Van Vleck propagator (Gutzwiller, 1967) as the sum over classical paths using the stationary phase approximation. The energy-dependent Green's function $G(\mathbf{q},\mathbf{q}';E)$ can now be written as the sum over all classical paths from $\mathbf{q}\to\mathbf{q}'$ for fixed energy and has the form

$$G_{sc}(\mathbf{q},\mathbf{q}';E)=\sum_{\substack{cl.tr\\ \mathbf{q}\to\mathbf{q}'}} A(\mathbf{q},\mathbf{q}';\hbar)e^{i/\hbar\, S(\mathbf{q},\mathbf{q}';E)}, \tag{37}$$

with $S(\mathbf{q},\mathbf{q}';E)=\int_{\mathbf{q}}^{\mathbf{q}'}\mathbf{p}\mathrm{d}\mathbf{q}$ being the action taken along the classical path and $A(\mathbf{q},\mathbf{q}';\hbar)$ being a path-dependent amplitude (Gutzwiller, 1967, 1990). The trace integral (34) may now be evaluated using the semiclassical expression (37). Alternative derivations of semiclassical trace formulas have been given by using quantum Poincaré maps (Bogomolny, 1992; Doron and Smilansky, 1992).

Closed semiclassical expressions for the trace (34) can be given for restricted classes of dynamical problems. These are the two extreme cases, integrable systems on the one hand and completely chaotic systems on the other. The trace can in both cases be written as a sum over *classical periodic orbits* of the system. The trace formulas are, however, very different in nature for the two extreme classical cases; this will have a profound influence on the interpretation and semiclassical calculation of the spectra of two-electron atoms in which both nearly integrable and chaotic classical dynamics are present.

In integrable problems, the phase space has a torus structure in terms of the constants of motions or action coordinates. The dynamics in each of the $f$-action coordinates $J_i$ are periodic with frequency $\omega_i$; periodic orbits of the system occur as continuous families on tori with rational frequency ratios $\omega_i/\omega_j$ for all $i,j$. The trace integration in Eq. (34) can be done analytically using the Green's function (37) (Berry and Tabor, 1976, 1977). The resulting periodic orbit formula coincides essentially with the semiclassical Einstein-Brillouin-Keller quantization, the multidimensional generalization of the WKB approximation (Berry and Tabor, 1976; Gutzwiller, 1990). A semiclassical quantization of integrable or near-integrable dynamics can thus be performed within the usual Einstein-Brillouin-Keller formalism; see Sec. IV.D.1.

The other extreme classical case is fully developed chaos, which is characterized by ergodic motion with uniform exponential separation of neighboring trajectories. All periodic orbits are unstable and isolated, forming a dense set of measure zero in phase space. The trace integral in Eq. (34) can be approximately evaluated by the method of stationary phase giving main contributions at periodic trajectories of the classical dynamics; this leads finally to Gutzwiller's trace formula (Gutzwiller, 1990), i.e.,

$$g_{sc}(E)=\overline{g}(E)-\frac{i}{\hbar}\sum_{po} T_{po}\sum_{r=1}^{\infty}\frac{1}{\sqrt{|\det(\mathbf{M}_{po}^r-\mathbf{1})|}} \times\exp\left[ir\frac{S_{po}(E)}{\hbar}-ir\sigma_{po}\frac{\pi}{2}\right]. \tag{38}$$

The first sum is taken over all unstable periodic orbits of the classical system, where the sum over $r$ accounts for the repetitions. The action $S$ is taken along the orbit and $T$ represents the period. The Monodromy or stability matrix $\mathbf{M}$ is the Jacobi matrix of the full phase-space flow in a reduced local phase-space coordinate system perpendicular to the trajectory and on the energy manifold. It describes the linearized dynamics in the neighborhood of the orbit after one revolution. The stability of a periodic orbit is characterized by the eigenvalues $\Lambda$ of $\mathbf{M}$.

The integer winding number $\sigma$, also called the Maslov index, counts twice the number of revolutions of the stable or unstable eigenvectors of $\mathbf{M}$ around the periodic trajectories (Creagh *et al.*, 1990; Robbins, 1991). The smooth part $\overline{g}(E)$ stems from the limit $\overline{g}(E)$

[10]Note that, for scattering problems, the trace is defined only after subtracting the asymptotic behavior in the separable limit, i.e., considering $g(E)=\mathrm{Tr}[G(E)-G_0(E)]$ with $G_0=(E-\hat{H}_0)^{-1}$ and $\hat{H}_0$ the Hamiltonian for noninteracting particles far from the interaction zone.

$=\lim_{\mathbf{q}\to\mathbf{q}'} G(\mathbf{q},\mathbf{q}')$ for direct paths $\mathbf{q}\to\mathbf{q}'$ of zero length. It is connected to the mean level density via

$$\overline{d}(E) = -\frac{1}{\pi}\operatorname{Im}\overline{g}(E) = \frac{1}{(2\pi\hbar)^f}\int\int \mathrm{d}q^f\,\mathrm{d}p^f\,\delta[E-H(\mathbf{p},\mathbf{q})], \tag{39}$$

being proportional to the classical phase-space volume on the energy manifold (Gutzwiller, 1990).

For uniformly chaotic systems, the largest eigenvalue of the Monodromy matrix increases typically as $\Lambda_{po} \approx \exp(T_{po}\lambda_0)$. Here $\lambda_0>0$ denotes the total Liapunov exponent of the classical dynamics corresponding to the mean separation of trajectories per unit time (Schuster, 1989). The amplitudes in Eq. (38) behave thus like $|\det(\mathbf{M}_{po}-\mathbf{1})|^{-1/2}\approx\exp(-T_{po}\lambda_0/2)$. The number $N(T)$ of orbits with period less than $T$, on the other hand, increases exponentially with $T$, i.e., $N(T)\approx\exp(h_t T)$, where $h_t$ is called the topological entropy; for uniformly chaotic and bound systems, we find typically $h_t\approx\lambda_0$ (Eckhardt and Aurell, 1989).

The above consideration shows that the Gutzwiller periodic orbit sum (38) is not absolutely convergent for real energies (Eckhardt and Aurell, 1989). In mathematical terms, one has to find a meromorphic extension of the trace $g_{sc}(E)$ in Eq. (38) as a function of the complex energy from the region of convergence onto (or below) the real energy axis.

Such a procedure is simplified in scaling systems in which the dynamics are up to a scaling transformation independent of the energy. The energy dependence of the actions is then of the form $S(E)=f(E)S_0$, and $f(E)$ is a universal scaling function; the amplitudes are energy independent. The trace $g_{sc}$ can now be written as a function of the complex variable $z=f(E)/\hbar$. The three-body Coulomb problem is such a scaling system, as will be shown in Sec. IV.B.1.

When constructing analytic continuations of semiclassical expressions, it is advantageous to consider a semiclassical approximation to the spectral determinant (36). Inserting the semiclassical expression (38) leads to (Miller, 1975; Voros, 1988)

$$D_{sc}(E)\sim e^{-i\pi\overline{N}(E)}\prod_{po}\times\exp\left[-\sum_{r=1}^{\infty}\frac{\exp[ir(S_{po}(E)/\hbar-\sigma_{po}\pi/2)]}{r\sqrt{|\det(\mathbf{M}_{po}^r-\mathbf{1})|}}\right] = e^{-i\pi\overline{N}(E)}\zeta_{sc}^{-1}(E). \tag{40}$$

The energy integration is carried out by using the relation $T_{po}=\partial S_{po}/\partial E$, and $\overline{N}(E)$ denotes the integrated mean level density, Eq. (39) (or mean level staircase function). The last equality defines the semiclassical zeta function, $\zeta_{sc}^{-1}(E)$.[11]

The product in Eq. (40) is again not absolutely convergent. However, the determinant structure of $D(E)$ allows one to expand the product in a controlled way, guided by the cumulant expansion for infinite matrices. These expansions can be shown to lead to convergent expressions, being analytic in a strip containing the real axis. The zeros of these functions are then the approximate eigenvalues of the corresponding quantum problems. Details will be presented in Sec. IV.A.2 and when applying this formalism to two-electron atoms in Sec. IV.D.

### 2. Semiclassical quantization for chaotic dynamics

In the following, we shall describe how to use periodic orbit information efficiently to obtain semiclassical estimates for individual eigenvalues. We shall focus on semiclassical quantization techniques for chaotic systems; a semiclassical quantization of integrable dynamics leads to the well-known Einstein-Brillouin-Keller quantization by writing the classical Hamiltonian in action-angle variables and exploiting the Bohr-Sommerfeld quantization conditions for the actions (Gutzwiller, 1990, and references therein). The Einstein-Brillouin-Keller formalism was used by Leopold and Percival (1980) in an early attempt to quantize helium assuming an integrable phase-space structure; see Sec. II.A.2. We shall come back to the Einstein-Brillouin-Keller quantization when discussing the stable so-called collinear frozen planet configuration in helium in Secs. IV.C.2.a and IV.D.1.

A semiclassical quantization of classically chaotic dynamics can be formulated in terms of all periodic orbits of the systems with the help of Eqs. (38) or (40). These periodic orbit formulas are sums or products over an exponentially increasing number of terms and are not absolutely convergent on the real energy axis; the outcome of the summation thus depends on the ordering of the individual terms in the sum. A natural ordering parameter for periodic orbit sums is the action or, equivalently, the period of the orbits. The minimal period needed to resolve structures on the scale of the mean level spacing $1/\overline{d}(E)$ is given by the so-called Heisenberg time

$$T_H = 2\pi\hbar\overline{d}(E). \tag{41}$$

Convergence of the trace (38) can be achieved by Gaussian smoothing (Aurich *et al.*, 1988; Sieber and

[11]The name originates from the similarity of Eq. (40), with the Riemann zeta function. Its representation both as a sum over the natural numbers, $\zeta_R(s)=\Sigma_n n^{-s}$, and as a product over the prime numbers, $\zeta_R(s)=\Pi_p(1-p^{-s})^{-1}$, is also not absolutely convergent for Im $s\leqslant 1$. An analytic continuation of the Riemann zeta function can, however, be given explicitly (Titchmarsh, 1986).

Steiner, 1990), which is equivalent to an effective cutoff in the summation. Inspired by the Riemann-Siegel relation for the Riemann zeta function (Titchmarsh, 1986), Berry and Keating (1990) expanded the semiclassical spectral determinant (40) by multiplying out the various factors. The terms in the resulting sum are then ordered with increasing period of the orbits and so-called composite orbits up to half the Heisenberg time. Similar methods have been reported by Sieber and Steiner (1991).

The techniques mentioned above are suitable for bound quantum systems only. In the following we shall introduce a slightly different concept based on quantum and classical Poincaré maps and their associated symbolic dynamics. This leads us to the well-controlled theory of spectral determinants for infinite matrices. These determinants are calculated in terms of so-called cumulant expansions, which provide a guide for periodic orbit expansions of semiclassical zeta functions valid for both bound spectra and resonances and hence appropriate for two-electron atoms.

The starting point is the semiclassical zeta function (40), which can be written in the form

$$\zeta^{-1}(E)=\det[1-T(E)], \tag{42}$$

with $T$ being a so-called transfer operator or quantum map associated with a classical Poincaré map of the system.[12]

Neither the classical Poincaré map nor the corresponding quantum transfer operators can in general be given analytically. The classical map is usually obtained by solving the equations of motion numerically. The quantum maps were discussed in the semiclassical context by Bogomolny (1992) and Doron and Smilansky (1992); methods to construct exact quantum maps have been proposed by Dietz and Smilansky (1993), Prosen (1994, 1995, 1996), and Rouvinez and Smilansky (1995).

Quantum eigenvalues correspond to energies $E$ for which $\det[1-T(E)]=0$. The determinant can be written in terms of traces by using the basic relation

$$\det(1-T)=\exp[\mathrm{Tr}\log(1-T)]=\exp\left(-\sum_{n=1}^{\infty}\frac{1}{n}\mathrm{Tr}\,T^n\right). \tag{43}$$

The traces of $T^n$ can in semiclassical approximation be written as the sum over all periodic orbits of the $n$th return of the classical Poincaré map, i.e., (Bogomolny, 1992)

$$\mathrm{Tr}\,T_{sc}^n(E)=\sum_{po}^{(n)}\frac{\exp((i/\hbar)S_{po}(E)-i\sigma_{po}(\pi/2))}{\sqrt{|\det(\mathbf{M}_{po}-\mathbf{1})|}}. \tag{44}$$

Inserting Eq. (44) into Eq. (43) leads again to the semiclassical zeta function Eq. (40) as products over periodic orbits. The computation of determinants and traces of infinite dimensional operators is well understood (Reed and Simon, 1972; Wirzba, 1997). The determinant can be written as a cumulant expansion

$$\zeta^{-1}(E)=\det[1-T(E)]=\sum_{m=0}^{\infty}c_m(E), \tag{45}$$

where the cumulant or curvature terms $c_m$ are defined recursively as

$$c_m=-\frac{1}{m}\sum_{k=0}^{m-1}\mathrm{Tr}\,T^{m-k}c_k;\quad c_0=1. \tag{46}$$

The sum converges faster than exponential for large $m$ under very general conditions (see Reed and Simon, 1972; Voros, 1987; Wirzba, 1997).

Writing out the first few terms in the expansion, we obtain

$$\zeta^{-1}(E)=1-\mathrm{Tr}\,T-\frac{1}{2}[\mathrm{Tr}\,T^2-(\mathrm{Tr}\,T)^2]-\frac{1}{3}\left(\mathrm{Tr}\,T^3-\frac{3}{2}\mathrm{Tr}\,T^2\,\mathrm{Tr}\,T+\frac{1}{2}(\mathrm{Tr}\,T)^3\right)-\frac{1}{4}\cdots. \tag{47}$$

The convergence of the cumulant expansion (45) originates from cancellations between the various traces. This means that an exponentially increasing number of periodic orbits contained in $\mathrm{Tr}\,T^n$ is balanced in a delicate way by products of shorter orbits to make the total curvature term $c_m$ decrease exponentially with $m$.

The cancellation mechanism in the cumulant expansion can be highlighted after writing Eq. (47) in terms of individual orbits. We may introduce a suitable symbolic dynamics, i.e., we assume that there is a one-to-one correspondence between trajectories in phase space and the set of all symbol sequences of $n$ different symbols (Artuso *et al.*, 1990; Cvitanović, 1998, and references therein). The symbolic dynamics are in general linked to a Poincaré surface of sections and the length of the code marks the iterates of the map. The (collinear) three-body Coulomb problem is a prototype of a physical system in which such a symbolic dynamics exists; see Sec. IV.B.2.

With the help of a symbolic code, the expansion (47) can be rewritten as a so-called cycle expansion (Cvitanović, 1988; Artuso *et al.*, 1990). For a binary code denoted by the symbols {0,1} (as, e.g., in the collinear three-body Coulomb problem), the cycle expansion for $\zeta^{-1}$ reads

$$\zeta_{sc}^{-1}=1-t_0-t_1-[t_{01}-t_0t_1]-[t_{001}-t_0t_{01}+t_{011}-t_{01}t_1]-\cdots, \tag{48}$$

[12] A quantum Poincaré map is as a discrete quantum propagator acting on wave functions in an $f-1$ dimensional coordinate space $\mathbf{q}=(q_1,\ldots,q_{f-1})$,

$$\psi_{n+1}(\mathbf{q}')=\int \mathrm{d}q^{f-1}\,T(\mathbf{q},\mathbf{q}';E)\psi_n(\mathbf{q}),$$

where the integral extends over a chosen Poincaré surface of section.

with

$$t_{po}=\frac{1}{\Pi_{j=1}^{f-1}\sqrt{\Lambda_{po,j}}}\exp\left(i\frac{S_{po}(E)}{\hbar}-i\sigma_{po}\frac{\pi}{2}\right) \tag{49}$$

and $\Lambda_{po,j}>1$ being the $f-1$ leading eigenvalues of the Monodromy matrix $\mathbf{M}_{po}$. [The denominator in Eq. (42) is here approximated by using $|\det(\mathbf{M}_{po}-\mathbf{1})| \approx\Pi_{j=1}^{f-1}\Lambda_{po,j}$; see Artuso *et al.*, 1990.] The expansion has the form of a perturbative series: the zeta function is dominated by short periodic orbits and the contributions of long orbits become negligible due to increasing cancellations between orbits and composite orbits.

The cycle expansion has been tested successfully for both bound and scattering problems (Cvitanović and Eckhardt, 1989; Tanner *et al.*, 1991; Wirzba, 1992) and was used to calculate for the first time bound states (including the ground state) and resonances in helium semiclassically in a consistent way (Ezra *et al.*, 1991). Still, the essential requirement for a semiclassical treatment of two-electron atoms is the understanding of the classical dynamics of this three-body Coulomb problem, which will be summarized below.

### B. Two-electron atoms: A classical analysis

In this section we discuss the classical phase-space dynamics of two-electron atoms, with an emphasis on helium. We first give a general characterization of the problem and describe the treatment of the various singularities present in the equations of motion. We then concentrate on total angular momentum $L=0$ and identify three lower-dimensional invariant subspaces of the full phase space. They are of special importance for doubly excited states and will be studied in detail.

#### 1. General overview: The classical Hamiltonian and its symmetries

##### *a. Integrals of motion, scaling properties, and regularization techniques*

The classical three-body system can be reduced to four degrees of freedom after eliminating the center-of-mass motion and incorporating the conservation of the total angular momentum. In the special case of zero angular momentum, the motion of the three particles is confined to a plane fixed in configuration space (Pars, 1965) and the problem reduces to three degrees of freedom. We shall as usual work in the infinite nucleus mass approximation. The classical Hamiltonian for a two-electron atom is then given by Eq. (1); the Hamiltonian including finite nucleus mass terms and after elimination of the center-of-mass coordinates can be found in Richter *et al.* (1993).

The energy dependence of the classical dynamics is equivalent to a scaling transformation of the classical motion in phase space, since the potential energy in Eq. (1) is a homogeneous function of the coordinates. Choosing the canonical transformation

$$\mathbf{r}_i\rightarrow\frac{1}{|E|}\mathbf{r}_i,\quad \mathbf{p}_i\rightarrow\sqrt{|E|}\mathbf{p}_i,\quad i=1,2 \tag{50}$$

and introducing a time transformation $t\rightarrow|E|^{-3/2}t$ eliminates the energy dependence in the classical Hamiltonian; the study of the classical dynamics can be restricted to the three distinct cases

$$H=\frac{\mathbf{p}_1^2}{2}+\frac{\mathbf{p}_2^2}{2}-\frac{Z}{r_1}-\frac{Z}{r_2}+\frac{1}{r_{12}}=\begin{cases}+1 & : \quad E>0\\ 0 & : \quad E=0\\ -1 & : \quad E<0.\end{cases} \tag{51}$$

The dynamics for other energy values are now obtained by the scaling transformation (50).

The $H=+1$ regime corresponds to the energy region in which three-body breakup is possible. There exist no periodic orbits of the electron pair and at least one electron always escapes to infinity. The classical dynamics for $E>0$ are important when studying the energy dependence of the total quantum cross section for three-particle fragmentation. The cross section can be deduced from purely classical considerations by studying the classical three-particle breakup along the so-called Wannier orbit (Wannier, 1953; Eckhardt, 1991). The resulting threshold law was first derived by Wannier (1953) in the limit $E\rightarrow0^+$ and was later extended to $E>0$ (Rost, 1994). A detailed discussion of this energy regime can be found in Rost (1995, 1998).

The classical dynamics for $H=-1$ are linked to the quantum energy regime $E<0$ containing the bound and resonance spectrum of two-electron atoms; see Fig. 5. Only one electron can escape classically and it will do so for most starting conditions. We shall discuss the classical aspects of this energy regime in Sec. IV.B.2.

The classical action $S$ and the (conserved) total angular momentum $\mathbf{L}$ scale as

$$S\rightarrow\frac{1}{\sqrt{|E|}}S,\quad \mathbf{L}\rightarrow\frac{1}{\sqrt{|E|}}\mathbf{L}. \tag{52}$$

Note that the angular momentum in the scaled coordinates converges to zero with increasing electronic excitation ($E\rightarrow0^-$) and fixed unscaled $\mathbf{L}$. The dynamics of *highly* doubly excited quantum states with moderate total angular momentum are thus semiclassically connected to a quantization of the planar configuration $\mathbf{L}=0$ in the scaled variables. This fact is exploited when considering the influence of the classical dynamics at $\mathbf{L}=0$ on quantum states with angular momentum $\mathbf{L}\neq0$; see Sec. IV.C.3. It also plays an important role when studying the cross section at the three-particle breakup threshold $E=0$ (Rost, 1998).

The equations of motion for the three-body Coulomb problem diverge whenever two of the three particles collide, i.e., an interparticle distance vanishes. The two-body collisions $r_1=0$, $r_2=0$, or $r_{12}=0$ can be regularized with the help of a so-called Kustaanheimo-Stiefel transformation (Kustaanheimo and Stiefel, 1965; Aarseth and

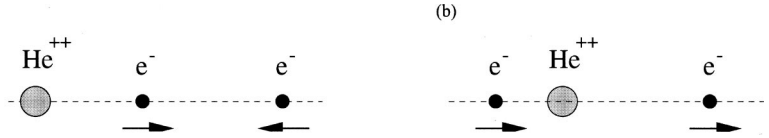


FIG. 13. The two collinear configurations: (a) the stable $Zee$ configuration and (b) the chaotic $eZe$ configuration.

Zare, 1974), which allows one to continue solutions of the classical equations of motion uniquely through the singular points. The transformation consists of a coordinate-dependent time transformation that stretches the time scale near the origin and a suitable canonical transformation in the coordinates (Richter *et al.*, 1993).

The singularity at the triple collision $r_1=r_2=r_{12}=0$, on the other hand, cannot be regularized and solutions going into or emerging from the singularity cannot be uniquely continued through this point. The dynamics near the triple collision are extremely sensitive to small changes in the initial conditions. The triple-collision singularity is indeed the main source for strong chaos in the three-body Coulomb problem, as discussed in more detail in Sec. IV.B.2.

#### *b. Symmetries and invariant subspaces*

The Hamiltonian for two-electron atoms, Eq. (1), has discrete symmetries being related to the parity transformation $(\mathbf{r}_1,\mathbf{r}_2)\rightarrow(-\mathbf{r}_1,-\mathbf{r}_2)$ and the particle exchange transformation $(\mathbf{r}_1,\mathbf{r}_2)\rightarrow(\mathbf{r}_2,\mathbf{r}_1)$. The latter symmetry is quantum mechanically linked to the total spin quantum number due to the antisymmetry of the full wave function (when neglecting spin orbit coupling; see Secs. II.B.1 and III.B.1).

The symmetries give rise to invariant subspaces in the full phase space. Trajectories that start in such a subspace will remain there for all times, thus reducing the relevant degrees of freedom of the dynamics. Invariant subspaces are an extremely useful tool for studying classical dynamics in a high-dimensional phase space. They serve as a low-dimensional window into the full dynamics; access to the full phase space in the vicinity of the symmetry plane can be obtained by studying the linearized dynamics in all degrees of freedom for trajectories in the symmetry plane.

The symmetry planes that exist for $L=0$ turn out to be crucial for an understanding of two-electron spectra and will be discussed in detail in the following section. The three existing invariant subspaces are:

(i) the *Wannier ridge*

$$r_1\equiv r_2;\ p_{r_1}\equiv p_{r_2};$$

(ii) the collinear $eZe$ configuration

$$\Theta\equiv\pi;\ p_\Theta\equiv 0;$$

(iii) the collinear $Zee$ configuration

$$\Theta\equiv 0;\ p_\Theta\equiv 0.$$

The particle exchange symmetry allows us to reduce the configuration space for the collinear configurations to the domain $r_1\geqslant r_2$, i.e., we can (and shall henceforth) always assume $r_1\geqslant r_2$ and treat an encounter with the symmetry line $r_1=r_2$ as hard wall reflection (Wintgen *et al.*, 1992); the Wannier ridge lies exactly in this symmetry plane $r_1=r_2$.

### 2. Invariant subspaces: Collinear configurations and the Wannier ridge

In the following, we shall discuss the three invariant subspaces mentioned above for $H=-1$. We concentrate first on the collinear configurations that form the backbone of the semiclassical quantization of helium introduced in Secs. IV.C and IV.D.

#### *a. Collinear helium: The Hamiltonian and general properties*

Collinear two-electron atoms in the energy regime below the double ionization threshold attracted attention only recently after their fundamental role for the semiclassical quantization of the helium spectrum was discovered (Ezra *et al.*, 1991). The classical dynamics of the collinear subspaces have been investigated in detail by Blümel and Reinhardt (1991), Ezra *et al.* (1991), Kim and Ezra (1991), Richter (1991), Richter *et al.* (1993), and Gaspard and Rice (1994). Collinear collision dynamics have also been studied by Gu and Yuan (1993) and Tang *et al.* (1996) and have been used to develop the classical $S$-matrix theory for reactive scattering in molecular problems by Miller (1974) and others.

Handke *et al.* (1993) and Dräger *et al.* (1994) studied the so-called $s$-wave helium, which is similar to the $eZe$ classical collinear dynamics; even so, the quantum arguments motivating this model are quite different. The model treats the electrons as pure $s$ waves, i.e., the classical dynamics of both electrons take place only in the radial direction. Electron-electron repulsion is included through an effective screening of the nucleus by the actual inner electron as seen by the then-outer electron. The screening is assumed to change abruptly whenever the electrons change places, i.e., the inner electron becomes the outer one and vice versa, which makes the classical dynamics nontrivial. Classical calculations for collinear three-particle Coulomb problems with mass ratios different from those found in two-electron atoms have been performed by Duan *et al.* (1999).

The collinear configurations in two-electron atoms are four-dimensional invariant subspaces of the six-dimensional phase space $\mathbf{L}=0$; the three particles move along a common axis with both electrons either on the same side of the nucleus ($Zee$ or $\Theta=0$ configuration) or on opposite sides of the nucleus ($eZe$ or $\Theta=\pi$ configuration); see Fig. 13. The two degrees of freedom are the

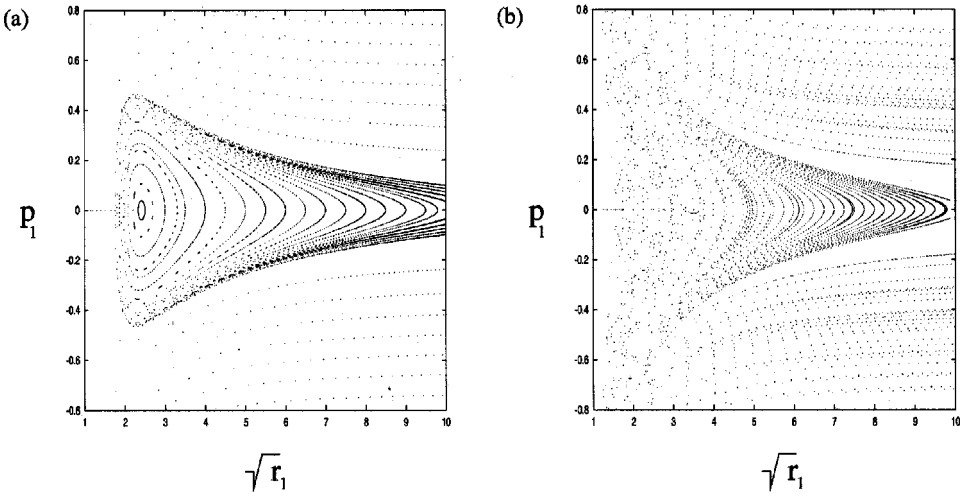


FIG. 14. Poincaré map ($r_2=0$) for the two collinear configurations and $Z=2$: (a) $\Theta=0$; (b) $\Theta=\pi$. The frozen planet orbit is at the center of the stable island in (a).

electron-nucleus distances $r_1$ and $r_2$. The collinear Hamiltonian is given by

$$H^{\pm}=\frac{p_1^2}{2}+\frac{p_2^2}{2}-\frac{Z}{r_1}-\frac{Z}{r_2}+\frac{1}{|r_1\pm r_2|}=-1, \tag{53}$$

and the $\pm$ signs correspond to the two possible configurations.

In the *Zee* case, surprisingly, the electron-electron repulsion leads to a stabilization of the dynamics for $Z>1$. The electrons cannot penetrate each other, and there is a well-defined inner and outer electron for all times. The inner electron bounces back and forth into the nucleus while the outer electron performs an oscillation at a finite distance from the nucleus, which is in turn driven by the motion of the inner electron; see Fig. 13(a). The dynamics can best be monitored in a Poincaré surface of section; see Fig. 14(a) (Richter, 1991; Wintgen *et al.*, 1994); we here choose $r_2=0$, i.e., we plot the momentum and position of the outer electron, whenever the inner electron hits the nucleus. The shortest periodic orbit, which is at the center of the large stable island, corresponds to a configuration in which the outer electron is almost frozen at a finite distance from the nucleus (frozen planet orbit; Richter and Wintgen, 1990b; Richter *et al.*, 1992).[13] The frozen planet orbit is indeed stable and the stable island surrounding it dominates the whole phase space for $Z=2$; see Fig. 14(a). The frozen planet orbit is also stable with respect to the $\Theta$ degree of freedom perpendicular to the symmetry plane, thus forming the center of a stable island in all six phase-space coordinates. This behavior persists over a wide range of $Z$ values (Richter, 1991) and under pertubations by a microwave field (Schlagheck and Buchleitner, 1998) as well as for angular momentum $L\neq 0$ (Yamamoto and Kaneko, 1993). The frozen planet orbit proves in particular that the dynamics of two-electron atoms are *not* ergodic.

This is in contrast to the $eZe$ configuration in which triple collisions can occur [see Fig. 13(b)]; the energy transfer between the electrons depends sensitively on how the particles approach the origin and chaos prevails. The fundamental difference in the dynamics in both cases can be seen in the Poincaré surface of sections; see Figs. 14(a) and 14(b). No stable islands are visible in the $eZe$ configuration, and the region near the origin in the Poincaré plane is completely structureless. In the following, we list some basic properties of the dynamics for the collinear subspaces (see Richter *et al.*, 1993; Blümel and Reinhardt, 1997; as well as Handke *et al.*, 1993, for the related $s$-wave helium):

- Both collinear configurations are unbound in the sense that one electron (say electron 1) can escape, i.e., ionize classically, with an arbitrary amount of kinetic energy. The Hamiltonian (53) has in the limit $r_1\to\infty$ the form of two noninteracting Kepler problems, i.e.,

$$H\underset{r_1\to\infty}{\to}\left(\frac{p_2^2}{2}-\frac{Z}{r_2}\right)+\left(\frac{p_1^2}{2}-\frac{Z-1}{r_1}\right). \tag{54}$$

  The dynamics in both configurations are equivalent in this limit, which is also reflected in the toruslike structure for large $r_1$ in both Figs. 14(a) and 14(b). Note, however, that the tori are not closed in the $eZe$ configuration when the outer electron returns to the nucleus. A typical trajectory alternates here between chaotic motion near the nucleus and time intervals with regular dynamics for $r_1\gg r_2$ until the outer electron eventually escapes to infinity without returning to the nucleus. The periodic orbit at $r_1\equiv\infty$, $p_1\equiv 0$ corresponds to the limiting case of an electron escaping with zero kinetic energy.
- There exists a symbolic dynamics for the chaotic $eZe$ configuration, which maps each trajectory one to one onto a binary symbol string. The symbols are

[13]The extreme localization of the outer electron justifies the use of $r_1$ as an adiabatic parameter in the molecular treatment of the corresponding quantum states; see Sec. III.B.4.

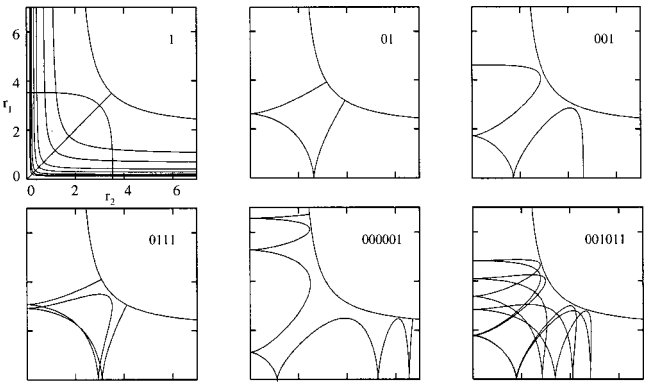


FIG. 15. Some unstable periodic orbits in the chaotic collinear $eZe$ configuration, shown together with their binary code; the fundamental asymmetric stretch orbit is displayed in the upper left corner together with the potential contours $V(r_1,r_2) = -Z/r_1 - Z/r_2 + 1/|r_1+r_2|$ in the classically allowed regime $V \leqslant -1$.

obtained from the rules

1, if a trajectory hits the line $r_1=r_2$ between two collisions with the nucleus $r_2=0$;
0, otherwise.

The symbolic dynamics are generated by the triple-collision orbits, i.e., those trajectories starting in or ending at the singular point $r_1=r_2=0$.

Periodic orbits in the $eZe$ subspace can be characterized by a periodic symbol string $\overline{a} = \ldots aaaa \ldots$ where $a$ is a finite symbol string of length $n$; the number of periodic orbits increases exponentially with the code length and thus with the period and the orbits are all unstable with respect to the dynamics in the collinear plane. The asymmetric stretch orbit $\overline{1}$ is the shortest orbit in this subspace; see upper left picture in Fig. 15. The marginally stable orbit $r_1 \equiv \infty$, $p_1 \equiv 0$ discussed above would have the notation $\overline{0}$ in our code. Some periodic orbits together with their code are displayed in Fig. 15.

- Strong chaos and electron escape in the $eZe$ configuration originates from the triple collision. Large energy and momentum transfer between the electrons that leads to subsequent ionization can happen only if the particles come close to the triple collision. The Wannier orbit running along the line $r_1=r_2$ is a triple-collision orbit; numerical evidence suggests that this orbit is infinitely unstable in the collinear subspace, i.e., for angular momentum $\mathbf{L}=0$ (Richter and Wintgen, 1990a; Kim and Ezra, 1991); see also the discussion in Secs. IV.B.2.b and IV.C.3.
- Both collinear configurations are stable with respect to linear perturbation perpendicular to the collinear phase space; the $Zee$ configuration is at the center of a six-dimensional stable island of the $L=0$ phase space. The $eZe$ configuration is stable in the bending motion corresponding to the dynamics in the $\Theta$ degree of freedom.

The last point is maybe the most important in the quantum context. *The collinear dynamics are disconnected from the rest of the $L=0$ phase space due to the stability in the $\Theta$ degree of freedom.* Two-electron atom eigenstates are localized along the collinear axis because there is an enhanced classical probability of remaining close to the collinear configuration (Wintgen *et al.*, 1994). The quantum and semiclassical consequences of this observation are discussed in Secs. IV.C and IV.D.

#### *b. The symmetry plane of the Wannier ridge*

The symmetry plane of symmetric collective electron motion $r_1 \equiv r_2 = r$, $p_{r_1} \equiv p_{r_2} = p_r$ is known as the Wannier ridge (Fano, 1983). The electron-pair motion in the phase-space region near the symmetry plane $r_1=r_2$ plays an important role in Wannier's classical description of the three-particle breakup at small energies $E>0$ (Wannier, 1953; Eckhardt, 1991). The classical dynamics for $E<0$ are, however, bound and ionization is prevented classically. The Wannier ridge was also proposed to be of importance for quantum resonances below the three-particle breakup threshold $E=0$, especially for symmetrically excited resonances (Fano, 1983; Harris *et al.*, 1990a, 1990b). We shall discuss this aspect in more detail at the end of the section.

The dynamics in the Wannier ridge subspace are of mixed behavior, i.e., classical chaotic regions and regular motion within stable islands coexist. The phase-space dynamics follow the typical KAM scenario (Arnold, 1979) from regular to chaotic dynamics when changing the nuclear charge from $Z=1/4$ to $Z=\infty$ (Richter, 1991; Richter *et al.*, 1993). In Figs. 16(a)–16(d), the phase-space structure is shown for various $Z$ values in the Poincaré surface of section $\Theta=\pi$. The coordinates $X$, $P_X$ correspond to $r$, $p_r$, respectively, after suitable rescaling (Richter *et al.*, 1993). The limit $Z \to 1/4$ is integrable (Richter *et al.*, 1993) and the phase space is filled by invariant tori grouped around the so-called Langmuir orbit (Langmuir, 1921); see Fig. 16(a). The Langmuir orbit corresponds to electron-pair dynamics exhibiting strong bending vibration as shown in Fig. 2(b). An increasing number of (resonant) tori are destroyed when $Z$ becomes larger; see Figs. 16(b)–16(d). Chains of elliptic and hyperbolic fixed points appear and chaotic bands are formed along the hyperbolic fixed points expanding with increasing $Z$.

The physically relevant cases $Z=1$ ($H^-$) and $Z=2$ (helium) [Figs. 16(b) and 16(c)] exhibit a mixed regular and chaotic phase space. The elliptic island around the Langmuir orbit is preserved and clearly dominates the Poincaré section. The Langmuir orbit becomes unstable at $Z \approx 5.6$ and a new orbit born at the bifurcation point converges to a collinear $Zee$ configuration in the limit $Z \to \infty$ (Richter, 1991; Müller and Burgdörfer, 1993). The limit of large nuclear charge $Z=100$ is depicted in Fig. 16(d). The phase space is now mainly covered with remnants of tori or so-called KAM tori (MacKay *et al.*, 1984).

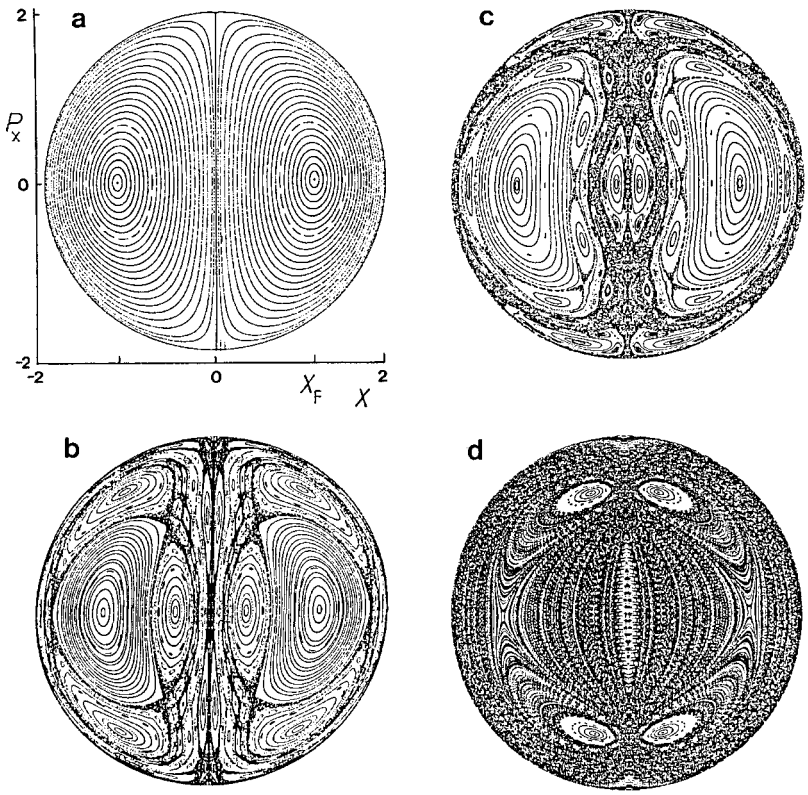


FIG. 16. Poincaré surface of section $\Theta=\pi$ in the Wannier ridge configuration for varying $Z$ values: (a) $Z=0.26$; (b) $Z=1$; (c) $Z=2$; (d) $Z=100$ (adapted from Richter *et al.*, 1993).

The Wannier ridge is, in contrast to the collinear subspaces, mostly unstable with respect to perturbations away from the symmetry plane. This is intuitively clear; a small asymmetry in the electron dynamics tends to get amplified due to the electron-electron repulsion and the trajectory "falls off" the Wannier ridge. Numerical stability analysis for helium shows that the 25 shortest periodic orbits on the Wannier ridge (apart from the Langmuir orbit) are all extremely unstable with respect to hyperangle $\alpha=\arctan(r_1/r_2)$ (Richter, 1991); the dynamics on the Wannier ridge are thus strongly coupled to the rest of the phase space due to the instability in $\alpha$. Localization of quantum states on the Wannier ridge can therefore not be expected semiclassically.

There is, however, one exception: the Langmuir orbit is only moderately unstable in $\alpha$ for most $Z$ values and is even stable for helium, i.e., $Z=2$ (Richter and Wintgen, 1990a). The Wannier ridge is thus strictly speaking not globally unstable in the $\alpha$ coordinate, as conjectured by Wesenberg *et al.* (1985) and Fano and Rau (1986). The stable island indicates the existence of sharp resonances in helium associated with a quantization of the Langmuir orbit; see also the discussion in Sec. IV.C.2.b.

Another "fundamental" mode on the Wannier ridge is the Wannier orbit $\Theta=\pi$, $p_\Theta=0$. It is the only orbit that exists both in the collinear subspace $eZe$ and on the Wannier ridge. (The Wannier orbit forms the boundary of the Poincaré surface in Fig. 16.) The orbit has attracted particular attention in the past, in models of the electron dynamics in symmetrically doubly excited states in $H^-$ and helium (Miller, 1972; Fano, 1983; Harris *et al.*, 1990a, 1990b; Sadeghpour, 1991). Studies by Richter and Wintgen (1990a) indicate, however, that the Wannier orbit is infinitely unstable for $L=0$, reflecting the nonregularizability of the dynamics at the triple-collision point. The influence of the Wannier orbit on the quantum spectrum can thus be dismissed on semiclassical grounds. The semiclassical prediction has been confirmed by quantum calculations. Wave functions of symmetrically excited states tend to be localized perpendicular to the Wannier orbit (Ezra *et al.*, 1991; Kim and Ezra, 1991; Richter and Wintgen, 1993). The Wannier orbit is also absent in a spectral Fourier analysis (Richter, 1991; Blümel and Reinhard, 1992; Qiu *et al.*, 1996) even for angular momentum $\mathbf{L}\neq 0$ (Grémaud and Gaspard, 1998). A detailed discussion is given in Sec. IV.C.3.

### C. Qualitative semiclassical analysis of the two-electron spectrum from fundamental periodic modes

#### 1. Classical interpretation of the spectral structure of two-electron atoms

The structure of the classical dynamics presented in the last section explains many details of the quantum spectrum qualitatively, including propensity rules and widths of resonances, without even referring explicitly to semiclassical arguments.

In the following, we shall restrict the discussion to $L=0$, i.e., we shall analyze the $^1S^e$ or $^3S^e$ spectrum of two-electron atoms, especially of helium, as shown in Fig. 5. Considering total angular momentum $L=0$ im-

plies $M=0$ and also $T=0$ [in Herrick's notation; see Eq. (18)]. We are thus dealing with states below the diagonal in Fig. 10; the transition (B), i.e., $\Delta m=-1$, in Eq. (19) does not occur.

The two collinear invariant subspaces discussed in Sec. IV.B.2 are stable with respect to perturbation in the angle $\Theta$; this implies an enhanced probability of staying close to the collinear configuration both classically and quantum mechanically, as well as localization of quantum states (resonances) on these configurations. The approximate quantum numbers associated with the collinear configurations can be identified by exploiting Herrick's relation (24) for the expectation value of the interelectronic angle $\Theta$, which for large excitation of the outer electron $n\to\infty$ reads

$$\langle\cos\Theta\rangle \underset{n\to\infty}{\to} -\frac{K}{N}=-\frac{N_1-N_2}{N_1+N_2+1} \tag{55}$$

[the above quantum numbers are introduced in Sec. III.B.1; see also Eq. (18)]. The Rydberg series with maximum $K=N-1$ and $\langle\cos\Theta\rangle\approx-1$ are linked to the $eZe$ configuration $\Theta=\pi$ (the corresponding series in Fig. 10 are those in the bottom row). The series with minimal $K=1-N$ and $\langle\cos\Theta\rangle\approx1$ are the states associated with the $Zee$ subspace and $\Theta=0$. These are the series directly below the diagonal in Fig. 10.

The existence of distinct noninteracting Rydberg series for fixed $N$ can semiclassically be related to the stability of the classical dynamics in the $\Theta$ degree of freedom. The Rydberg series with maximal/minimal $K$ interact least with the rest of the spectrum because the classical dynamics near the corresponding collinear subspaces are disconnected from the rest of the classical phase space. The dynamics *in* the $eZe$ configuration are, however, strongly chaotic. We thus expect mixing between series with different $N$ but maximal $K$, i.e., $\Delta N=-1$, $\Delta K=-1$, which is exactly the propensity rule (A), i.e., $\Delta N_1=-1$ listed in Eq. (19). The $Zee$ configuration is fully stable in all degrees of freedom. Interaction between series localized in this collinear subspace, i.e., between series that have minimal $K$ but different $N$ quantum numbers, is exponentially suppressed. This in turn corresponds to the suppression of transition (C) in Eq. (19), i.e., $\Delta N=-1$, $\Delta K=1$, or equivalently $\Delta N_2=-1$, as discussed in a completely different context in Sec. III.B.3.a.

The difference in the resonance widths can be understood along the same lines. The states associated with the $Zee$ configuration can only decay via (dynamical) tunneling (semiclassically described by complex classical paths) and thus have extremely small decay widths and very long lifetimes. The quantum states as well as the classical dynamics are trapped in the classically stable island, and autoionization is exponentially suppressed (Richter and Wintgen, 1991). In the $eZe$ subspace, classical escape is fast along the collinear axis due to the chaotic dynamics. The typical resonance widths are thus orders of magnitude larger than in the stable collinear configuration. Classical escape happens when the two electrons approach the nucleus almost symmetrically along the Wannier orbit, allowing for large momentum transfer between the particles; see also Sec. IV.B.2.a. The Wannier orbit being the link between the collinear $eZe$ configuration and the unstable Wannier-ridge subspace (Sec. IV.B.2.b) is thus an effective escape channel, in agreement with the findings in the molecular adiabatic picture; see Sec. III.B.3.a and Fig. 9. More detailed studies of resonance widths in this $K$ regime were undertaken by Blümel and Reinhardt (1992, 1997) and Burgdörfer *et al.* (1997); they studied in particular the transition from regular resonance structures into the Ericson regime of overlapping and strongly interacting resonances (Ericson, 1960), where an assignment of quantum numbers loses its meaning.

The picture is less clear for intermediate $K$ values in a given $N$ manifold. The classical phase space has not been studied systematically in this region, i.e., for $\Theta\approx\pi/2$. The dynamics are expected to be mixing here in all degrees of freedom, i.e., there are no regions of stability shielded from the rest of the phase space. Numerical studies of the quantum spectrum indicate increasing interference between all Rydberg series. A breakdown of any approximate scheme of quantum numbers in the regime $K\approx0$ and $N\geqslant9$ is indeed observed (Bürgers *et al.*, 1995; Rost and Tanner, 1997). The largest resonance widths in each $N$ manifold are typically found in this intermediate $K$ regime, where classical escape can occur along two degrees of freedom.

### 2. Single-periodic-orbit quantization

In order to get quantitative semiclassical approximations for two-electron resonance positions, a detailed knowledge of the periodic orbits of the system is essential; see Sec. IV.A. We cannot hope to obtain the full spectrum including all the Rydberg series in each $N$ manifold, even when restricting ourselves to $S$ states; the high dimensionality of the classical phase space makes a systematic study of the full set of periodic orbits almost impossible. However, a description of Rydberg series that correspond to classical configurations centered on the collinear subspaces is feasible in light of the previous paragraph. In particular, symmetrically excited intrashell states with $\langle r_1\rangle\approx\langle r_2\rangle$ and wave functions concentrated near the origin can be semiclassically reached by considering the fundamental short periodic orbits only. A full semiclassical treatment of asymmetrically excited states, including complete Rydberg series up to the various single-ionization thresholds, will be presented in Sec. IV.D.

#### *a. The frozen planet orbit*

The two-electron states corresponding to the $Zee$ configuration can be treated within an Einstein-Brillouin-Keller quantization; see Sec. IV.A.2. The center of the classical stability island [see Fig. 14(a)] is dominated by the behavior around the fixed point, the frozen planet periodic orbit. The dynamics in the vicinity of this central orbit can be well described by a harmonic

TABLE II. Total binding energies $-E$ for $^1S^e$ states obtained by single periodic orbit (PO) quantization of the asymmetric stretch orbit Eq. (58) and the frozen planet orbit Eq. (56), compared with full quantum-mechanical (QM) calculations based on complex rotation (Bürgers *et al.*, 1995).

| Asymmetric stretch orbit | | | Frozen planet orbit | | |
|---|---|---|---|---|---|
| $(N,K)_n$ | PO | QM | $(N,K)_n$ | PO | QM |
| $(1,0)_1$ | 3.097 | 2.904 | | | |
| $(2,1)_2$ | 0.804 | 0.778 | $(2,-1)_2$ | | |
| $(3,2)_3$ | 0.362 | 0.354 | $(3,-2)_3$ | 0.248 | 0.257 |
| $(4,3)_4$ | 0.205 | 0.201 | $(4,-3)_4$ | 0.1394 | 0.1411 |
| $(5,4)_5$ | 0.1317 | 0.1294 | $(5,-4)_5$ | 0.0892 | 0.0896 |
| $(6,5)_6$ | 0.0917 | 0.0903 | $(6,-5)_6$ | 0.061 89 | 0.062 05 |
| $(7,6)_7$ | 0.0675 | 0.0665 | $(7,-6)_7$ | 0.045 46 | 0.045 54 |
| $(8,7)_8$ | 0.0517 | 0.0510 | $(8,-7)_8$ | 0.034 80 | 0.034 84 |
| $(9,8)_9$ | 0.0409 | 0.0403 | $(9,-8)_9$ | 0.027 49 | 0.027 52 |
| $(10,9)_10$ | 0.0332 | 0.0327 | $(10,-9)_10$ | 0.022 27 | 0.022 28 |

approximation. The winding numbers, i.e., the frequency ratios $\omega_1/\omega_2$ for the motion on and perpendicular to the frozen planet orbit, are approximately constant for tori close to the central fixed point. This makes it possible to perform a harmonic-oscillator quantization of the core region of the stable island by considering the frozen planet orbit and its normal modes only; the corresponding quantum states are called the frozen planet states. Richter and Wintgen (1990b, 1991) were able to give a simple double Rydberg formula for collinear *Zee* resonance states,

$$E_{m,k,\bar{n}} = -\frac{(S_{\mathrm{FP}}/2\pi)^2}{\left[\left(m+\frac{1}{2}\right)+2\left(k+\frac{1}{2}\right)\sigma_1+\left(\bar{n}+\frac{1}{2}\right)\sigma_2\right]^2},$$

$$m,k,\bar{n}=0,1,2,\ldots, \tag{56}$$

which is similar to semiempirical formulas like Eq. (33), described in Sec. III.E.2. The parameters entering the Rydberg formula are now completely determined in terms of classical properties of the frozen planet orbit; $S_{\mathrm{FP}}/2$ is the (scaled) action of the orbit and $\sigma_1$, $\sigma_2$ are the winding numbers for the dynamics in the $\Theta$ degree of freedom perpendicular to the collinear subspace and for the dynamics in the collinear plane, respectively. (We have $S_{\mathrm{FP}}/2\pi=1.4915$, $\sigma_1=0.4616$, and $\sigma_2=0.0677$ for helium.) The classical parameters are obtained by integrating the linearized dynamics in the neighborhood of the orbit over all degrees of freedom. There are two equivalent degrees of freedom perpendicular to the collinear space, which give rise to the additional factor 2 in Eq. (56). The quantum numbers $(m,k,\bar{n})$ can be related to excitation (of normal modes) parallel $(m)$ and perpendicular $(\bar{n})$ to the periodic orbit and to excitation in the bending degree of freedom $(k)$. We obtain the following identification with the Herrick/Stark quantum numbers $(N,K)_n$ in Eq. (18) and the MO quantum numbers $(\bar{n}_\mu,\bar{n}_\lambda)_{\bar{n}}$ for planetary atom states introduced in Sec. III.B.4:

| frozen planet | $r_>$adiabatic | Herrick/Stark | |
|---|---|---|---|
| $m$ | $=\bar{n}_\mu=$ | $\frac{1}{2}(N-K-1)$ | (57a) |
| $k$ | $=\bar{n}_\lambda=$ | $\frac{1}{2}(N+K-1)$ | (57b) |
| $\bar{n}$ | $=\bar{n}=$ | $n-N.$ | (57c) |

A semiclassical description of the *Zee* configuration is thus equivalent to the molecular adiabatic approximation of planetary atom states (with $r_1=r_>$ being the adiabatic invariant; cf. Sec. III.B.4).

The results from Eq. (56) are in good agreement with full quantum calculations for moderate excitation in $k$ and $\bar{n}$, as can be seen from Table II. The frozen planet approximation becomes increasingly better in the semiclassical limit $N\to\infty$ and exceeds even results obtained from the adiabatic MO approximation in Sec. III.B.4 (Richter *et al.*, 1992).

The localization of *Zee* quantum states on the frozen planet orbit can be observed in the probability densities of numerically obtained quantum wave functions in the $\Theta=0$ plane; see Fig. 17. The excitations along $(m)$ and perpendicular $(\bar{n})$ to the periodic orbit are clearly visible as a regular nodal pattern in the wave functions.

The collinear alignment is weakened with increasing excitation in $k$ and the approximations leading to Eq. (56) break down in this limit. Similarly, the limit $\bar{n}\to\infty$ violates the assumption of being close to the center of the island. Equation (56) indeed does not converge to the correct single ionization thresholds for $\bar{n}\to\infty$, as has been pointed out by Ostrovsky and Prudov (1993), and nonharmonic corrections have to be included in a full Einstein-Brillouin-Keller calculation (Wintgen and Richter, 1994); see also Sec. IV.D.1.

The frozen planet configuration does not exist for $H^-$, i.e., $Z=1$, where the *Zee* subspace is purely repulsive (Richter *et al.*, 1992; Gaspard and Rice, 1994). The existence of frozen planet states also plays an important part in the possible formation of nondispersive two-electron wave packets in helium driven by an electromagnetic field (Schlagheck and Buchleitner, 1999); the classical

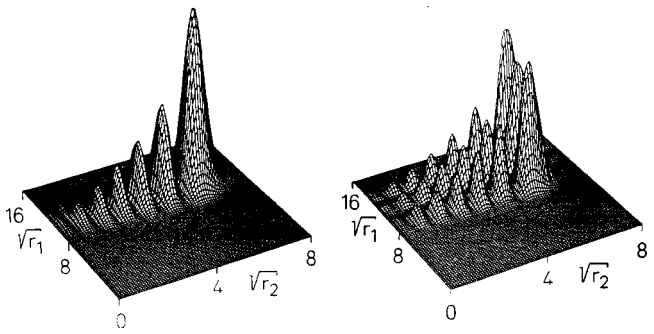


FIG. 17. Frozen planet states, localized along the classical frozen planet orbit [Fig. 13(a)], corresponding to the quantum numbers $m,k,\bar{n}$: (a) $m,k,\bar{n}=6,0,0$; (b) $m,k,\bar{n}=(6,0,2)$ in $^1S^e$ helium; the corresponding $(N,K)_n$ notation is (a) $(7,-6)_7$ and (b) $(7,-6)_9$. The completely symmetrized version of the wave functions is obtained by reflection on the axis $r_1=r_2$ (from Richter *et al.*, 1992).

frozen planet configuration has futhermore been observed for mass ratios different from those of two-electron atoms and has led to the prediction of a new form of a quasistable binding mechanism for antiprotons in atoms (Richter *et al.*, 1991).

### b. The Langmuir orbit

A semiclassical quantization of the Langmuir orbit [see Fig. 2(b)] has been proposed by several authors to approximate the helium ground state (Langmuir, 1921; Dimitrijević and Grujić, 1984; Wesenberg *et al.*, 1985). However, the attempts failed due to the use of incorrect quantization conditions, i.e., an incorrect consideration of the motion perpendicular to the periodic orbit. Richter and Wintgen (1990a) predicted long-lived resonant states for helium with energies given by a double Rydberg formula like Eq. (56) after discovering that the Langmuir orbit is stable in all degrees of freedom; see also Sec. IV.B.2.b. The phase-space volume covered by the stable island around the Langmuir orbit is, however, extremely small yielding upper bounds for the number of states associated with the island (Berry, 1983). Long-lived resonant states localized on the Langmuir orbit are expected only in the limit of extremely high double excitation (Richter and Wintgen, 1990a); Müller and Burgdörfer (1993) give $N\geqslant 500$ as an estimate for the first Langmuir resonance. Müller *et al.* (1992) extended the double-Rydberg formula to low energies and thus obtained approximations for low-lying resonance energies with $N\leqslant 15$ and moderately doubly excited states. They proposed that these Langmuir states correspond to symmetrically excited resonances with maximal bending excitation belonging to the energetically uppermost Rydberg series with minimal $K=1-N$ quantum number (Müller and Burgdörfer, 1993). The semiclassical results of the last section and quantum calculations for doubly excited states in helium with principal quantum numbers $N\leqslant 10$ suggest, however, that resonances belonging to minimal $K$ are of the frozen-planet type and are related to the collinear $Zee$ configuration (Richter and Wintgen, 1993). The Langmuir orbit is expected to play an important role for intermediate $K$ values, $K\approx 0$, and this point of view is supported by results from spectral Fourier transformation (Qiu *et al.*, 1996); see also Sec. IV.C.3.

### c. The asymmetric stretch orbit

The $eZe$ collinear configuration is energetically the most favored subspace, with both electrons being far apart on opposite sites of the nucleus; the configuration is thus a candidate for a semiclassical quantization of the ground state and symmetrically excited intrashell states (corresponding to maximal $K=N-1$ and $N=n$). The fundamental mode in the $eZe$ dynamics close to the nucleus is characterized by the shortest periodic orbit, the asymmetric stretch orbit in Fig. 15. Even though the dynamics in the $eZe$ configuration are chaotic and all periodic orbits including the asymmetric stretch orbit are unstable, we may try to perform a single periodic orbit quantization in a way similar to that outlined in the last few paragraphs. This step will be justified in more detail in Sec. IV.D. A naive asymmetric stretch quantization indeed provides a surprisingly accurate double Rydberg formula for intrashell resonances in two-electron atoms (Ezra *et al.*, 1991; Wintgen *et al.*, 1992):

$$E_{m,k}=-\frac{(S_{\mathrm{AS}}/2\pi)^2}{\left[m+\frac{1}{2}+2\left(k+\frac{1}{2}\right)\sigma_{AS}\right]^2},\quad m,k=0,1,2,\ldots. \tag{58}$$

We obtain $S_{\mathrm{AS}}/2\pi=1.8290$ for the periodic orbit action in helium and $\sigma_{AS}=0.5393$ for the winding number for the dynamics in the bending degree of freedom. The quantum numbers $m$ and $k$ describe excitation along and perpendicular to the orbit, which in turn correspond to intrashell excitation and vibrational excitation in the bending degree of freedom, respectively. We obtain the following identification with the Herrick and MO quantum numbers in Eq. (18):

| asymmetric stretch | $r_{12}$ adiabatic | Herrick/Stark | |
|---|---|---|---|
| $m=$ | $[n_\mu/2]=$ | $\frac{1}{2}(N+K-1),$ | (59a) |
| $k=$ | $n_\lambda=$ | $\frac{1}{2}(N-K-1).$ | (59b) |

Note that the quantum number $\bar{n}$ in Eq. (57c) representing asymmetric excitation perpendicular to the orbit within the collinear plane is absent here due to the instability of the orbit. The collinear $eZe$ quantum numbers are indeed equivalent to the quantum numbers obtained from the molecular approximation [cf. Eq. (18)] with fixed interelectronic axis as described in Sec. III.B.1.

A comparison of Eq. (58) with quantum results is shown in Table II for symmetrically excited states $N=n$, i.e., the lowest states in each Rydberg series $K$

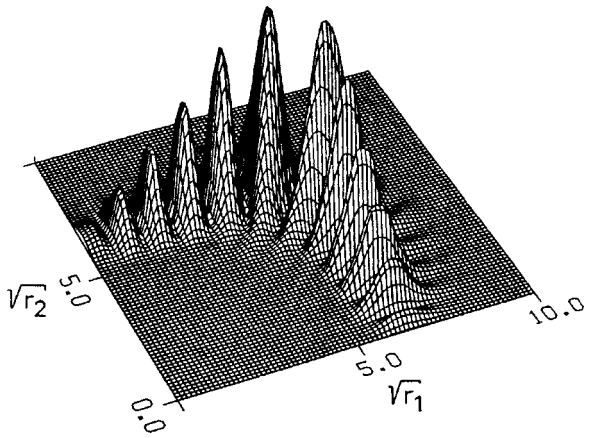


FIG. 18. The $(m,l,k)=(5,0,0)$ wave function (projected onto $\Theta=\pi$) in $^3S^e$ helium; $(N,K)_n=(6,5)_6$; the localization along the asymmetric stretch orbit [see Fig. 13(b)] is clearly visible (from Wintgen *et al.*, 1992).

$=N-1$. The overall good agreement (including the ground state) emphasizes the importance of the asymmetric stretch orbit as a fundamental mode for both the bound and the resonance spectrum in two-electron atoms; see also Table I. The agreement of the Heisenberg-Sommerfeld model, Fig. (3), is not purely accidental; it captures the main ingredients of the dynamics by introducing asymmetric near-collinear motion. Equation (58) also explains semiclassically the existence of double-Rydberg formula found by Rau (1983) and Molina (1989) for symmetrically excited (intrashell) resonances; see Eq. (33) and the discussion in Sec. III.E.2. Müller and co-workers were able to give a semiempirical triple Rydberg formula that contains the semiclassical expressions in Eq. (58) in the limit $K=N-1$ but covers a wide range in $K$ and $N$, reproducing true quantum results with astonishing accuracy (Müller, 1993; Qiu *et al.*, 1996).

The localization of intrashell wave functions on the asymmetric stretch orbit is shown in Fig. 18. The nodal pattern corresponds to excitation along the orbit described by the $m$ quantum number. The tendency of wave functions being repelled from the (very unstable) triple collision and from the Wannier orbit $r_1=r_2$ can be observed here. Similar localization phenomena are found in collinear $ABA$ molecules, where the corresponding wave functions are known as hyperspherical modes (Bisseling *et al.*, 1987, and references therein).

To resolve asymmetric states with $n>N$, more detailed information about the chaotic electron dynamics is needed. This information is provided by including more unstable periodic orbits, which can be incorporated into a quantization schema when making use of the cycle-expansion technique discussed in Sec. IV.A.2. We shall present details in Sec. IV.D.2.

### 3. Spectral Fourier analysis

The connection between classical periodic orbits and quantum traces as outlined in Sec. IV.A.1 allows one to analyze experimental or numerical quantum spectra by Fourier transformation. The method is based on Gutzwiller's formula (38), which for scaling systems has the form

$$d(z)=\sum_n \delta(z-z_n)\approx \bar{d}(z)+\sum_{po} A_{po}e^{izS_{po}}. \tag{60}$$

The sum is taken over all periodic orbits $(po)$ of the system and $z$ is the scaling parameter; we have $S(E)/\hbar=z(E;\hbar)S_{\rm po}=(\hbar\sqrt{-E})^{-1}S_{\rm po}$ [cf. Eq. (52)], for two-electron atoms, and $z_n$ are the scaled quantum eigenvalues. According to Eq. (60), a Fourier transformation of the quantum density of states with respect to $z$ (after subtracting the smooth background $\bar{d}$ on both sides) reveals peaks at the actions of classical periodic orbits. The technique is especially useful for analyzing "chaotic" spectra, i.e., spectra that show no obvious structure in terms of good or approximate quantum numbers. The Fourier transformation uncovers long-range correlations between quantum eigenvalues that may pass unobserved when studying a raw spectrum showing strong level interference on short energy scales (Eichmann *et al.*, 1988). The related scaled energy spectroscopy was first applied to hydrogen in a constant magnetic field (Wintgen, 1987; Holle *et al.*, 1988; Friedrich and Wintgen, 1989) and has now become a standard tool in atomic and molecular spectroscopy.

Scaled energy spectroscopy was first applied to helium by Kim and Ezra (1991) and Richter (1991), who noticed that the Wannier orbit was indeed absent from the Fourier spectrum. This result could be traced back to the fact that the Wannier orbit is infinitely unstable (see also Sec. IV.B.2.b), leading to a vanishing amplitude $A_{\rm po}$ in Gutzwiller's formula [Eq. (60)]. Similar results were reported by Blümel and Reinhard (1992) for the two-dimensional collinear model and by Dräger *et al.* (1994) for the $s$-wave model. The most thorough study of the Fourier-transformed helium $^1S^e$ spectrum has so far been undertaken by Qiu *et al.* (1996; see also Burgdörfer *et al.*, 1997) based on *ab initio* quantum calculations by Bürgers *et al.* (1995). Their results confirm the picture drawn in the previous paragraphs; the asymmetric stretch orbit and the frozen planet orbit dominate the Fourier spectrum for quantum states with maximal and minimal $K$, respectively. The resolution of the Fourier analysis could be considerably enhanced by extrapolating an empirical formula for the $^1S^e$ spectrum (Burgdörfer *et al.*, 1995) to energies above the $N=15$ threshold. Up to 100 orbits of the collinear subspaces could be identified in the Fourier spectrum of the empirical double-Rydberg formula; see Fig. 19. Interestingly, the contribution of the Langmuir orbit was found to dominate the spectrum for intermediate $K$ values, i.e., $K\approx 0$, and $N>15$.

Recently, Gremaud and Gaspard (1998) studied the Fourier transformation of the total $^1S^e$ *and* $^1P^o$ helium spectrum up to $N=7$. As expected from the classical angular momentum scaling in Eq. (52), the Fourier spectrum in both cases is dominated by the collinear asym-

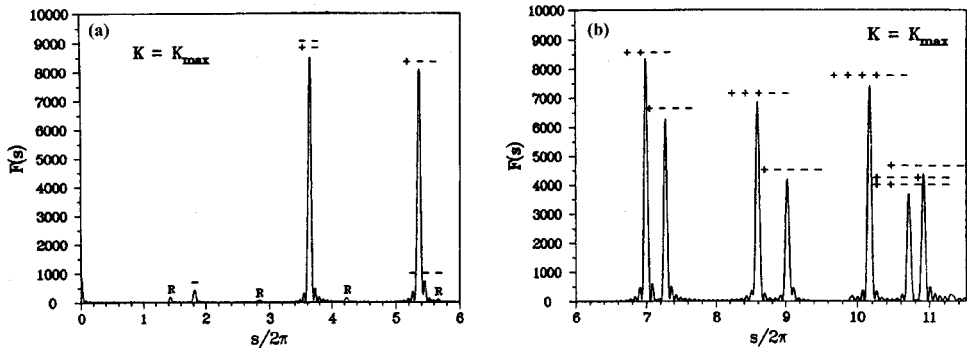


FIG. 19. Fourier transformation of the ${}^1S^e\ (N,N-1)_n$ spectrum corresponding to the chaotic $eZe$ configuration. Dominant peaks are visible at the actions $s$ of various periodic orbits, cf. Fig. 15. Note that the symbol code is $(+,-)$ here corresponding to (0,1) in the notation of Sec. IV.B.2.a (from Qiu *et al.*, 1996).

metric stretch and frozen planet orbits in the $L=0$ classical dynamics. Even $P$ wave functions localized on the asymmetric stretch orbits were found. This again emphasizes the importance of the asymmetric stretch and the frozen planet orbits as the fundamental modes in two-electron atoms. The connection between quantum states with $L\neq 0$ and the classical $L=0$ dynamics can be understood in terms of the scaling relation (52).

### D. Quantitative determination of resonances from semiclassical summation techniques

The semiclassical approximations for bound and resonance states in two-electron atoms in Secs. IV.C.2.a and IV.C.2.c were based on a quantization of the shortest periodic orbits in the collinear subspaces. The double Rydberg formulas (56) and (58) provide good approximations for low-lying states in the corresponding $(N,K)_n$ series, i.e., for $N\approx n$. They fail, however, to reproduce both asymmetrically excited states and Rydberg series converging to the various single ionization thresholds $I_N-Z^2/2N^2$. Resonances close to the thresholds belong to extremely asymmetric states $\langle r_1\rangle \gg \langle r_2\rangle$ and can only be resolved semiclassically, if the classical dynamics in the limit $r_1\to\infty$ are taken appropriately into account. We first consider the almost integrable $Zee$ configuration, which can be treated within the more conventional framework of Einstein-Brillouin-Keller quantization. We shall then use the cycle expansion technique and obtain asymmetric excited resonances $n\geqslant N$ for chaotic collinear $eZe$ states by including long unstable periodic orbits. A special periodic orbit summation technique is introduced in Sec. IV.D.3, which contains the dynamics in the limit $r_1\to\infty$. The corresponding zeta functions resolve the correct Rydberg structure and a semiclassical quantum defect theory can be derived.

#### 1. Einstein-Brillouin-Keller quantization of asymmetric electronic excitations

The double Rydberg formula (56) is based on a harmonic approximation of the torus structure in Fig. 14(a) in the vicinity of the center fixed point. In order to describe the full dynamics of the stable island in the whole collinear subspace, we may take advantage of the near-integrable nature of the $Zee$ configuration. Local canonical transformations to action/angle variables can be found in principle, in which the two-electron atom Hamiltonian takes on the form

$$H(p_1,r_1,p_2,r_2,\Theta,p_\Theta)=H(J_1,J_2,J_3,\phi_1,\phi_2,\phi_3)\approx H(J_1,J_2,J_3), \tag{61}$$

and the usual Einstein-Brillouin-Keller quantization may be performed as indicated in Sec. IV.A.2. There is in general no procedure to derive the local action (and conjugated angle) variables analytically. Methods to determine such transformations numerically have been developed by Bohigas *et al.* (1993; see also Percival, 1974, and Martens and Ezra, 1987), and applied to the collinear $Zee$ problem by Wintgen and Richter (1994).

Following Wintgen and Richter (1994), we may characterize the torus structure in Fig. 14(a) not by actions $J_1$, $J_2$ but in terms of a winding number $\alpha=\omega_2/\omega_1$ with $\omega_i=\partial H/\partial J_i$, $i=1,2$ being the frequencies. The winding number of an (approximately) closed curve in Fig. 14(a) can be determined numerically by integrating a trajectory on that curve. The action $S=\int p\ \mathrm{d}q$ of a trajectory after the first return to the Poincaré section can again be obtained numerically but may be written alternatively for fixed energy as

$$S(\alpha)=2\pi[J_1(\alpha)+\alpha J_2(\alpha)]. \tag{62}$$

In the notation above, $J_1$ represents approximately the radial motion of the inner electron and $J_2$ the radial motion of the outer electron. A third degree of freedom, $J_3$, is identified with the bending degree of freedom and we have $J_3=0$ in the collinear plane. A second important relation between actions and winding numbers holds on the energy manifold. Using $dE=\omega_1\,dJ_1+\omega_2\,dJ_2=0$, we obtain

$$\frac{\partial S}{\partial \alpha}=2\pi J_2(\alpha). \tag{63}$$

The frozen planet orbit corresponds to $S(\alpha_{\mathrm{FP}})=S_{\mathrm{FP}}$ with $\alpha_{\mathrm{FP}}$ ($=0.067\,650$ for helium) being the stability index of the periodic orbit in the collinear plane; see Sec. IV.C.2.a. The periodic orbit condition implies $dS/d\alpha|_{\alpha_{\mathrm{FP}}}=2\pi J_2=0$.

For vanishing electron-electron interaction in the limit $r_1 \to \infty$ we obtain $J_1 \to \infty$ and $\alpha \to 0$. The collinear Hamiltonian (53) then approaches the independent electron limit, Eq. (54), and the action $S(\alpha)$ can be given analytically, i.e.,

$$\lim_{\alpha \to 0} S(\alpha) = \frac{2\pi Z}{\sqrt{-2E}} \left[ 1 + \left( \frac{Z-1}{Z} \alpha \right)^{2/3} \right]^{3/2}. \tag{64}$$

The third degree of freedom $J_3$ perpendicular to the collinear configuration gives rise to an additional term in Eq. (62), which for small $J_3 \neq 0$ can again be written as a function of $\alpha$ only, i.e.,

$$S(\alpha) = 2\pi [J_1(\alpha) + \alpha J_2(\alpha) + 2\alpha_3(\alpha) J_3(\alpha)].$$

The winding number $\alpha_3$ as a function of $\alpha$ is obtained from the linearized dynamics perpendicular to the collinear plane (Wintgen and Richter, 1994).

Inserting the Einstein-Brillouin-Keller quantization condition $J_1 = m + \frac{1}{2}$, $J_2 = \overline{n} + \frac{1}{2}$, $J_3 = k + \frac{1}{2}$ in Eqs. (62) and (63) together with the (numerically obtained) $S(\alpha)$ curve, and exploiting the scaling relation for the actions (52), leads to quantized energy levels $E_{m,k,\overline{n}}$.

The quantum numbers $(m,k,\overline{n})$ are identical to those in Eq. (57). However, the Rydberg structure of the two-electron spectrum together with the correct single ionization thresholds is now fully reproduced, which is guaranteed by incorporating the asymptotic $S(\alpha)$ behavior, Eq. (64). Moreover, the quantitative agreement is remarkably good even down to the lowest states in each series, in which strong electron-electron interaction near the frozen planet orbit contributes dominantly (Wintgen and Richter, 1994).

Ostrovsky (1992) and Ostrovsky and Prudov (1993) proposed an alternative approach by expanding the electron-electron interaction in a multipole series leading to an independent electron-type approximation. The model reproduces the structure of Rydberg series but cannot account for the correlated electron dynamics, which are reflected in the formation of the frozen planet configuration.

### 2. Semiclassical zeta function and symmetrically excited states

A semiclassical treatment of the classically chaotic collinear dynamics ($\Theta = \pi$) cannot rely on a torus quantization, as indicated in the previous section, and must fall back upon the periodic orbit theory developed in Sec. IV.A. Ezra *et al.* (1991; see also Wintgen *et al.*, 1992) were the first to study the semiclassical $eZe$ spectrum including all relevant degrees of freedom. Similar collinear models (neglecting, however, the stable degree of freedom perpendicular to the collinear subspace) were studied by Blümel and Reinhard (1992) and Dräger *et al.* (1994).

The two-electron bound states or resonances associated with the $eZe$ collinear space can be expressed as the zeros of the semiclassical zeta function (40) written as a product over all periodic orbits. For the collinear subspace (including all degrees of freedom in the Monodromy matrix $\mathbf{M}$), it has the form

$$\zeta_{sc}^{-1}(z) = \prod_{k=0}^{\infty} \zeta_k^{-1}(z) = \prod_{k=0}^{\infty} \prod_{l=0}^{\infty} \prod_{po} (1 - t_{po}^{(k,l)}). \tag{65}$$

The products over $k$ and $l$ originate from an expansion of $|\det(\mathbf{M} - \mathbf{1})|^{-1/2}$ in Eq. (40) in terms of the stable $(k)$ and unstable $(l)$ eigenvalues of $\mathbf{M}$. The higher terms in $l$ corresponding to the unstable degree of freedom can in general be neglected and we will set $l = 0$ henceforth. The index $k$ accounts for the stable bending dynamics in the angle $\Theta$ and corresponds to an approximate quantum number, the vibrational quantum number introduced in Eq. (59) in Sec. IV.C.2.c. The spectrum associated with a given $k$ quantum number corresponds to the zeros of the individual zeta functions $\zeta_k^{-1}$.

The periodic orbit weights $t_{po}^{(k)}$ in Eq. (65) are of the form

$$t_{po}^{(k)}(z) = \frac{1}{\sqrt{\Lambda_{po}}} \exp\left[ iz S_{po} - i n_{po} \pi - 4\pi i \left( k + \frac{1}{2} \right) \sigma_{po} \right]. \tag{66}$$

Here $\Lambda_{po}$ is the eigenvalue of $\mathbf{M}$ along the unstable direction; the winding number in the unstable degree of freedom is linked to the code length $n_{po}$ of the periodic orbit in the binary symbolic dynamics introduced in Sec. IV.B.2.a. The winding number associated with the stable degree of freedom is $\sigma_{po}$. The energy dependence is contained in the scaling variable $z = \hbar^{-1}(-E)^{-1/2}$.

The zeta functions $\zeta_k^{-1}$ above can be rewritten in terms of a cumulant expansion; see Sec. IV.A.2. Including only the first term in a binary cycle expansion, as in Eq. (48), leads to a quantization condition

$$\zeta_k^{-1} \approx 1 - t_1^{(k)} \overset{!}{=} 0. \tag{67}$$

The term $t_1^{(k)}$ is the contribution from the asymmetric stretch orbit, the fundamental periodic mode of the collinear configuration (see Fig. 15). Note that the orbit "0" is absent in collinear two-electron atoms. The quantization condition given by Eq. (67) is the leading term in a zeta function expansion and justifies the single periodic orbit quantization (58) introduced in Sec. IV.C.2.c.

The unstable asymmetric stretch orbit can only account for the phase-space region $r_1 \approx r_2$ and thus for intrashell states; the dynamics of asymmetric electron motion are represented by longer periodic orbits, as shown in Fig. 15. The contributions of these orbits are included by taking into account higher terms in a cycle expansion as introduced in Sec. IV.A.2 for each of the semiclassical zeta functions $\zeta_k^{-1}$ separately. By making use of the symbolic dynamics, we obtain an expanded zeta function of the form (48), i.e.,

$$\zeta_k^{-1}(z) = \sum_{j=0}^{\infty} c_j = 1 - [t_0^{(k)} - t_1^{(k)}] - [t_{01}^{(k)} - t_0^{(k)} t_1^{(k)}] - [t_{001}^{(k)} - t_0^{(k)} t_{01}^{(k)} + t_{011}^{(k)} - t_{01}^{(k)} t_1^{(k)}] - \cdots. \tag{68}$$

TABLE III. Real part of the zeros of $\zeta_0^{-1}$ obtained by cycle expansion of length $j$. The exact quantum energies are in the last column. The states are labeled by their principal quantum numbers. A line as entry indicates a missing zero at that level of approximation.

| $N$ | $n$ | $j=1$ | $j=4$ | $j=8$ | $j=12$ | $j=16$ | $-E_{\mathrm{qm}}$ |
|---|---|---|---|---|---|---|---|
| 1 | 1 | 3.0970 | 2.9692 | 2.9001 | 2.9390 | 2.9248 | 2.9037 |
| 2 | 2 | 0.8044 | 0.7714 | 0.7744 | 0.7730 | 0.7727 | 0.7779 |
| 2 | 3 | | 0.5698 | 0.5906 | 0.5916 | 0.5902 | 0.5899 |
| 2 | 4 | | | | 0.5383 | 0.5429 | 0.5449 |
| 3 | 3 | 0.3622 | 0.3472 | 0.3543 | 0.3535 | 0.3503 | 0.3535 |
| 3 | 4 | | | 0.2812 | 0.2808 | 0.2808 | 0.2811 |
| 3 | 5 | | | 0.2550 | 0.2561 | 0.2559 | 0.2560 |
| 3 | 6 | | | | 0.2416 | 0.2433 | 0.2438 |
| 4 | 4 | 0.2050 | 0.1962 | 0.1980 | 0.2004 | 0.2012 | 0.2010 |
| 4 | 5 | | 0.1655 | 0.1650 | 0.1654 | 0.1657 | 0.1657 |
| 4 | 6 | | | 0.1508 | 0.1505 | 0.1507 | 0.1508 |
| 4 | 7 | | | 0.1413 | 0.1426 | 0.1426 | 0.1426 |

The weights $t_{\mathrm{po}}^{(k)}$ are given by Eq. (66) and the cumulant terms $c_j$ defined in Eq. (45) contain all contributions of orbits and composite orbits having the same total symbol length $j$. The expanded zeta functions depend only on the classical actions, stability indices, and winding numbers, which have to be determined numerically by integrating the equations of motion along the periodic orbits (Richter *et al.*, 1993). We set $t_0=0$ in Eq. (68) due to the absence of the orbit "0." This fact has serious consequences related to the existence of Rydberg series and will be discussed in Sec. IV.D.3.

The cycle-expanded zeta functions, Eq. (68), yield good approximations of the energies for intrashell resonant states $n=N$; cf. Table III. Moreover, subsequent states with $n>N$ in each Rydberg series are gradually revealed with increasing $j$, i.e., by including higher cumulants and thus longer and longer orbits in the cycle expansion.

Even interference effects between states in overlapping Rydberg series for $N\geqslant 4$ can be resolved semiclassically (Wintgen *et al.*, 1994). Results of equal quality have been obtained for $H^-$ (including weak-magnetic-field effects) by Gaspard and Rice (1994). Moderate excitation in $\Theta$ can be accounted for by choosing $k>0$ in Eq. (68) (Wintgen *et al.*, 1992). Classical and semiclassical studies beyond the linear approximation in the $\Theta$ dynamics have been reported by Grujić and Simonović (1995).

### 3. Rydberg series and semiclassical quantum defect theory for collinear *eZe* states

The cycle-expansion technique presented above provides results of considerable accuracy for intra-shell resonant states and states with moderate asymmetric excitation. However, it cannot resolve the Rydberg structure at the single ionization thresholds, which must include the classical dynamics in the limit $r_1\to\infty$ corresponding to very long periodic orbits and thus long symbol codes. A connection of the phase-space regions for small and large $r_1$ is less obvious than in the *Zee* configuration, in which invariant tori provide the transition. The classical dynamics in the collinear *eZe* subspace show a gradual change from chaos to regular dynamics with increasing $r_1$, cf. Fig. 14(b), and a smooth link between these two limits can be provided by the periodic orbits of the system, as will be shown next.

Tanner and Wintgen (1995) proposed to rewrite the expansion (68) in a way that includes regular orbits stretching out along the $r_1$ axis up to infinity (an example of such an orbit is the 000 001 orbit in Fig. 15) before dealing with the complicated chaotic dynamics near the nucleus (represented, for example, by the 001 011 orbit in Fig. 15). The new expansion schema for the zeta function (65) corresponds to switching from the binary alphabet (0,1) to an infinite letter alphabet according to the rule (Tanner *et al.*, 1996; Rost and Tanner, 1997)

$$10^{n-1}\to n;\quad 10^{n-1}10^{m-1}\to nm\quad \ldots,$$

and $0^n$ stands for $n$ 0's occurring successively in a row. The expansion is now written in terms of infinite sums over the regular 0 tails explicitly, i.e.,

$$\zeta_k^{-1}(z)=1-\sum_{n=1}^{\infty} t_n^{(k)}-\sum_{m=1}^{\infty}\sum_{n=1}^{\infty}\frac{1}{2}(t_{mn}^{(k)}-t_m^{(k)}t_n^{(k)})-\sum_{l=1}^{\infty}\sum_{m=1}^{\infty}\sum_{n=1}^{\infty}\ldots, \tag{69}$$

and the periodic orbit weights are again given by Eq. (66). The fundamental term $1-\Sigma_{n=1}^{\infty}t_n^{(k)}$ contains periodic orbits with code $10^{n-1}$. It can be seen as the building block for the zeta function; its zeros reproduce the gross structure of the Rydberg spectrum. Subsequent terms in Eq. (69) give corrections that account for interactions between overlapping Rydberg series corresponding to different $N$ quantum numbers.

A quasi-Einstein-Brillouin-Keller formula can be derived revealing the basic structure of the spectrum by approximating the zeta function by its fundamental term only (Tanner and Wintgen, 1995; Rost and Tanner, 1997), i.e.,

$$\zeta_k^{-1}(z) \approx 1 - \sum_{n=1}^{\infty} t_n^{(k)}(z) \approx 1 - \sum_{m=-\infty}^{\infty} \int_1^{\infty} dn\, e^{2\pi i m n}\, t_n^{(k)}(z). \quad (70)$$

Poisson summation has been used in the last step and $n$ is now a continuous variable. Approximating the integrals by stationary phase yields the condition

$$\frac{\partial}{\partial n}\left[ z\frac{S(n)}{2\pi} - \left(m+\frac{1}{2}\right)n - 2\left(k+\frac{1}{2}\right)\sigma(n)\right] = 0, \quad (71)$$

with $S(n)$ corresponding to the actions of periodic orbits with symbol codes $01^{n-1}$. The quantization condition $\zeta_k^{-1}(E) \approx 1 - \Sigma_{n=1}^{\infty} t_n^{(k)} \overset{!}{=} 0$ implies (in stationary phase approximation) the phase quantization

$$z\frac{S(n)}{2\pi} - \left(m+\frac{1}{2}\right)n - 2\left(k+\frac{1}{2}\right)\sigma(n) = \bar{n} + \frac{1}{8}, \quad (72)$$

with integer $\bar{n} \geq 0$. Equations (71) and (72) correspond exactly to the Einstein-Brillouin-Keller quantization in Eqs. (62) and (63). The regular chaos transition producing nonclosed tori in phase space leads to the unusual action quantization condition $\bar{n} + 1/8$ for the motion of the outer electron.

The quasi-Einstein-Brillouin-Keller quantization using Eqs. (71) and (72) in the same way as in Sec. IV.D.1 reproduces Rydberg series converging to the correct ionization thresholds and coincide well with full three-dimensional quantum calculations, especially in the large $\bar{n}$ limit (Tanner and Wintgen, 1995). It does not capture the interaction between overlapping Rydberg series manifesting itself in perturber states. These states can be resolved by including higher terms in the expansion (69) (Tanner and Wintgen, 1995).

The quasi-Einstein-Brillouin-Keller formalism allows the derivation of a simple estimate for quantum defects at threshold energies. The quantum defect $\nu_{N,K}(E)$ is defined as the smooth function through the points (Friedrich, 1998)

$$E_{(N,K)_n} = I_N - \frac{1}{2[n - \nu(E_{(N,K)_n})]^2}, \quad (73)$$

where $n \geq N$ counts the states successively up to the threshold energy $I_N$. The quasi-Einstein-Brillouin-Keller approximation for the threshold values $\nu_{N,K}$ is given by the simple formula (Rost and Tanner, 1997)

$$\nu_{N,K}(I_N) = (1+s_0)\,N - 2\left(k+\frac{1}{2}\right)\sigma_0 - \frac{1}{8} + n_{\mathrm{per}}, \quad (74)$$

where $n_{\mathrm{per}}$ counts the number of perturber states in the $N$ series and $s_0$, $\sigma_0$ are coefficients determined by periodic orbit data (one obtains $s_0 = -0.437\,09$, $\sigma_0 = 0.304\,91$ for helium). Equation (74) is in good agreement with quantum results (see Table IV). The unusual phase 1/8, arising from the nonclosure of the tori in phase space, is especially crucial at the thresholds.

TABLE IV. Quantum defects at the various threshold energies $I_N = -2/N^2$ (from Rost and Tanner, 1997).

| $N$ | 1 | 2 | 3 | 4 | 5 | 6 | 7 |
|---|---|---|---|---|---|---|---|
| MQDT | 0.140 | 0.685 | 1.272 | 2.785 | 3.410 | 4.953 | 6.391 |
| QEBK | 0.133 | 0.696 | 1.259 | 2.822 | 3.385 | 4.948 | 6.510 |

The infinite periodic orbit sums thus account for the quasiregular dynamics in the separable limit of noninteracting electrons. The Rydberg series structure of the spectrum is correctly described, and the resonances follow a simple Einstein-Brillouin-Keller quantization scheme near the thresholds. The chaoticity of the central phase-space region plays, however, a crucial role in reproducing mixing and interference between overlapping series.

## V. CONCLUSION AND OUTLOOK

### A. Summary

We can distinguish roughly three periods in which characteristic problems in two-electron atoms, most clearly exemplified in helium, have been addressed. These periods reflect a shift in interest towards higher excitation energies.

#### 1. Helium after 1920: The quest for quantum mechanics

The failure of the old quantum theory to describe a stable two-electron atom, as described in Sec. II, triggered the invention and development of quantum mechanics. Once the basic formalism had been established by Heisenberg and Schrödinger, early variational calculations produced remarkably good results for the ground state. This quick success was possible because the variational technique was already known (the Rayleigh-Ritz variational principle). The central-field approximation together with the Hartree-Fock self-consistent-field method finally made it possible to understand and compute large parts of the periodic table, including excited bound states of helium. The pictures and ideas developed in a semiclassical context for two-electron atoms within the old quantum mechanics were obsolete and quickly forgotten in view of the success of the new quantum wave mechanics.

#### 2. Helium after 1960: The need to go beyond the Hartree-Fock approximation

With the seminal synchrotron absorption experiments leading to doubly excited states in the early 1960's it became clear that the effective single-particle picture, familiar from the successful Hartree-Fock approximation, was inadequate for two-electron resonances. As a

consequence, sophisticated alternative quantum approximations were developed over the next 30 years. The most important concepts were a group-theoretical approach and two adiabatic approximations, as described in Sec. III. These concepts successfully explained the high degree of nontrivial regularity in the spectra of two-electron resonances, i.e., features that could not and cannot be accounted for by an effective single-particle picture. Rather, they are intrinsically related to the *correlated* dynamics of two electrons.

#### 3. Helium after 1990: The quest for new concepts to understand the extreme excitation regime

Over the last decade the regime of extremely high excitation of both electrons, i.e., $N \approx n \geq 10$, has become feasible both experimentally and computationally. For these high excitations the approximate quantum numbers begin to lose their meaning and the regularities in the two-electron resonance spectrum start to dissolve. Moreover, even if applicable, the spectroscopic concept of isolated resonances identified by a set of quantum numbers becomes very questionable if the density of resonances per unit energy tends to infinity, which is the case towards the three-body breakup limit $E=0$ with $N \approx n \to \infty$. Hence one needs an alternative concept to understand two-electron dynamics in this regime of extreme double excitation. This concept is provided by the modern semiclassical approach. Its development over the last few years, reviewed in Sec. IV, reveals impressive progress in the quantitative description of the resonances by cycle expansion and the quasi-Einstein-Brillouin-Keller approach. The backbone of these semiclassical descriptions are the periodic orbits of the full classical two-electron system without approximations.

It is very gratifying to see that from the shortest and simplest periodic orbits and from their stability properties one can draw a picture of two-electron excitation dynamics that agrees perfectly well with the results of the quantum approximations explaining the regular spectrum of intermediate double excitation. The asymmetric stretch and the frozen planet orbit can carry quantized two-electron resonances. The third fundamental collinear orbit, the Wannier orbit, is too unstable for resonance formation. Instead, it represents the main decay path for the resonances.

However, the periodic orbits have one advantage that goes beyond the simple structural picture discussed above: A representation of the spectra in terms of periodic orbits, in particular through periodic orbit spectroscopy, does not rely on an explicit quantization scheme based on the quasiseparability of the problem into (collective) coordinates or the existence of approximate quantum numbers. This advantage might lead the way into the extreme excitation regime, where the increase of resonances renders meaningless a description in terms of assigned quantum numbers. Moreover, the limit of high excitations naturally calls for semiclassical methods. One tool, which has already proved very useful for characterizing dynamical features in the extreme excitation limit for hydrogen in a magnetic field, is scaled periodic orbit spectroscopy. As described in Sec. IV.C.3, the incredibly complex energy spectrum with many (overlapping) resonances can look quite ordered, if properly Fourier transformed into the time domain in which peaks at certain times indicate the periods of relevant periodic orbits.

### B. Outlook

An important and interesting issue for the future is two-electron dynamics in the extreme excitation limit towards the three-body breakup threshold.

- Which kinds of resonances will survive as isolated identifiable structures?
- Will collective effects arise and which observable signature do they produce?
- Is chaotic behavior directly observable?

We expect that most of these questions can be discussed theoretically in the context of classical nonlinear dynamics. Some of them have already been addressed. In particular, it has been argued that Ericson fluctuations (Ericson, 1960) may occur in two-electron spectra (Rost and Wintgen, 1996; Blümel and Reinhardt, 1997; Burgdörfer *et al.*, 1997; Grémaud and Delande, 1997). This shows that, in the extreme excitation regime, features could be possible that are common to many few-body systems.

Working towards a solution of these questions can make the helium atom once again a catalyst for the development of novel concepts and perspectives for few-body physics.

## ACKNOWLEDGMENTS

We have written this review in memory of Dieter Wintgen and his pioneering contributions to ''quantum chaos'' in atomic physics. His distinct knowledge both in atomic physics and in modern nonlinear dynamics triggered the revival of modern semiclassical methods in two-electron atoms. With two of the authors being former Ph.D. students of Dieter and the third a collaborator on several projects, we all shared with him interest, insight, and esteem for the intricacy of the three-body Coulomb problem.

We acknowledge fruitful collaboration with J. S. Briggs, J. T. Broad, A. Bürgers, M. Domke, G. Ezra, J. Feagin, D. Herschbach, G. Kaindl, E. A. Solovev, R. Thürwächter, A. Vollweiter, and D. Wintgen. For frequent discussions on two-electron dynamics we thank R. Blümel, E. Bogomolny, J. Burgdörfer, P. Cvitanović, D. Delande, U. Eichmann, H. Friedrich, C. H. Greene, R. Gersbacher, H. Klar, W. Sandner, and V. Schmidt. We would also like to thank Jon Keating for carefully reading parts of the manuscript. Finally, we are grateful for the financial support of this work by the Deutsche Forschungsgemeinschaft (DFG), in particular within the Sonderforschungsbereich 276 at Freiburg University. Partial support from the DFG under Contract No.

Wi877/2 (K.R.), Wi877/5 (G.T.), TA181/1 (G.T.) and under the Gerhard Hess-Programm (J.M.R.), as well as from the A. von Humboldt Foundation (K.R., J.M.R.) and the Deutscher Akademischer Austauschdienst (J.M.R.), is also acknowledged. We also thank the Isaac Newton Institute for Mathematical Sciences, Cambridge, where part of this review was prepared.

## REFERENCES

Aarseth, S. J., and K. Zare, 1974, Celest. Mech. **10**, 185.
Abramov, D. I., V. V. Gusev, and L. I. Ponomarev, 1997, Phys. At. Nucl. **60**, 1133.
Abrashkevich, A. G., D. G. Abrashkevich, and M. Shapiro, 1995, Comput. Phys. Commun. **90**, 311.
Arnold, V. I., 1979, *Mathematical Methods in Classical Mechanics* (Springer, New York).
Arnold, V. I., 1991, Ed., *Dynamical Systems III; Mathematical Aspects of Classical and Celestical Mechanics* (Springer, Berlin).
Artuso, R., E. Aurell, and P. Cvitanović, 1990, Nonlinearity **3**, 325 and 361.
Atsumi, T., T. Isihara, M. Koyama, and M. Matsuzawa, 1990, Phys. Rev. A **42**, 6391.
Aurich, R., M. Sieber, and F. Steiner, 1988, Phys. Rev. Lett. **61**, 483.
Aymar, M., C. H. Greene, and E. Luc-Koenig, 1996, Rev. Mod. Phys. **68**, 1015.
Bachau, H., 1984, J. Phys. B **17**, 1771.
Bachau, H., 1988, J. Phys. B **21**, 3547.
Bachelard, G., 1941, *Le Nouvel Esprit Scientifique* (Presses Universitaires de France, Paris), p. 152.
Balian, R. C., and C. Bloch, 1972, Ann. Phys. (Paris) **69**, 76.
Balian, R. C., and C. Bloch, 1974, Ann. Phys. (Paris) **85**, 514.
Balslev, E., and J. M. Combes, 1971, Commun. Math. Phys. **22**, 280.
Belov, A. A., and D. V. Khveshchenko, 1985, Sov. Phys. JETP **62**, 1138.
Bergeson, S. D., *et al.*, 1998, Phys. Rev. Lett. **80**, 3475.
Berry, M. V., 1983, in *Chaotic Behaviour of Deterministic Systems*, edited by G. Iooss (North-Holland, Amsterdam), p. 172.
Berry, M. V., and J. P. Keating, 1990, J. Phys. A **23**, 4839.
Berry, M. V., and M. Tabor, 1976, Proc. R. Soc. London, Ser. A **349**, 101.
Berry, M. V., and M. Tabor, 1977, J. Phys. A **10**, 371.
Bethe, H. A., and E. E. Salpeter, 1977, *Quantum Mechanics of One- and Two-Eelectron Atoms* (Plenum, New York).
Bhatia, A. K., and A. Temkin, 1975, Phys. Rev. A **11**, 2018.
Bhatia, A. K., and A. Temkin, 1984, Phys. Rev. A **29**, 1895.
Bisseling, R. H., R. Kossloff, J. Manz, F. Mrugala, J. Römelt, and G. Weichselbaum, 1987, J. Chem. Phys. **86**, 2626.
Bloomfield, L. A., R. R. Freeman, W. E. Cooke, and J. Bokor, 1984, Phys. Rev. Lett. **53**, 2234.
Blümel, R., and W. P. Reinhardt, 1992, *Directions in Chaos Vol. 4*, edited by D. H. Feng and J.-M. Yuan (World Scientific, Singapore), p. 245.
Blümel, R., and W. P. Reinhardt, 1997, *Chaos in Atomic Physics* (Cambridge University Press, Cambridge).
Bogomolny, E., 1992, Nonlinearity **5**, 805.
Bohigas, O., 1991, in *Chaos and Quantum Physics*, Les Houches, Session LII 1989, edited by M. J. Giannoni, A. Voros, and J. Zinn-Justin (Elsevier, Amsterdam), p. 87.
Bohigas, O., S. Tomsovic, and D. Ullmo, 1993, Phys. Rep. **223**, 44.
Bohr, N., 1913, Philos. Mag. **26**, 476.
Born, M., 1925, *Vorlesungen über Atommechanik* (Springer, Berlin); English translation: Lectures on *the Mechanics of the Atom* (Ungar, New York, 1927).
Born, M., and W. Heisenberg, 1923, Z. Phys. **16**, 229.
Brotton, S. J., S. Cvejanovic, F. J. Currell, N. J. Bowring, and F. H. Read, 1997, Phys. Rev. A **55**, 318.
Buckmann, S. J., P. Hammond, F. H. Read, and G. C. King, 1983, J. Phys. B **16**, 4039.
Buckmann, S. J., and D. S. Newman, 1987, J. Phys. B **20**, L711.
Buckman, S. J., and C. W. Clark, 1994, Rev. Mod. Phys. **66**, 539.
Burgdörfer, J., Y. Qiu, and J. Müller, 1997, *Classical, Semiclassical and Quantum Dynamics in Atoms*, edited by H. Friedrich and B. Eckhardt (Springer-Verlag, Berlin), p. 304.
Burgdörfer, J., X. Yang, and J. Müller, 1995, Chaos Solitons Fractals **5**, 1235.
Bürgers, A., D. Wintgen, and J.-M. Rost, 1995, J. Phys. B **28**, 3163.
Byron, F. W., and C. J. Joachain, 1989, Phys. Rep. **179**, 212.
Camus, P., T. F. Gallagher, J. M. Lecomte, P. Pillet, L. Pruvost, and J. Boulmer, 1989, Phys. Rev. Lett. **62**, 2365.
Cassidy, D. C., 1995, *Werner Heisenberg* (Spektrum Akademischer Verlag Heidelberg), Sec. II.8: ''Der blonde Bauernjunge.''
Chen, Z., C. G. Bao, and C. D. Lin, 1992, J. Phys. B **25**, 61.
Chrysos, M., G. Aspromallis, Y. Komninos, and C. A. Nicolaides, 1992, Phys. Rev. A **46**, 5789.
Chrysos, M. Y., Y. Komninos, Th. Mercouris, and C. A. Nicolaides, 1990, Phys. Rev. A **42**, 2634.
Cooper, J. W., U. Fano, and F. Prats, 1963, Phys. Rev. Lett. **10**, 518.
Cortés, M., and F. Martin, 1993, Phys. Rev. A **48**, 1227.
Creagh, S. C., J. M. Robbins, and R. G. Littlejohn, 1990, Phys. Rev. A **42**, 1907.
Cvitanović, P., 1988, Phys. Rev. Lett. **61**, 2729.
Cvitanović, P., and B. Eckhardt, 1989, Phys. Rev. Lett. **63**, 823.
Cvitanović, P., 1998, *Classical and Quantum Chaos: A Cyclist Treatise (Das Buch)*, http://www.nbi.dk/ChaosBook/.
Dietz, B., and U. Smilansky, 1993, Chaos **3**, 581.
Dimitrijević, M. S., and P. V. Grujić, 1984, Z. Naturforsch. Teil A **39A**, 930.
Dmitrieva, I. K., and G. I. Plindov, 1988, J. Phys. B **21**, 3055.
Dmitrieva, I. K., and G. I. Plindov, 1988b, Opt. Spectrosc. **64**, 162.
Dmitrieva, I. K., and G. I. Plindov, 1989, J. Phys. B **22**, 1297.
Dmitrieva, I. K., and G. I. Plindov, 1990, J. Phys. B **23**, 693.
Dmitrieva, I. K., and G. I. Plindov, 1991, J. Phys. B **24**, 3149.
Domke, M., G. Remmers, and G. Kaindl, 1992, Phys. Rev. Lett. **69**, 1171.
Domke, M., K. Schulz, G. Remmers, A. Gutiérrez, G. Kaindl, and D. Wintgen, 1995, Phys. Rev. A **51**, R4309.
Domke, M., K. Schulz, G. Remmers, G. Kaindl, and D. Wintgen, 1996, Phys. Rev. A **53**, 1424.
Domke, M., C. Xue, A. Puschmann, T. Mandel, E. Hudson, D. A. Shirley, G. Kaindl, C. H. Greene, H. R. Sadeghpour, and H. Petersen, 1991, Phys. Rev. Lett. **66**, 1306.
Doolen, G. D., J. Nuttall, and R. W. Stagat, 1974, Phys. Rev. A **10**, 1612.
Doron, E., and U. Smilansky, 1992, Nonlinearity **5**, 1055.

Drake, G. W. F., 1988, Nucl. Instrum. Methods Phys. Res. B **31**, 7.
Drake, G. W. F., 1993, in *Long-Range Casimir Forces: Theory and Recent Experiments on Atomic Systems*, edited by F. S. Levin and D. A. Micha (Plenum, New York), p. 107.
Dräger, M., G. Handke, W. Ihra, and H. Friedrich, 1994, Phys. Rev. A **50**, 3793.
Duan, Y., C. Browne, and J.-M. Yuan, 1999, Phys. Rev. A **59**, 238.
Eckhardt, B., 1991, Habilitationsschrift (Universität Marburg).
Eckhardt, B., and E. Aurell, 1989, Europhys. Lett. **9**, 509.
Eichmann, U., P. Brockmann, V. Lange, and W. Sandner, 1989, J. Phys. B **22**, L361.
Eichmann, U., V. Lange, and W. Sandner, 1990, Phys. Rev. Lett. **64**, 274.
Eichmann, U., V. Lange, and W. Sandner, 1992, Phys. Rev. Lett. **68**, 21.
Eichmann, U., K. Richter, D. Wintgen, and W. Sandner, 1988, Phys. Rev. Lett. **61**, 2438.
Eikema, K. S. E., W. Ubachs, W. Vassen, and W. Hogervorst, 1996, Phys. Rev. Lett. **76**, 1216.
Einstein, A., 1917, Verh. Dtsch. Phys. Ges. **19**, 82.
Ericson, T., 1960, Phys. Rev. Lett. **5**, 430.
Ezra, G. S., K. Richter, G. Tanner, and D. Wintgen, 1991, J. Phys. B **24**, L413.
Fano, U., 1961, Phys. Rev. **124**, 1866.
Fano, U., 1983, Rep. Prog. Phys. **46**, 97.
Fano, U., and J. W. Cooper, 1965, Phys. Rev. **137**, A1364.
Fano, U., and A. R. P. Rau, 1986, *Atomic Collisions and Spectra* (Academic Press, New York).
Feagin, J. M., and J. S. Briggs, 1986, Phys. Rev. Lett. **57**, 984.
Feagin, J. M., and J. S. Briggs, 1988, Phys. Rev. A **37**, 4599.
Feynman, R. P., and A. R. Hibbs, 1965, *Quantum Mechanics and Path Integrals* (McGraw-Hill, New York).
Friedrich, H., 1998, *Theoretical Atomic Physics* (Springer, Berlin).
Friedrich, H., and D. Wintgen, 1989, Phys. Rep. **183**, 37.
Froese-Fischer, C., and M. Indrees, 1990, J. Phys. B **23**, 679.
Fukuda, H., N. Koyama, and M. Matsuzawa, 1987, J. Phys. B **20**, 2959.
Gallagher, T., 1994, *Rydberg Atoms* (Cambridge University Press, Cambridge).
Gaspard, P., and S. A. Rice, 1994, Phys. Rev. A **48**, 838.
Gerasimovich, E. A., I. K. Dmitrieva, and G. I. Plindov, 1996, J. Phys. B **29**, 5227.
Goldstein, H., 1980, *Classical Mechanics* (Addison-Wesley, Reading, MA).
Gou, B. C., Z. Chen, and C. D. Lin, 1991, Phys. Rev. A **43**, 3260.
Grémaud, B., and D. Delande, 1997, Europhys. Lett. **40**, 363.
Grémaud, B., and P. Gaspard, 1998, J. Phys. B **31**, 1671.
Grujić, P. V., and N. S. Simonović, 1995, J. Phys. B **28**, 1159.
Gu, Y., and J.-M. Yuan, 1993, Phys. Rev. A **47**, R2442.
Guhr, T., A. M. Müller-Groeling, and H. A. Weidenmüller, 1998, Phys. Rep. **299**, 189.
Gutzwiller, M. C., 1967, J. Math. Phys. **8**, 1979.
Gutzwiller, M. C., 1971, J. Math. Phys. **12**, 343.
Gutzwiller, M. C., 1990, *Chaos in Classical and Quantum Mechanics* (Springer, New York).
Gutzwiller, M. C., 1995, in *Few Body Problems in Physics*, AIP Conf. Proc. No. 334, edited by F. Gross (AIP, Woodbury, New York), p. 275.
Gutzwiller, M. C., 1998, Rev. Mod. Phys. **70**, 589.
Halzen F., and A. D. Martin, 1984, *Quarks and Leptons: An Introductory Course in Modern Particle Physics* (Wiley, New York).
Hamacher, P., and J. Hinze, 1989, J. Phys. B **22**, 3397.
Handke, G., M. Dräger, and H. Friedrich, 1993, Physica A **197**, 113.
Harris, P. G., H. C. Bryant, A. H. Mohaghegli, R. A. Reeder, H. Sharifian, H. Tootoonchi, C. Y. Tang, J. B. Donahue, C. R. Quick, D. C. Rislove, and W. W. Smith, 1990a, Phys. Rev. Lett. **65**, 309.
Harris, P. G., H. C. Bryant, A. H. Mohaghegli, R. Reeder, C. Y. Tang, J. B. Donahue, and C. R. Quick, 1990b, Phys. Rev. A **42**, 6443.
Hayes, M. A., and M. P. Scott, 1988, J. Phys. B **21**, 1499.
Heim, T. A., G. B. Armen, and A. R. P. Rau, 1997, Phys. Rev. A **55**, 2674.
Heisenberg, W., 1922, letter to Sommerfeld, 28 October 1922; archive of the *Deutsches Museum*, Munich.
Heisenberg, W., 1925, Z. Phys. **33**, 879.
Heisenberg, W., 1926, Z. Phys. **39**, 499.
Heitmann, D., and J. P. Kotthaus, 1993, Phys. Today **46**(6), 56.
Heller, E. J., and S. Tomsovic, 1993, Phys. Today **46**(7), 38.
Hernandez, M. I., and D. C. Clary, 1996, J. Chem. Phys. **104**, 8413.
Herrick, D. R., 1975a, Phys. Rev. A **12**, 413.
Herrick, D. R., 1975b, J. Math. Phys. **16**, 281.
Herrick, D. R., 1983, Adv. Chem. Phys. **52**, 1.
Herrick, D. R., and M. E. Kellman, 1980, Phys. Rev. A **21**, 418.
Herrick, D. R., M. E. Kellman, and R. D. Poliak, 1980, Phys. Rev. A **22**, 1517.
Herrick, D. R., and A. O. Sinanoglu, 1975, Phys. Rev. A **11**, 97.
Herrick, D. R., and F. H. Stillinger, 1975, Phys. Rev. A **11**, 42.
Herschbach, D. R., 1986, J. Chem. Phys. **84**, 838.
Herschbach, D. R., 1993, Dudley Herschbach Festschrift, J. Chem. Phys. **97**, special issue.
Herschbach, D. R., O. Goscinsci, and J. S. Avery, 1993, Eds., *Dimensional Scaling in Chemical Physics* (Kluwer, Dordrecht).
Hicks, P. J., and J. Comer, 1975, J. Phys. A **8**, 1866.
Ho, Y. K., 1983, Phys. Rep. **99**, 1.
Ho, Y. K., 1986, Phys. Rev. A **34**, 4402.
Ho, Y. K., 1989, Z. Phys. D: At., Mol. Clusters **11**, 277.
Ho, Y. K., 1990, J. Phys. B **23**, L71.
Ho, Y. K., 1992, Phys. Rev. A **45**, 148.
Ho, Y. K., and A. K. Bhatia, 1992, Phys. Rev. A **45**, 6268.
Ho, Y. K., and J. Callaway, 1985, J. Phys. A **18**, 3481.
Hogervorst, W., 1993, Comments At. Mol. Phys. **29**, 245.
Holle, A., J. Main, G. Wiebusch, H. Rottke, and K. H. Welge, 1988, Phys. Rev. Lett. **61**, 161.
Hunter, G., and H. O. Pritchard, 1967a, J. Chem. Phys. **46**, 2146.
Hunter, G., and H. O. Pritchard, 1967b, J. Chem. Phys. **46**, 2153.
Hunter, G., B. F. Gray, and H. O. Pritchard, 1968, J. Chem. Phys. **45**, 3806.
Hunter, III, J. E., and R. S. Berry, 1987, Phys. Rev. A **36**, 3042.
Hylleraas, E. A., 1928, Z. Phys. **48**, 469.
Hylleraas, E. A., 1929, Z. Phys. **54**, 347.
James, H. M., and A. S. Coolidge, 1937, Phys. Rev. **51**, 857.
Jones, R. R., and T. F. Gallagher, 1990, Phys. Rev. A **42**, 2655.
Junker, B. R., 1982, Adv. At. Mol. Phys. **18**, 207.
Keller, J. B., 1958, Ann. Phys. (N.Y.) **4**, 180.
Kellman, M. E., 1994, Phys. Rev. Lett. **73**, 2543.

Kellman, M. E., and D. R. Herrick, 1980, Phys. Rev. A **22**, 1536.
Kellner, G. W., 1927, Z. Phys. **44**, 91.
Kemble, E. C., 1921, Philos. Mag. **42**, 123.
Kilgus, G., *et al.*, 1990, Phys. Rev. Lett. **64**, 737.
Kim, J. H., and G. S. Ezra, 1991, in *Proceedings of the Adriatico Conference on Quantum Chaos*, edited by H. Cerdeira *et al.* (World Scientific, Singapore), p. 436.
Kinoshita, T., 1959, Phys. Rev. **115**, 366.
Klar, H., 1986, Phys. Rev. Lett. **57**, 66.
Klar, H., and M. Klar, 1980, J. Phys. B **13**, 1057.
Kossmann, H., B. Krässig, and V. Schmidt, 1988, J. Phys. B **21**, 1489.
Koyama, N., H. Fukuda, T. Motoyama, and M. Matsuzawa, 1986, J. Phys. B **19**, L331.
Koyama, N., A. Takafuji, and M. Matsuzawa, 1989, J. Phys. B **22**, 553.
Kramers, H. A., 1923, Z. Phys. **13**, 312.
Kustaanheimo, P., and E. Stiefel, 1965, J. Reine Angew Math. **278**, 204P.
Landé, A., 1919, Phys. Z. **20**, 228.
Langmuir, I., 1921, Phys. Rev. **17**, 339.
Leopold, J. G., and I. C. Percival, 1980, J. Phys. B **13**, 1037.
Leopold, J. G., I. C. Percival, and A. S. Tworkowski, 1980, J. Phys. B **13**, 1025.
Lin, C. D., 1982a, Phys. Rev. A **25**, 76.
Lin, C. D., 1982b, Phys. Rev. A **26**, 2305.
Lin, C. D., 1983a, Phys. Rev. Lett. **51**, 1348.
Lin, C. D., 1983b, Phys. Rev. A **27**, 22.
Lin, C. D., 1984, Phys. Rev. A **29**, 1019.
Lin, C. D., 1986, Adv. At. Mol. Phys. **22**, 77.
Lin, C. D., 1989, Phys. Rev. A **39**, 4355.
Lin, C. D., 1995, Phys. Rep. **257**, 1.
Lin, C. D., and J. Macek, 1984, Phys. Rev. A **29**, 2317.
Lin, C. D., and S. Watanabe, 1987, Phys. Rev. A **35**, 4499.
Liu, C. H., N. Y. Du, and A. F. Starace, 1991, Phys. Rev. A **43**, 5891.
Lyman, T., 1924, Astrophys. J. **60**, 1.
Macek, J., 1968, J. Phys. B **1**, 831.
Macias, A., and A. Riera, 1986a, Europhys. Lett. **2**, 351.
Macias, A., and A. Riera, 1986b, Phys. Lett. A **119**, 28.
Mack, M., J. H. Nijland, P. van der Straten, A. Niehaus, and R. Morgenstern, 1989, Phys. Rev. A **39**, 3846.
MacKay, R. S., J. D. Meiss, and I. C. Percival, 1984, Phys. Rev. Lett. **52**, 697.
Madden, R. P., and K. Codling, 1963, Phys. Rev. Lett. **10**, 516.
Mandelshtam, V. A., T. R. Ravuri, and H. S. Taylor, 1993, Phys. Rev. Lett. **70**, 1932.
Martens, C. C., and S. E. Ezra, 1987, J. Chem. Phys. **86**, 279.
Martin, F., A. Riera, M. Yanez, and H. Bachau, 1988, J. Phys. B **21**, 2261.
Mehra, J., and H. Rechenberg, 1982, *The Historical Development of Quantum Theory* (Springer-Verlag, Heidelberg); see in particular Vol. I, Part 2 and Vol. II, Chap. 3.
Menzel, A., S. P. Frigo, S. B. Whitfield, C. D. Caldwell, and M. O. Krause, 1996, Phys. Rev. A **54**, 2080.
Menzel, A., S. P. Frigo, S. B. Whitfield, C. D. Caldwell, M. O. Krause, J.-Z. Tang, and I. Shimamura, 1995, Phys. Rev. Lett. **75**, 1479.
Miller, W. H., 1972, J. Chem. Phys. **56**, 38.
Miller, W. H., 1974, Adv. Chem. Phys. **25**, 69.
Miller, W. H., 1975, J. Chem. Phys. **63**, 996.
Molina, Q., 1989, Phys. Rev. A **39**, 3298.
Montesquieu, A. B., 1988, J. Phys. B **21**, 3387.
Moretto-Capelle, P., D. Bordenave-Montesquieu, A. Bordenave-Montesquieu, A. L. Godunov, and V. A. Schipakov, 1997, Phys. Rev. Lett. **79**, 5230.
Morgan, H. D., and D. L. Ederer, 1984, Phys. Rev. A **29**, 1901.
Morita, N., and T. Suzuki, 1988, J. Phys. B **21**, L439.
Müller, J., 1993, Ph.D. thesis (University of Frankfurt); published in Reihe Physik (Verlag Deutsch, Frankfurt), **19**, 1.
Müller, J., and J. Burgdörfer, 1993, Phys. Rev. Lett. **70**, 2375.
Müller, J., J. Burgdörfer, and D. W. Noid, 1992, Phys. Rev. A **45**, 1471.
Müller, J., X. Yang, and J. Burgdörfer, 1994, Phys. Rev. A **49**, 2470.
Nikitin, S. I., and V. N. Ostrovsky, 1982, J. Phys. B **15**, 1609, and references therein.
Ostrovsky, V. N., 1992, Phys. Rev. A **46**, R5309.
Ostrovsky, V. N., and N. V. Prudov, 1993, J. Phys. B **26**, L263.
Oza, D. H., 1986, Phys. Rev. A **33**, 824.
Park, C. H., A. F. Starace, J. Tan, and C. D. Lin, 1991, Phys. Rev. A **33**, 1000.
Pars, L. A., 1965, *A Treatise on Analytical Dynamics* (Heinemann, London).
Pan, C., A. F. Starace, and C. H. Greene, 1994, J. Phys. B **27**, L137.
Pauli, W., 1922, Ann. Phys. (Leipzig) IV **68**, 177.
Pekeris, C. L., 1958, Phys. Rev. **112**, 1649.
Pekeris, C. L., 1959, Phys. Rev. **115**, 1216.
Pelikan, E., and H. Klar, 1983, Z. Phys. A **310**, 153.
Percival, I. C., 1974, J. Phys. A **7**, 794.
Percival, I. C., 1977, Proc. R. Soc. London, Ser. A **353**, 289.
Prosen, T., 1994, J. Phys. A **27**, L709.
Prosen, T., 1995, J. Phys. A **28**, 4133.
Prosen, T., 1996, Physica D **91**, 244.
Qiu, Y., J. Müller, and J. Burgdörfer, 1996, Phys. Rev. A **54**, 1922.
Rau, A. R. P., 1983, J. Phys. B **16**, L699.
Rau, A. R. P., 1984, Phys. Rep. **110**, 369.
Read, F. H., 1977, J. Phys. B **12**, 449.
Read, F. H., 1982, Aust. J. Phys. **35**, 475.
Read, F. H., 1990, J. Phys. B **23**, 951.
Reed, M., and B. Simon, 1972, *Methods of Modern Mathematical Physics* (Academic Press, New York); see Vol. I Chap. VI and Vol. IV Chap. XIII.
Reinhardt, W. P., 1982, Annu. Rev. Phys. Chem. **33**, 223.
Richter, K., 1991, *Semiklassik von Zwei-Elektronen-Atomen*, Ph.D. thesis, Universität Freiburg.
Richter, K., J. S. Briggs, D. Wintgen, and E. A. Solov'ev, 1992, J. Phys. B **25**, 3929.
Richter, K., J. M. Rost, R. Thürwächter, J. S. Briggs, D. Wintgen, and E. A. Solov'ev, 1991, Phys. Rev. Lett. **66**, 149.
Richter, K., G. Tanner, and D. Wintgen, 1993, Phys. Rev. A **48**, 4182.
Richter, K., and D. Wintgen, 1990a, J. Phys. B **23**, L197.
Richter, K., and D. Wintgen, 1990b, Phys. Rev. Lett. **65**, 1965.
Richter, K., and D. Wintgen, 1991, J. Phys. B **24**, L565.
Richter, K., and D. Wintgen, 1992, in *Atomic Physics 13*, edited by H. Walther, T. W. Hänsch, and B. Neizert (American Institute of Physics, New York), p. 388.
Richter, K., and D. Wintgen, 1993, J. Phys. B **26**, 3719.
Robbins, J. M., 1991, Nonlinearity **4**, 343.
Rost, J. M., 1994, Phys. Rev. Lett. **72**, 1998.
Rost, J. M., 1995, J. Phys. B **28**, 3003.
Rost, J. M., 1998, Phys. Rep. **297**, 271.

Rost, J. M., and J. S. Briggs, 1988, J. Phys. B **21**, L233.
Rost, J. M., and J. S. Briggs, 1989, J. Phys. B **22**, 3587.
Rost, J. M., and J. S. Briggs, 1990, J. Phys. B **23**, L339.
Rost, J. M., and J. S. Briggs, 1991, J. Phys. B **24**, 4293.
Rost, J. M., J. S. Briggs, and J. M. Feagin, 1991, Phys. Rev. Lett. **66**, 1642.
Rost, J. M., R. Gersbacher, K. Richter, J. S. Briggs, and D. Wintgen, 1991, J. Phys. B **24**, 2455.
Rost, J. M., K. Schulz, M. Domke, and G. Kaindl, 1997, J. Phys. B **30**, 4663.
Rost, J. M., S. M. Sung, D. R. Herschbach, and J. S. Briggs, 1992, Phys. Rev. A **46**, 2410.
Rost, J. M., and G. Tanner, 1997, in *Classical, Semiclassical and Quantum Dynamics in Atoms*, edited by H. Friedrich and B. Eckhardt (Lecture Notes in Physics 485, Springer, Berlin), p. 274.
Rost, J. M., and D. Wintgen, 1996, Europhys. Lett. **35**, 19.
Roussel, F., M. Cheret, L. Chen, T. Bolzinger, G. Spiess, J. Hare, and M. Gross, 1990, Phys. Rev. Lett. **65**, 3112.
Rouvinez, C., and U. Smilansky, 1995, J. Phys. A **28**, 77.
Sadeghpour, H. R., 1991, Phys. Rev. A **43**, 5821.
Sadeghpour, H. R., and C. H. Greene, 1990, Phys. Rev. Lett. **65**, 313.
Sadeghpour, H. R., C. H. Greene, and M. Cavagnero, 1992, Phys. Rev. A **45**, 1587.
Sakaue, H. A., *et al.*, 1990, J. Phys. B **23**, L401.
Sánchez, I., and F. Martin, 1993, Phys. Rev. A **48**, 1243.
Schiff, L. I., 1968, *Quantum Mechanics* (McGraw-Hill, Singapore).
Schlagheck, P., and A. Buchleitner, 1998, J. Phys. A **31**, L489.
Schlagheck, P., and A. Buchleitner, 1999, Europhys. Lett. **46**, 24.
Schrödinger, E., 1926, Ann. Phys. (Leipzig) **79**, 361.
Schulz, K., G. Kaindl, M. Domke, J. D. Bozek, P. A. Heimann, A. S. Schlachter, and J. M. Rost, 1996, Phys. Rev. Lett. **77**, 3086.
Schuster, H. G., 1989, *Deterministic Chaos* (VCH, Weinheim).
Seaton, M. J., 1983, Rep. Prog. Phys. **64**, 167.
Seng, M., M. Halka, K.-D. Heber, and W. Sandner, 1995, Phys. Rev. Lett. **74**, 3344.
Sieber, M., and F. Steiner, 1990, Phys. Lett. A **144**, 159.
Sieber, M., and F. Steiner, 1991, Phys. Rev. Lett. **67**, 1941.
Sinanoglu, O., and D. E. Herrick, 1975, J. Chem. Phys. **62**, 886.
Slater, J. C., 1927, Proc. Natl. Acad. Sci. USA **13**, 423.
Slater, J. C., 1977, *Quantum Theory of Matter* (Krieger, Huntington).
Sokell, E, A. A. Wills, P. Hammond, M. A. MacDonald, and M. K. Odling-Smee, 1996, J. Phys. B **29**, L863.
Solov'ev, E. A., 1985, Zh. Éksp. Teor. Fiz. **89**, 1991 [Sov. Phys. JETP **62**, 1148].
Sommerfeld, A., 1923, J. Opt. Soc. Am. **7**, 509.
Starace, A. F., 1988, *Fundamental Processes of Atomic Dynamics*, edited by J. S. Briggs, H. Kleinpoppen, and H. O. Lutz (Plenum, New York).
Starace, A. F., 1993, in *Many-Body Theory of Atomic Structure and Photoionization*, edited by T.-N. Chang (World Scientific, Singapore), p. 107.
Stolterfoht, N., C. C. Havener, R. A. Phaneuf, J. K. Swenson, S. M. Shafroth, and F. W. Meyer, 1986, Phys. Rev. Lett. **57**, 74.
Strand, M. P., and W. P. Reinhardt, 1979, J. Chem. Phys. **70**, 3812.
Tang, J. Z., and I. Shimamura, 1994, Phys. Rev. A **50**, 1321.
Tang, J. Z., S. Watanabe, and M. Matsuzawa, 1992a, Phys. Rev. A **46**, 2437.
Tang, J. Z., S. Watanabe, M. Matsuzawa, and C. D. Lin, 1992b, Phys. Rev. Lett. **69**, 1633.
Tang, X., Y. Gu, and J.-M. Yuan, 1996, Phys. Rev. A **54**, 496.
Tanner, G., K. Hansen, and J. Main, 1996, Nonlinearity **9**, 1641.
Tanner, G., P. Scherer, E. B. Bogomolny, B. Eckhardt, and D. Wintgen, 1991, Phys. Rev. Lett. **67**, 2410.
Tanner, G., and D. Wintgen, 1995, Phys. Rev. Lett. **75**, 2928.
Titchmarsh, E. C., 1986, *The Theory of the Riemann Zeta Function* (Clarendon Press, Oxford).
Tolstikhin, O. I., S. Watanabe, and M. Matsuzawa, 1995, Phys. Rev. Lett. **74**, 3573.
Unsöld, A., 1927, Ann. Phys. (Leipzig) **82**, 355.
van den Brink, J. P., G. Nienhuis, J. van Eck, and H. G. M. Heideman, 1989, J. Phys. B **22**, 3501.
Van Vleck, J. H., 1922, Philos. Mag. **44**, 842.
Vollweiter, A., J. M. Rost, and J. S. Briggs, 1991, J. Phys. B **24**, L155.
Voros, A., 1987, Commun. Math. Phys. **110**, 439.
Voros, A., 1988, J. Math. Phys. **21**, 685.
Wang, H., 1986, J. Phys. B **19**, 3401.
Wannier, G., 1953, Phys. Rev. **90**, 817.
Watanabe, S., and C. D. Lin, 1986, Phys. Rev. A **34**, 823.
Wesenberg, G. E., D. W. Noid, and J. B. Delos, 1985, Chem. Phys. Lett. **118**, 72.
Wintgen, D., 1987, Phys. Rev. Lett. **58**, 1589.
D. Wintgen, 1994, private communication.
Wintgen, D., A. Bürgers, K. Richter, and G. Tanner, 1994, Prog. Theor. Phys. Suppl. **116**, 121.
Wintgen, D., and D. Delande, 1993, J. Phys. B **26**, L399.
Wintgen, D., and K. Richter, 1994, Comments At. Mol. Phys. **29**, 261.
Wintgen, D., K. Richter, and G. Tanner, 1992, Chaos **2**, 19.
Wirzba, A., 1992, Chaos **2**, 77.
Wirzba, A., 1997, Habilitationsschrift (Gesellschaft für Schwerionenforschung mbH, Darmstadt).
Witten, E., 1980, Phys. Today **33**(7), 38.
Woodruff, P. R., and J. A. R. Samson, 1982, Phys. Rev. A **25**, 848.
Wulfman, C., 1968, Phys. Lett. **26A**, 397.
Wulfman, C., 1973, Chem. Phys. Lett. **23**, 370.
Yamamoto, T., and K. Kaneko, 1993, Phys. Rev. Lett. **70**, 1928.
Yuh, H. J., G. S. Ezra, P. Rehmus, and R. S. Berry, 1981, Phys. Rev. Lett. **47**, 497.
Zubek, M., G. C. King, P. M. Rutter, and F. H. Read, 1989, J. Phys. B **22**, 3411.